

Collapsing Bubble Bed in a Downcomer with the Introduction of Solvent

Seng How Kuan

Department of Mining and Materials Engineering
McGill University
Montreal, Canada

August 2012

A thesis submitted to McGill University
in partial fulfillment of the requirements of the degree of
Doctor of Philosophy

© Seng How Kuan, 2012

In the memory of my parents,

Tong Hai and Kim Lay.

東海和金麗

“爸，媽，我得到博士了”

To the memory of Dr. S. Ramachandra Rao
(1936 - 2012)

Abstract

The original goal was to use a downcomer to create swarms of solvent-coated bubbles to scale-up the air-assisted solvent extraction (AASX) process. The downcomer provides a close-packed bubble bed considered attractive for solvent coating and fast extraction kinetics. During initial testing, the bubble bed was observed to collapse upon introduction of solvent, evident from decreasing gas holdup, decreasing aspirated air rate, and formation of air slugs. Neither changing solvent introduction technique, solvent composition nor addition of frother or salt alleviated the situation. In many cases collapse was complete (air rate became zero) at less than 900 ppm solvent. Thus, the focus shifted to address this phenomenon. Because conditions in the bubble bed approach those of foam (gas holdup over 45%), the de-foaming action of oil droplets was thought to be responsible, the solvent taking the role of de-foaming agent. The mechanism is related to oil droplets bridging and/or spreading to destabilize the inter-bubble film. Testing two hydrophobic solids, talc and graphite, showed that solids did not collapse the bed suggesting that the solvent's ability to spread gives the de-foaming (bed collapse) effect. A setup was established to view coalescence of two bubbles held in proximity when exposed to circulating dispersions of solvent, solid and solvent/solid. Conditions giving coalescence generally agreed with those yielding bed collapse, including the MIBC/talc system which resisted coalescence and bed collapse on introduction of solvent. Solvent bridging was captured on video although spreading was not observed. In conclusion the downcomer is not suited to AASX. The unit is used in Jameson Cells employed to remove solvent droplets in SX plants. The solvent levels appear to be less than 200 ppm where collapse is only partial and the phenomenon may not be noticed in those applications.

Resumé

Le premier objectif de la recherche consistait à faire usage d'une goulotte de façon à créer des bulles enrobées de solvant afin d'augmenter l'échelle de mesure pour l'extraction au solvant par air assisté (AASX). La goulotte assure un contact plus étroit entre la bulle et le solvant et celui est considéré comme avantageux pour l'enrobage des bulles du solvant et pour la cinétique d'extraction rapide. Lors des tests initiaux, l'effondrement du lit formé par les bulles dans la goulotte, était observé à l'introduction du solvant comme le démontre le bas niveau du gaz, la diminution du débit de l'air aspiré, et la formation des grandes bulles d'air. L'on a observé qu'en changeant de technique d'introduction du solvant, la composition du solvant, et en ajoutant du sel et du moussant, le problème restait entier. Puisque les conditions dans le lit des bulles dans la goulotte avoisinent celles de la mousse (niveau de gaz plus que 45%), les propriétés des gouttelettes de solvant étaient tenues pour responsables, les gouttelettes de solvant jouant le rôle d'agent démousseur. Ce faisant, la recherche s'est penchée sur ce phénomène. Le mécanisme est lié à l'action de formation de pont (entre les bulles) et/ou l'enrobage des bulles par des gouttelettes de solvant. Celles-ci déstabilisent le film entre les bulles. Plus d'investigations sur les effets des matériaux hydrophobes sur la stabilité du lit des bulles en comparant le solvant à deux solides hydrophobes, le talc et le graphite, avaient révélé que les solides n'avaient pas produit l'effondrement, sinon favorisé la stabilité: Ceci suggère l'habileté du solvant à s'étaler, ce qui confère la propriété démoussante (effondrement du lit). En conséquence, un montage avait été fait pour visualiser la coalescence entre deux bulles de plus près, lorsque celles-ci étaient exposées à la circulation des dispersions de solvant, solide et des mélanges solvant/solides. Les résultats ont montré que les conditions entraînant la coalescence s'accordaient bien avec celles qui engendraient l'effondrement du lit dans la goulotte. Le pont formé entre les bulles et le solvant avait été capté par vidéo alors que l'étalement ne l'était pas. En conclusion, la goulotte n'est pas indiquée pour l'extraction au solvant par air assisté (AASX). L'unité est utilisée dans la cellule de Jameson pour éliminer les gouttelettes de solvant dans les unités d'extraction. Le niveau de solvant est moins de 200 ppm et dans ce cas, l'effondrement est partiel et le phénomène n'est peut-être pas observé dans ces applications.

Contribution of authors

This thesis is manuscript-based. All the manuscripts are co-authored with Prof. James A. Finch in his capacity as research supervisor. The manuscripts are presented as Chapters 3, 4, and 5 of the thesis and will be presented for publication. The candidate designed and conducted the experiments. The candidate wrote every chapter and considered the comments from the supervisor in generating the final versions.

The thesis is organized into seven chapters, three of which (Chapters 3, 4, and 5) are stand-alone chapters and will be presented for publication. A chapter is included (Chapter 6) to provide a unifying discussion of the results in Chapter 3, 4, and 5. The thesis also includes an introduction (Chapter 1), a literature review (Chapter 2) and a conclusion (Chapter 7). Additional information was included in the Appendix section.

Acknowledgements

I would like to extend my warmest gratitude to Professor Finch for his guidance and support in carrying out this work. His enthusiasm, kindness, and patience made this work possible, especially during times when things did not work and motivation was low.

Also, I would like to express my appreciation to Dr. Cesar Gomez for his valuable insights and suggestions on the work and to Dr. Miguel Maldonado and Ray Langlois for their assistance in the experimental setup. Thanks also to the rest of the Finch group for their help, camaraderie and support: Dr. Barnabe Ngabe, Dr. Jan Nettet, Amir Nazari, Frank Rosenblum, Hope Tan, Azin Zangooi, Jarrett Quinn, Adam Jordens, Sarah Jung, Jennifer Radman, Marc Nassif, Nalini Singh, Mitra Mirnezami, Peng Bo Chu, and Joel Ross. Special thanks go to Wei Zhang for his invaluable help in moving the setup over three different laboratories and also for providing motivation for me to complete this work by finishing his PhD in a little over 2 years.

Table of Contents

ABSTRACT	VI
RESUMÉ	VII
CONTRIBUTION OF AUTHORS	VIII
ACKNOWLEDGEMENTS	IX
TABLE OF CONTENTS	X
LIST OF FIGURES	XIII
LIST OF TABLES	XVII
CHAPTER 1 - INTRODUCTION	1
1.1 GENERAL BACKGROUND.....	1
1.2 OBJECTIVES OF THESIS.....	4
1.3 STRUCTURE OF THESIS.....	5
1.4 REFERENCES	7
CHAPTER 2 – LITERATURE REVIEW	9
2.1 SOLVENT EXTRACTION	9
2.1.1 <i>General Principles</i>	9
2.1.2 <i>Extractants, Diluents and Modifiers</i>	10
2.1.3 <i>Solvent Extraction Circuits</i>	11
2.3 SOLVENT EXTRACTION IN THE TREATMENT OF EFFLUENT STREAMS	12
2.3.1 <i>Acid Mine Drainage (AMD)</i>	14
2.4 SOLVENT-COATED BUBBLES.....	15
2.4.1 <i>Previous Bubble Coating Work</i>	15
2.4.2 <i>Contact Angle and Induction Time</i>	16
2.4.3 <i>Thermodynamics of Coating</i>	17
2.4.4 <i>Mechanism of Bubble-Oil Droplet Attachment</i>	17
2.4.5 <i>Air-Assisted Solvent Extraction (AASX)</i>	20
2.4.6 <i>Aerosol Technique for Solvent Extraction</i>	21
2.5 THE DOWNCOMER.....	23
2.6 SURFACTANT AND SALT ACTION ON BUBBLE SIZE REDUCTION	25
2.6.1 <i>Coalescence prevention</i>	25
2.6.2 <i>Break-up</i>	28
2.7 REFERENCES	30
CHAPTER 3 - COLLAPSING BUBBLE BED IN THE DOWNCOMER WITH THE INTRODUCTION OF SOLVENT	37
3.1 INTRODUCTION.....	37
3.2 EXPERIMENTAL	38
3.2.1 <i>General setup</i>	38
3.2.2 <i>Solvent injection</i>	41

3.2.3 <i>Materials and methods</i>	46
3.2.4 <i>Estimating solvent rate</i>	47
3.3 RESULTS	49
3.3.1 <i>Extraction and turbidity</i>	49
3.3.2 <i>Collapsing bubble bed</i>	51
3.3.2.1 LIX:Kerosene 1:29.....	51
3.3.2.1.1 Gas holdup and air rate	51
3.3.2.1.2 Bubble size.....	53
3.3.2.2 Effect of LIX to kerosene ratio	54
3.3.2.3 Effect of injection method	56
3.3.3 <i>Effect of aeration after stopping solvent injection</i>	58
3.4 DISCUSSION.....	60
3.5 CONCLUSIONS	67
3.6 REFERENCES	68
CHAPTER 4 - EFFECT OF HYDROPHOBIC MATERIAL ON BUBBLE BED IN THE DOWNCOMER.....	70
4.1 INTRODUCTION.....	70
4.2 THEORY OF FOAMING DESTABILIZATION BY HYDROPHOBIC MATERIAL	70
4.3 EXPERIMENTAL	74
4.3.1 <i>General setup</i>	74
4.3.2 <i>Materials and methods</i>	74
4.4 RESULTS	75
4.4.1 <i>Effect of hydrophobic liquid (solvent)</i>	75
4.4.2 <i>Effect of hydrophobic solids</i>	75
4.4.2.1 Talc	75
4.4.2.3 Graphite.....	78
4.4.3 <i>Effect of hydrophobic solids and solvent</i>	79
4.4.3.1 Gas holdup	79
4.4.3.2 Bubble images.....	83
4.4.3.3 Froth buildup in the presence of solids	87
4.5 DISCUSSION.....	89
4.5.1 <i>In MIBC system</i>	89
4.5.2 <i>In PPG 425 system</i>	90
4.5.3 <i>In the NaCl system</i>	91
4.5.3.1 Talc	91
4.5.3.2 Graphite.....	92
4.5.3 <i>Bubble bed collapse and industrial practice of organic removal using Jameson Cells</i>	93
4.6 CONCLUSIONS	94
4.7 REFERENCES	95
CHAPTER 5 – SOLVENT DROPLET-BUBBLE CONTACT IN PRESENCE OF FROTHERS, SALT AND HYDROPHOBIC SOLIDS	98
5.1 INTRODUCTION.....	98
5.2 EXPERIMENTAL	98
5.2.1 <i>General setup and procedure</i>	98

5.2.2 Materials and methods.....	100
5.3 RESULTS	101
5.3.1 Setup 1: Droplet contacting the two bubbles.....	101
5.3.1.1 $D_d/D_b > 1$	101
5.3.1.2 $D_d/D_b < 1$	104
5.3.2 Setup 2: Circulating dispersions.....	105
5.3.2.1 Water only.....	105
5.3.2.1.1 Water and solvent	105
5.3.2.2.2 Water and talc or graphite.....	106
5.3.2.2 In presence of MIBC.....	107
5.3.2.2.1 MIBC alone.....	107
5.3.2.2.2 MIBC and solvent.....	108
5.3.2.2.3 MIBC and talc.....	108
5.3.2.2.4 MIBC, talc and solvent	109
5.3.2.3 In presence of PPG 425.....	109
5.3.2.3.1 PPG 425 alone.....	109
5.3.2.3.2 PPG 425 and solvent.....	110
5.3.2.3.3 PPG 425 and talc.....	111
5.3.2.3.4 PPG 425, talc, and solvent	112
5.3.2.4 In presence of NaCl	112
5.3.2.4.1 NaCl alone	112
5.3.2.4.2 NaCl and solvent.....	113
5.3.2.4.3 NaCl and talc.....	113
5.3.2.4.4 NaCl, talc and solvent.....	114
5.3.2.4.5 NaCl and graphite	114
5.3.2.4.6 NaCl, graphite, and solvent.....	115
5.3.2.5 Summary.....	116
5.3.3 Surface and interfacial tensions.....	116
5.4 DISCUSSION.....	117
5.5 CONCLUSIONS	121
5.6 REFERENCES	122
CHAPTER 6 – UNIFYING DISCUSSION	123
6.1 SUMMARY OF FINDINGS.....	123
6.2 SOLVENT BRIDGING AND SPREADING EFFECT	125
6.3 SOLIDS BRIDGING EFFECT.....	125
6.4 THE MIBC/TALC COMBINATION	126
6.5 INDUSTRIAL USE OF DOWNCOMER IN ORGANIC REMOVAL	126
6.6 REFERENCES	127
CHAPTER 7 – CONCLUSIONS, CONTRIBUTIONS, AND FUTURE WORK ..	128
7.1 CONCLUSIONS	128
7.2 CONTRIBUTIONS TO KNOWLEDGE	130
7.3 SUGGESTIONS FOR FUTURE WORK.....	130
7.4 REFERENCES	131
APPENDICES	132

List of Figures

Fig. 2.1. Structure of D2EHPA.....	10
Fig. 2.2. Structure of LIX 65N.	10
Fig. 2.3. A typical solvent extraction flowsheet (adapted from Rydberg et. al., 2004)....	11
Fig. 2.4. Solute concentration ranges for separation techniques (adapted from Kentish and Stevens, 2001).....	13
Fig. 2.5. Mechanisms for gas bubble capture of oil droplets suspended in water	19
Fig. 2.6. Experimental setup of AASX to produce a stream of solvent-coated bubbles ..	20
Fig. 2.7. Comparison of extraction as function of solvent volume using solvent droplet and solvent coated bubble.....	21
Fig. 2.8. Aerosol technique for solvent coating in AASX.....	22
Fig. 2.9. Example extraction experiment.....	23
Fig. 2.10. Jameson cell operation	24
Fig. 2.11. a) Before stretching, surfactant molecules distributed uniformly at interface b) After stretching, local surface tension increases as a consequence of lower surface concentration of surfactant.....	26
Fig. 2.12. Break-up mechanism.....	30
Fig. 3.1. General setup.....	40
Fig. 3.2. McGill Bubble Size Analyzer.	41
Fig. 3.3. Method 1: Experimental setup for solvent injection	42
Fig. 3.4. Method 1: Point of solvent discharge.....	43
Fig. 3.5. Method 2: Experimental setup for introduction of solvent into solution	44
Fig. 3.6. Method 3: Experimental setup for introduction of solvent as aerosol into the air inlet	45
Fig. 3.7. Solvent rate versus $1/D_{32}$ simulating conditions from water to frother or salt solutions	49
Fig. 3.8. Extraction as a function of solvent addition in presence of MIBC, PPG 425 and NaCl.	50
Fig. 3.9. Turbidity as a function of solvent addition in presence of MIBC, PPG 425 and NaCl.	51
Fig. 3.10. Gas holdup in separation tank as a function of solvent addition in presence of MIBC, PPG 425 and NaCl.....	52
Fig. 3.11. Gas holdup in separation tank as a function of time in presence of MIBC, PPG 425 and NaCl illustrating stabilisation of gas holdup when solvent injection is stopped at 12 minutes.	52
Fig. 3.12. Air rate as a function of solvent addition in presence of MIBC, PPG 425 and NaCl. Note that gas rate was calculated based on the cross sectional area of the separation tank.	53
Fig. 3.13. (a) Bubbles in water. (b) Bubbles with addition of 50 ppm MIBC. (c) Bubbles after 33.33 mL solvent injection in presence of 50 ppm MIBC.	53
Fig. 3.14. (a) Bubbles in water. (b) Bubbles with addition of 10 ppm PPG 425. (c) Bubbles after 33.33 mL solvent injection in presence of 10 ppm PPG 425.	54
Fig. 3.15. (a) Bubbles in water. (b) Bubbles with the addition of 0.4 M NaCl. (c) Bubbles after 33.33 mL solvent injection in presence of 0.4 M NaCl.....	54

Fig. 3.16. Gas holdup before solvent addition with 0.8M NaCl.....	55
Fig. 3.17. Gas holdup as a function of solvent addition and LIX to kerosene ratio	55
Fig. 3.18. Air rate as a function of solvent addition and LIX to kerosene ratio.	56
Fig. 3.19. Comparison of gas holdup data for the three solvent introduction techniques (into bubble bed, into solution and aerosol) for MIBC systems.	57
Fig. 3.20. Comparison of gas holdup data for the three solvent introduction techniques for PPG 425 systems.....	57
Fig. 3.21. Comparison of gas holdup data for the three solvent introduction techniques for NaCl systems.	58
Fig. 3.22. Turbidity as a function of time during and after solvent addition in presence of MIBC, PPG 425 and NaCl.....	58
Fig. 3.23. Extraction as a function of time during and after solvent addition in presence of MIBC, PPG 425 and NaCl.....	59
Fig. 3.24. Gas holdup as a function of time during and after solvent addition in presence of MIBC, PPG 425 and NaCl.	60
Fig. 3.25. Film rupture caused by spreading of oil droplet.....	62
Fig. 3.26 (a) Droplet does not enter interface when; (b) Droplet enters interface when ; (c) Droplet spreads at interface when.....	64
Fig. 3.27. (a) Stable oil bridge formation (b) Unstable oil bridge formation (c) Stable oil bridge at equilibrium after deformation.....	65
Fig. 3.28 (a) Oil droplet enters interface; (b) Oil bridge formation; (c) Oil bridge is stretched with time; (d) Film ruptures.	66
Fig. 4.1. (a) Interaction of a glass bead =102° with a film of liquid; (b) Interaction of a glass bead =74° with a film of liquid	72
Fig. 4.2. The gas holdup in separation tank as a function of solvent addition in presence of MIBC, PPG 425 and NaCl	75
Fig. 4.3. The effect of talc up to 0.07 % w/w on gas holdup and bubble size in presence of MIBC, PPG 425 and NaCl.....	76
Fig. 4.4 Effect of talc up to 1 % w/w on gas holdup and bubble size in presence of 50 ppm MIBC	77
Fig. 4.5. Effect of talc up to 1 % w/w on gas holdup and bubble size in presence of 10 ppm PPG 425	77
Fig. 4.6. Effect of talc up to 1 % w/w on gas holdup and bubble size in presence of NaCl	78
Fig. 4.7. Effect of graphite up to 1 % w/w on gas holdup and bubble size in presence of NaCl	79
Fig. 4.8. Combined effect of talc and solvent on gas holdup in presence of 50 ppm MIBC	80
Fig. 4.9. Combined effects of talc and solvent on gas holdup in presence of 10 ppm PPG 425.....	81
Fig. 4.10. Combined effect of talc and solvent on gas holdup in presence of 0.4M NaCl	82
Fig. 4.11. Combined effect of graphite and solvent on gas holdup in presence of 0.4M NaCl	83
Fig. 4.12. Bubble images for the following sequence: (a) Water alone; (b) After addition of 50 ppm MIBC; (c) After addition of 0.07 % w/w talc; (d) After addition of 0.5%	

w/w talc; (e) After addition of 1 % w/w talc; (f) After addition of 33.3 mL solvent (A/O 900).....	84
Fig. 4.13. Bubble images for the following sequence: (a) Water only; (b) After addition of 10 ppm PPG 425; (c) After addition of 0.07 % w/w talc; (d) After addition of 0.5 % w/w talc; (e) After addition of 1 % w/w talc; (f) After addition of 33.3 mL solvent (A/O 900).....	85
Fig. 4.14. Bubble images for the following sequence: (a) Water only; (b) After addition of 0.4M NaCl; (c) After addition of 0.07 % w/w talc; (d) After addition of 0.5% w/w talc; (e) After addition of 1 % w/w talc; (f) After addition of 33.3 mL solvent (A/O 900).....	86
Fig. 4.15. Bubble images for the following sequence: (a) Water only; (b) After addition of 0.4M NaCl; (c) After addition of 0.07 % w/w graphite; (d) After addition of 0.5% w/w graphite; (e) After addition of 1 % w/w graphite; (f) After addition of 33.3 mL solvent (A/O of 900).....	87
Fig. 4.16. In presence of 0.4 M NaCl: (a) Froth build-up in launder after the addition of 0.5 % w/w talc; (b) Froth collapse after subsequent solvent addition	88
Fig. 4.17. In presence of 0.4 M NaCl: (a) Froth build-up in launder after the addition of 1% w/w talc; (b) Froth collapse after subsequent solvent addition	88
Fig. 4.18. Coalescence inhibiting effect due to packing of talc particles and MIBC molecules at the air-water interface.....	90
Fig. 4.19. (a) Frother orientation at air-water interface comparing PPG 425 with two OH end groups to frothers with one OH end group (i.e., alcohols, e.g. MIBC); (b) Removal of PPG 425 from interface by adsorption on talc	91
Fig. 4.20. Gas holdup as a function of solvent concentration in presence of MIBC, PPG 425 and NaCl.....	94
Fig. 5.1. Setup 1: Contacting two bubbles with a solvent droplet.....	99
Fig. 5.2. Setup 2: Contacting circulating dispersion past the bubbles.....	100
Fig 5.3. Setup 1: Solvent droplet in contact with two bubbles in presence of 50 ppm MIBC	102
Fig 5.4. Setup 1: Solvent droplet formed at capillary in contact with two bubbles in water	102
Fig 5.5. Setup 1: Solvent droplet formed at capillary in contact with two bubbles in presence of 10 ppm PPG 425.....	103
Fig 5.6. Setup 1: Solvent droplet formed with syringe in contact with two bubbles in presence of 10 ppm PPG 425:.....	104
Fig. 5.7. Setup 2: Two bubbles in water only.....	105
Fig. 5.8. Setup 2: Solvent droplet colliding with bubble and spreading (ca. 3 s).....	106
Fig. 5.9. Setup 2: Build-up of solvent layer through time (ca. 37 s).....	106
Fig. 5.10. Setup 2: Water and 0.02 % w/w talc, time from a to c, ca. 65-70 s.....	107
Fig. 5.11. Setup 2: Water and 0.02 % w/w graphite, time from a to c, ca. 65-70 s.....	107
Fig. 5.12. Setup 2: 50 ppm MIBC.....	108
Fig. 5.13. Setup 2: 50 ppm MIBC and 1600 ppm solvent (time from a to c, ca. 65 - 70s)	108
Fig. 5.14. Setup 2: 50 ppm MIBC and 0.02 % w/w talc.....	109
Fig. 5.15. Setup 2: 50 ppm MIBC, 0.02 % w/w talc, and 1600 ppm solvent.....	109
Fig. 5.16. Setup 2: 10 ppm PPG 425.....	110

Fig 5.17. Setup 2: 10 ppm PPG 425 and 1600 ppm solvent.....	110
Fig. 5.18. Setup 2: Solvent droplet attaches (a) and bridges the two bubbles (b – d) causing coalescence (e – f) with 10 ppm PPG 425.....	111
Fig. 5.19. Setup 2: 10 ppm PPG 425 and 0.02 % w/w talc.....	112
Fig. 5.20. Setup 2: 10 ppm PPG 425, 0.02 % w/w talc and 1600 ppm solvent.....	112
Fig. 5.21. Setup 2: 0.4 M NaCl.....	113
Fig. 5.22. Setup 2: 0.4 M NaCl and 1600 ppm solvent.....	113
Fig. 5.23. Setup 2: 0.4 M NaCl and 0.02 % w/w talc.....	114
Fig. 5.24. Setup 2: 0.4 M NaCl, 0.02 % w/w talc and 1600 ppm solvent.....	114
Fig. 5.25. Setup 2: 0.4 M NaCl and 0.02 % w/w graphite.....	115
Fig. 5.26. Setup 2: 0.4 M NaCl, 0.02 % w/w graphite and 1600 ppm solvent.....	115
A1. (a) Bubbles in water. (b) Bubbles with addition of 90ppm MIBC. (c) Bubbles after 33.3 mL solvent injection in the presence of 90ppm MIBC.....	133
A2. (a) Bubbles in water. (b) Bubbles with addition of 30ppm PPG 425. (c) Bubbles after 33.3 mL solvent injection in the presence of 30ppm PPG 425.....	133
A3. (a) Bubbles in water. (b) Bubbles with addition of 0.8M NaCl. (c) Bubbles after 33.3 mL solvent injection in the presence of 0.8M NaCl.....	133
A4. Copper extraction with respect to solvent addition at different LIX to kerosene ratios.....	134
A5. Change of turbidity with respect to solvent addition at different LIX to kerosene ratios.....	134
A6. Comparison of turbidity data for the three solvent introduction techniques (in bubble bed, in solution and in air) for MIBC systems.....	135
A7. Comparison of turbidity data for the three solvent introduction techniques for PPG 425 systems.....	135
A8. Comparison of turbidity data for the three solvent introduction techniques for NaCl systems.....	136
A9. Effect of silicone oil concentration in solvent on gas holdup of separation tank. ...	136
A10. Solvent droplet in contact with two bubbles in presence of 50 ppm MIBC, LIX:Kerosene 1:29.....	137
A11. Solvent droplet in contact with two bubbles in presence of 0.4 M NaCl, LIX:Kerosene 1:29.....	137
B1. Oxime molecule.....	138
B2. Formation of copper complex with two oxime molecules.....	138
B3. Molecular structure of 4-methyl-2-pentanol or methyl isobutyl carbinol (MIBC)..	139
B4. Molecular structure of polypropylene glycol (PPG 425).....	139

List of Tables

Table 2.1. Comparison of active water treatment methods (Reed, 1998).....	12
Table 2.2. Composition of AMD for selected ore types (mg/L) (Ritcey, 1989).....	15
Table 2.3. Surface and interfacial tensions (in mJ/m ²) to compute the spreading coefficient,	17
Table 3.1. The frothers/salt used.	46
Table 3.2. Chemical composition of the extractant.....	46
Table 5.1 Coalescence, yes or no, for each condition tested.....	116
Table 5.2. Measurements of interfacial tensions and computation of E, B and S coefficients for solvent (LIX:kerosene 1:29)-aqueous solution systems.....	117
Table 5.3. Observations of bubble bed collapse in downcomer and coalescence event in the bubble contact setup in presence of MIBC, PPG 425 and NaCl with talc, graphite and/or solvent.....	120

Chapter 1 - Introduction

1.1 General Background

For the first half of the 20th century, solvent extraction found application in organic chemistry to separate or purify substances (Cox and Rydberg, 2004). In the 50s, uranium recovery became the first major commercial application of solvent extraction (SX) technology in the hydrometallurgical industry. The process was later used as a separation and purification process for other metals, most notably copper, with the opening of the Ranchers Bluebird and Bagdad solvent extraction (SX) plant in the late 60's (Sole et al., 2005). An established process today, solvent extraction is generally restricted to concentrated solutions (> 500 mg/L) and requires an aqueous to solvent (a/o) ratio of ca. 1 (Kentish and Stevens, 2001). When applied to dilute solutions, solvent losses, high capital costs, phase disengagement difficulties and large solvent inventory count among some of the disadvantages of SX. The ambition was to extend SX to dilute streams, such as acid mine drainage which led to the concept of using solvent-coated bubbles (Chen et al., 2003).

The concept of using a coated bubble is partly based on its use in flotation that can be traced to Taggart (1927) who suggested that an oil film spread on a bubble would enhance the collection of hydrophobic particles by forming compact gas/oil/solid agglomerates. Misra and Anazia (1987) pursued the idea for fine coal flotation and discovered that the induction time for bubble attachment was significantly reduced when the bubble was encapsulated in oil. Wang et al. (1988) developed a method of converting kerosene (collector for coal) into gaseous state under controlled temperature and then introducing the gasified collector to air bubbles. The gaseous molecules condensed on the inner surface of the bubble which thus become collector-coated and this enhanced collection of coal particles. Peng and Li (1991) developed a similar technique of collector addition for coal flotation systems where the hydrocarbon-oil collector was converted into gaseous state under controlled temperature and then introduced into the air stream

and dispersed into the flotation cell. They found using the technique that coal particles as large as 600 – 1000 μm were floated faster with less collector than when using the conventional collector addition route. Maiolo and Pelton (1998) used an aerosol generator to produce a mist of silicone oil to coat bubbles and reported enhanced ink (i.e., carbon) removal rate from recycled paper pulp. Gomez et al. (2001) later confirmed this in continuous testing using a flotation column at a deinking plant. Su et al. (2006) demonstrated that bitumen flotation recovery from poor processing ores could be greatly enhanced using oily bubbles (air bubbles coated with a thin layer of oil) instead of air bubbles alone. All work on organic-coated bubbles to date stems from laboratory scale efforts and despite their apparent success, no scaled-up process of coating swarms of bubbles has been developed.

Chen et al. (2003) first described the use of solvent-coated bubbles in solvent extraction. Termed air-assisted solvent extraction (AASX), the method involved spreading of a kerosene-based solvent over a bubble by carefully passing air through a thin plug of solvent replenished from a reservoir. Spreading was shown to be thermodynamically favored. Tarkan and Finch (2005) gave further proof of concept by exploiting the foaming properties of kerosene-based solvents to inject foam through an orifice to produce solvent-coated bubbles. Metal recovery and ease of phase separation were demonstrated but scale up using multiple orifices did not appear feasible (Tarkan and Finch, 2006).

Tarkan et al. (2012) returned to the aerosol coating technique of Maiolo and Pelton (1998) combined with the Venturi bubble generator employed by Gomez et al. (2001). The technique, however, was limited by the delivery rate of aerosol using the ultrasonic generator (which was only ca. 80mL/h) and thus the extraction time was long (about 2 hours in the example quoted). In this regard the ultrasonic aerosol generator approach did not meet the ‘scale up’ criterion. As alternative coating methods, various configurations of Venturi tube were attempted including drawing both air and solvent through the same suction port (Tarkan et al., 2012). None have been successful so far, with visible evidence of tramp solvent droplets in the aqueous phase. It was inferred that the contact time to

coat bubbles was not adequate in the Venturi throat, bubble/droplet contact experiments suggesting at least 1s (i.e., induction time) was required (Chen et al., 2003).

This led to the present work whereby a downcomer, familiar from the Jameson Cell, was tested as a ‘coating reactor’. In a downcomer, the feed stream is introduced vertically downwards through an orifice to aspirate and shear air into bubbles. Since the bubbles tend to rise against the down-flowing liquid this creates a high gas holdup (over 45% as measured by Summers et al., 1995) inside the downcomer. This high gas holdup region will be referred to as the ‘bubble bed’. This bubble bed was anticipated as well suited for solvent to contact and coat bubbles, the typical retention time in the downcomer of a few seconds exceeding the estimated 1s induction time needed for solvent to coat bubbles. In addition, the high gas holdup in the downcomer suggested fast extraction kinetics. Some encouragement for this use of a downcomer is the fact that Jameson Cells are employed to recover solvent droplets from electrolyte in SX plants, essentially a de-oiling application (Miller and Readett, 1992; Miller et al., 1997; Young et al., 2006).

1.2 Objectives of Thesis

The original goal of the research was to develop a method to create swarms of solvent-coated bubbles using the downcomer to treat dilute metal solutions such as AMD (Acid Mine Drainage). During the initial tests, collapse of the bubble bed in the downcomer was observed upon introduction of solvent. The collapse was evident from a decreasing gas holdup, decreasing aspirated air rate, and increasing bubble size. Thus, the focus shifted to address this phenomenon with the following sub-objectives:

1. To determine the factors controlling collapse of the bubble bed through studying the chemistry of the solvent, presence of surfactants (frothers) and salts in the aqueous phase, and method of solvent injection;
2. Recognizing the possible collapse mechanism was due to the hydrophobic nature of the solvent, to determine the effects of hydrophobic solids (talc and graphite) on the bubble bed;
3. To determine the effect on bubble bed stability when introducing solvent in the presence of hydrophobic solids and frother or salt;
4. To propose and test mechanisms of bubble bed collapse.

1.3 Structure of Thesis

The thesis is manuscript-based. It is organized into seven chapters, three of which (Chapters 3, 4, and 5) are stand-alone chapters and will be presented for publication. A chapter is included (Chapter 6) to provide a unifying discussion of the results in Chapters 3, 4, and 5. The thesis starts with an introduction (Chapter 1), a literature review (Chapter 2) and ends with a conclusion chapter (Chapter 7). Additional information is included in an Appendix. The following is a summary of all the chapters:

Chapter 1 – Introduction

A brief background to the research is presented. The thesis objectives and structure are outlined.

Chapter 2 – Literature review

A review of the solvent extraction process, solvent-coated bubbles, the Jameson downcomer and the role of surfactant and salt in bubble size reduction is presented.

Chapter 3 – Collapsing bubble bed in the downcomer with introduction of solvent

The chapter outlines an approach to solvent coating of bubbles based on the downcomer principle used in the Jameson Cell. The issue of collapsing bubble bed is introduced together with efforts to control the collapse. Antifoaming literature was consulted to propose an explanation based on solvent bridging and spreading.

Chapter 4 – Effect of hydrophobic material on bubble bed in the downcomer

This chapter investigates the effect on the bubble bed of hydrophobic solids as a counterpart to hydrophobic liquids (solvent). It is noted that hydrophobic solids did not collapse the bubble bed.

Chapter 5 – Droplet-bubble contact in presence of frothers, salt, and hydrophobic solids

A set-up specifically designed to observe droplet-bubble contact in presence of frothers, salt and hydrophobic solids and liquids (solvent) is outlined. Direct evidence of bridging leading to bubble coalescence is presented.

Chapter 6 – Unifying discussion

The chapter brings together the important findings as well as a commentary on the research undertaken to identify the bubble bed collapse mechanism.

Chapter 7 – Conclusions, Contributions, and Future Work

Conclusions, contributions and suggestions for future work are presented.

1.4 References

Chen, F., Finch, J.A., Distin, P.A., Gomez, C.O., 2003. Air assisted solvent extraction. *Canadian Metallurgical Quarterly* 42, 277–280.

Cox, M., Rydberg, J., 2004. Introduction to solvent extraction. *Solvent Extraction and Practice*. Marcel Dekker, Inc., New York.

Gomez, C.O., Acuna, C., Finch, J.A., Pelton, R., 2001. Aerosol enhanced flotation deinking of recycled paper. *Pulp & Paper Canada* 102, 28–30.

Kentish, S.E., Stevens, G.W., 2001. Innovations in separations technology for the recycling and re-use of liquid waste streams. *Chemical Engineering Journal* 84, 149–159.

Maiolo, J., Pelton, R., 1998. Aerosol-enhanced flotation—a possible approach to improved flotation deinking. *Journal of Pulp and Paper Science* 24, 324–328.

Miller, G.M., Readett, D. J., 1992. The Mount Isa Mines Limited copper solvent extraction and electrowinning plant. *Minerals Engineering* 5 (10-12), 1335-1343.

Miller, G.M., Readett, D.J., Hutchinson, P., 1997. Experience in operating the Girilambone copper SX-EW plant in changing chemical environments. *Minerals Engineering* 10(5), 467-481.

Misra, M., Anazia, I., 1987. Ultrafine coal flotation by gas phase transport of atomized reagents. *Minerals and Metallurgical Processing* (November), 233–236.

Peng, F.F., Li, H.R., 1991. Oil-coated air bubble flotation to improve coal flotation rate and recovery. Society for Mining, Metallurgy and Exploration, Inc., Preprint Number 91-77, pp. 1–9.

Sole, K.C., Feather, A.M., Cole, P.M., 2005. Solvent extraction in South Africa: An update of some recent hydrometallurgical developments. *Hydrometallurgy* 78, 52 – 78.

Summers, A.J., Manqiu, X., Finch, J., 1995. Technical note: Effect of level in separation tank on downcomer behaviour in a Jameson Cell, *Minerals Engineering* 8 (12), 1607 – 1613.

Su, L., Xu, Z., Masliyah, J., 2006. Role of oily bubbles in enhancing bitumen flotation. *Minerals Engineering* 19, 641-650.

Taggart, A.F., 1927. *Handbook of Ore Dressing*. John Wiley & Sons, New York.

Tarkan, H. M., Finch, J.A., 2005. Air-assisted solvent extraction: towards a novel extraction process. *Minerals Engineering* 18, 83-88.

Tarkan, H.M., Kuan, S.H., Finch, J.A., 2012. Studies on Air-assisted solvent extraction. *Separation technologies for minerals, coal and earth resources*. Society for Mining, Metallurgy and Exploration, Inc. (SME), 317-324.

Wang, Z.N., Wang, H.F., Qiao, G.L., 1988. High selective coal flotation by gasfication of hydrocarbon collector, 13th International Conference on Coal & Slurry Technology, April 12–15, Denver, USA.

Young, M.F., Barnes, K.E., Anderson, G.S., Pease, J.D., 2006. Jameson Cell: The ‘comeback’ in base metal applications using improved design and flow sheets. *Proceedings, 38th Annual Meeting of the Canadian Mineral Processors*, January 17-19, 2006, Ottawa, Canada, 311-332.

Chapter 2 – Literature review

2.1 Solvent Extraction

2.1.1 General Principles

The term solvent extraction refers to the distribution of a solute between immiscible liquid phases in contact with each other (Rydberg et. al., 2004). One of the phases is generally aqueous-based and the other generally an organic-based or solvent. Solute A, which initially is dissolved in one of the two liquids, is eventually distributed between both phases. Reaching an equilibrium distribution, the solute is at concentration $[A]_{aq}$ in the aqueous layer and at concentration $[A]_{org}$ in the organic layer. The distribution ratio D is given by

$$D = \frac{[A]_{org}}{[A]_{aq}} \quad (2.1)$$

In principle, D can be written for more than one solute (solute A, B etc); D is known as the distribution coefficient or distribution factor. In industrial applications, the percentage extraction %E is more often used, given by

$$\%E = \frac{100D}{(1 + D)} \quad (2.2)$$

Solutes have differing solubilities in a liquid due to variations in the strength of the solute/solvent interaction. Hence, in a system of two immiscible (or only partially miscible) solvents, different solutes become unevenly distributed between the two phases, forming the basis of selectivity in the solvent extraction technique. Because all solutes (organic as well as inorganic) can be made more or less soluble in either the aqueous or

organic phases by appropriate chemical control, the number of potential applications of solvent extraction is almost limitless.

2.1.2 Extractants, Diluents and Modifiers

The solvent consists of extractant, diluent and modifier. For systems involving compound formation, extractants are divided into types: acidic and chelating. Among the acidic, organic derivatives of phosphoric acids (e.g. D2EHPA (Figure 2.1)) and carboxylic acids are the most important. The LIX (Figures 2.2), KELEX and ACORGA type extractants are considered chelating extractants. Other groups of extractants include ones involving ion association and others solvation. Extractants using ion association are limited to amines and quaternary ammonium compounds. Extractants using solvation are divided into two groups: organic reagents containing oxygen bonded to carbon (ethers, ketones) and oxygen or sulphur bonded to phosphorus (TBP, TOPO, CYANEX 471).

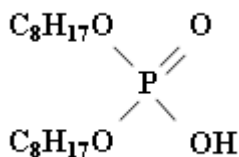


Fig. 2.1. Structure of D2EHPA.

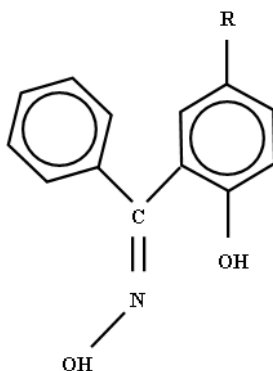


Fig. 2.2. Structure of LIX 65N.

Diluents are organic liquids in which the extractant and modifier are dissolved to form the solvent. Diluents are used to decrease the viscosity of extractant, provide a suitable concentration of extractant and improve dispersion properties of the solvent. Modifiers are used to assist phase disengagement, overcome formation of a third phase, influence mass transfer and reduce entrainment of the solvent.

2.1.3 Solvent Extraction Circuits

Figure 2.3 shows a typical solvent extraction flowsheet. The incoming aqueous solution, the feed, is contacted with the (recycled) solvent in the extraction phase. The depleted phase then becomes the raffinate and the enriched solvent phase becomes the extract (pregnant solvent). The raffinate undergoes a solvent recovery stage to remove entrained solvent before being discarded. Other solutes that are co-extracted with the main solute are removed with an aqueous scrub solution in a scrub stage producing a scrub extract and a scrub raffinate (containing impurities). The scrub raffinate is returned to the feed solution to maintain an overall water balance while the scrubbed extract is contacted with another aqueous solution to strip (back-extract) the desired component. The stripped solvent undergoes a regeneration process to prepare for recycle. The loaded (pregnant) strip solution is subsequently treated to remove the desired product and the strip solution is recycled.

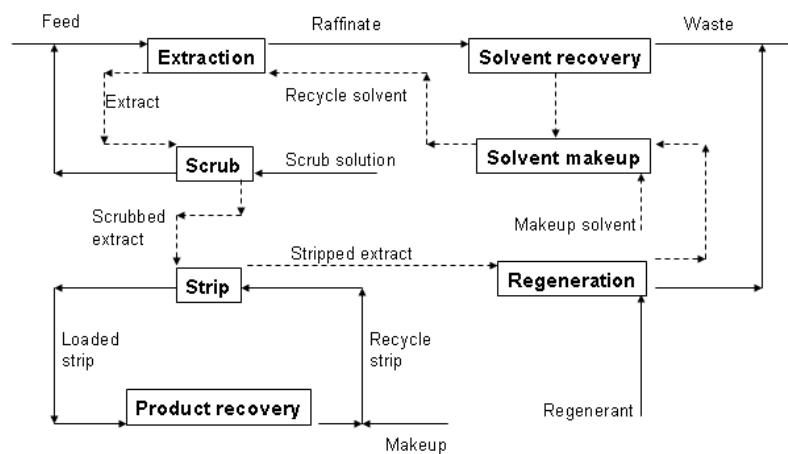


Fig. 2.3. A typical solvent extraction flowsheet (adapted from Rydberg et. al., 2004).

2.3 Solvent Extraction in the Treatment of Effluent Streams

Metal discharge limits for industrial effluents vary with jurisdiction. Though it is not possible to list general wastewater discharge limits, there is increasing regulatory pressure to reduce them. As regulations become tighter, new technologies must be developed. Traditionally, wastewater streams have been treated by a combination of physico-chemical processes such as flocculation, precipitation and filtration, and biological processes such as activated sludge and biofilm processes (Kentish and Stevens, 2001).

A comparison of some wastewater treatment methods is given in Table 2.1. As noted, solvent extraction is generally applied to concentrations > 500 mg/L making it unsuited to many wastewaters. Figure 2.4 shows the solute concentration range encountered for some separation technologies. The challenge in this thesis is to extend solvent extraction to the concentration ranges encountered in effluents such as acid mine drainage (AMD).

Table 2.1. Comparison of active water treatment methods (Reed, 1998).

Process	Chemical/Energy input	Metal reclamation	Major advantages	Major disadvantages
Chemical precipitation	Precipitant, flocculant, acid base; mixing and fluid handling	Metal sludge	Well established, low effluent concentrations	High chemical dosages, several unit operations
Electrolytic recovery	Electrical power	Solid metal scrap	Well-established; direct recovery of solid metal; no chemical consumption	Energy intensive; high capital costs; reduced efficiency at dilute concentrations
Ion-exchange	Regenerated solutions; fluid handling	Concentrated soluble metal stream	Highly selective, effectiveness < 100 mg/L	Chemical regeneration requirements, adsorbent expense; prone to fouling in mixed waste

				streams
Disposable adsorbents	Replacement adsorbent; fluid handling	Metal immobilizes on solid adsorbent	Simple metal remove process; low adsorbent cost; effective < 100 mg/L	Selectivity, recurring cost of new adsorbent, disposal cost of spent adsorbent
Membranes	Extractant for liquid-supported membrane; fluid handling	Concentrated soluble metal stream	Selective; continuous concentrated metal solution recycle	Membrane durability, fouling
Liquid-liquid solvent extraction	Organic solvent/water contact; loading and stripping in mixer and settlers or columns	Concentrated soluble metal stream	Selective; continuous concentrated metal solution recycle	Capital costs; solvent loss to air/water; solvent disposal

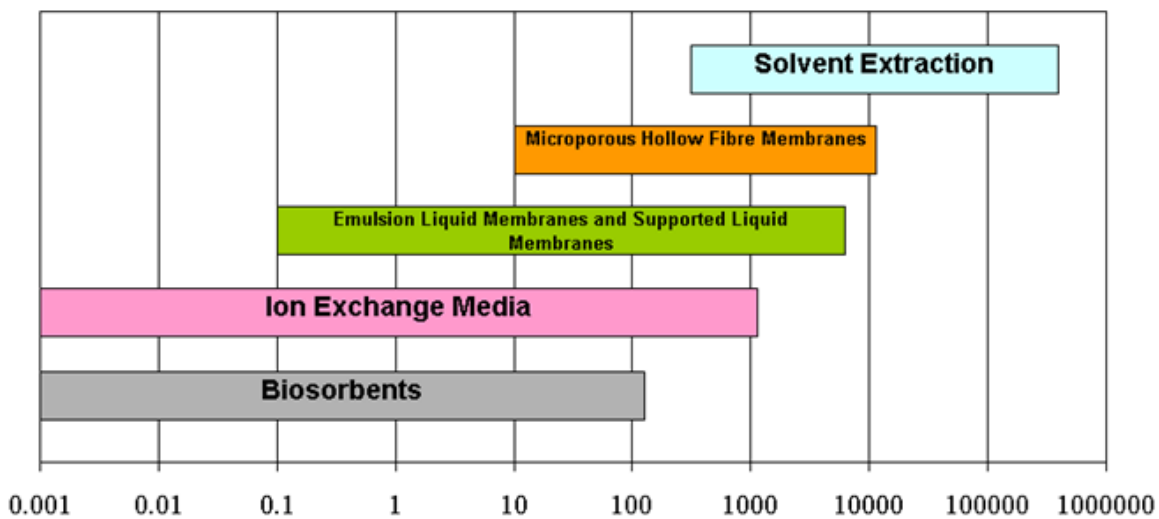
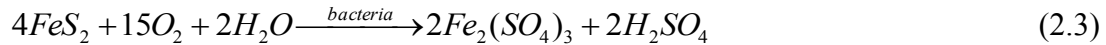


Fig. 2.4. Solute concentration ranges (in mg/L) for separation techniques (adapted from Kentish and Stevens, 2001).

2.3.1 Acid Mine Drainage (AMD)

Acid mine drainage (AMD) is an example of the large volumes of dilute metal-bearing effluents generated in the metal extraction and processing industries. AMD is generated when there is chemical reaction between water, oxygen and sulphur-bearing metallic minerals, particularly iron sulphides. The process is oxidation and could take place chemically or biologically. If the process is biological, *Thiobacillus ferrooxidans* is the most important bacterium, gaining energy for growth from the oxidation of reduced sulphur compounds and ferrous iron (Evangelou, 1995). The reactions for the mechanisms (direct and indirect) are (Younger et. al., 2002):

- Direct:



- Indirect:



Further oxidation is contributed by the ferric ions, making iron sulphides (particularly pyrite and pyrrhotite) important in acid generation. Other sulphide minerals also produce acid drainage but are less effective than the iron sulphides and may better be considered as leached by the acid. Composition of AMD depends on the source; Table 2.2 shows some examples.

Table 2.2. Composition of AMD for selected ore types (mg/L) (Ritcey, 1989).

	Ore type						
	Uranium	Gold	Iron	Copper	Cu-Pb-Zn	Cu-Ni	Cu-Mo
pH	2.3	7.6	6.4	3.8	2.0-7.9	7.5	7.7
Aluminium	10	0.6	-	-	-	-	-
Calcium	52	240	-	-	120	-	-
Cobalt	416	-	-	-	-	0.01	0.004
Copper	3.6	0.24	0.1	83	76	0.15	0.02
Iron	30-3 200	3.6	1.3	0.08-48	8.5-3 200	1.2	0.21
Lead	0.7	-	0.1	0.006	0.02-90	-	0.1
Uranium	67	-	-	-	-	-	-
Zinc	11	-	0.06	0.01-91	0.04-1.60	0.01	0.13

2.4 Solvent-Coated Bubbles

The need is to treat large volumes cheaply. If solvent could be carried as a thin layer on bubbles this could provide a high specific surface area with high aqueous to organic (a/o) ratio while maintaining rapid phase disengagement due to the buoyancy provided by the air core (Tarkan and Finch, 2005).

2.4.1 Previous Bubble Coating Work

Oil coated bubbles have been suggested as aids to flotation, a concept that can be traced to Taggart (1927) who suggested that an oil film spread on a bubble would enhance the collection of hydrophobic particles. Misra and Anazia (1987) pursued the idea for fine coal flotation and discovered that the induction time for bubble attachment was significantly reduced when the bubble was encapsulated in oil. Wang et al. (1988) and Peng and Li (1991) developed a method of converting hydrocarbon-oil collectors for coal

(e.g. kerosene) into gaseous state under controlled temperature and then introducing the gasified collector to air bubbles. The gaseous molecules condensed on the inner surface of the bubble which thus becomes collector-coated and enhances collection of coal particles. Maiolo and Pelton (1998) and Gomez et al. (2001) used an aerosol generator to produce a mist of silicone oil to coat bubbles and reported enhanced ink (i.e., carbon) removal rate from recycled paper pulp. Su et al. (2006) demonstrated that bitumen flotation recovery could be enhanced using oily bubbles (air bubbles coated with a thin layer of oil) instead of air bubbles alone.

2.4.2 Contact Angle and Induction Time

The coating process is governed by bubble-solvent interaction. This is akin to studying wettability. Several methods have been developed to determine wettability notably contact angle and induction time. Both these measures have been used in flotation studies to provide some guidance to the process. Contact angle has been the more widely used. However, contact angle is a thermodynamic (equilibrium) measure and has limitations describing dynamic conditions such as flotation (Laskowski and Iskra, 1970; Lekki and Laskowski, 1971; Ye et al., 1989; Yoon and Jordan, 1991; Peng, 1996). Induction time, on the other hand, can provide dynamic information and is considered a more reliable marker than contact angle for predicting flotation response (Su et al., 2006).

Relating to the coating process, induction time is a measure of the time required to form a stable, three-phase contact between a gas bubble and a solvent droplet brought into contact in an aqueous medium. The induction time is used to quantify the attachment process. As an example, Gu et al. (2004) found that the induction time of bubble-bitumen droplet attachment was greatly reduced by increasing solution temperature and decreasing bubble size.

2.4.3 Thermodynamics of Coating

The tendency to spread and the stability of the resulting organic film on a bubble is described thermodynamically by the spreading coefficient, S (Adamson, 1990). For the case of AASX, the equation can be written as (Chen et al. 2003):

$$S = \gamma_{A/W} - (\gamma_{O/W} + \gamma_{O/A}) \quad (2.6)$$

where γ is surface/interfacial tension and subscripts A, O and W refer to air, oil and water, respectively. If $S > 0$, coating (spreading of organic film on a bubble) occurs spontaneously. Using data from literature for kerosene systems (Table 2.3), S is found to be positive meaning that the formation of a stable solvent coating on a bubble is favoured (Chen et. al., 2003).

Table 2.3. Surface and interfacial tensions (in mJ/m²) to compute the spreading coefficient, S (Chen et al., 2003). Solvent was 3% DEHPA in kerosene.

Aqueous phase	$\gamma_{A/W}^*$	$\gamma_{O/W}$	$\gamma_{O/A}$	S
Water	72.36	20.38	25.22	26.76
0.1 M Cu ₂ SO ₄	72.30	18.88	25.22	28.20

2.4.4 Mechanism of Bubble-Oil Droplet Attachment

Rawlins and Ly (2012) reviewed four mechanisms for gas bubble capture of oil droplets suspended in water (Figure 2.5): (a) direct impingement with full or partial encapsulation by chemical adhesion; (b) hydrodynamic capture of oil droplets in the wake of a rising bubble; (c) clustering of bubbles to form a buoyant mat; and (d) bubble nucleation, coalescence, and growth on the surface of an oil droplet to result in full or partial

* $\gamma_{W/A}$, $\gamma_{O/A}$ and $\gamma_{W/O}$ are the surface tension of the aqueous phase and the oil phase and interfacial tension of the oil - aqueous interface, respectively.

encapsulation. Process (a) is often considered relevant for oil droplet flotation (a growing application for environmental applications), i.e., where the droplet size is comparable to the bubble size and full or partial encapsulation of the bubble by the oil droplet can occur (Strickland, 1980; Oliveira et al., 1999; Grattoni et al., 2003; Moosai and Dawe, 2003; Niewiadomski et al., 2007). The droplet is envisaged to collide with the bubble and the intervening water film then ruptures to allow the hydrocarbon liquid and gas to come in contact (Niewiadomski et al. 2007). Full encapsulation occurs when the oil completely covers the gas bubble surface; should the droplet size not be sufficient for full encapsulation, the oil droplet may form a lens on the downstream side (refer to Figure 2.5a). Sylvester and Byeseda (1980) proposed mechanism (b) where bubbles of 200-700 μm diameter were observed to capture much smaller oil droplets of 1- 15 μm diameter in the hydrodynamic wake of the rising bubble, instead of through adhesion to the surface. In this case the oil droplet has insufficient momentum to rupture the water layer at the bubble surface but is small enough to become trapped in the turbulent wake. The third mechanism (c) sees bubble and droplet clusters forming a buoyant ‘mat’ that rises (Rodrigues and Rubio, 2007). Fuerstenau et al. (2007) observed the formation of bubble clusters in mineral flotation in which the bubbles are held together by bridging particles. In oil flotation, the oil droplets can act as a bridging structure to form a cluster or mat of bubbles. The fourth mechanism (d) relates to dissolved gas flotation (DGF) where gas bubbles nucleate on particle/droplet surfaces, then grow to sufficient size to result in levitation (flotation) (Oliveira et al., 1999; Rodrigues and Rubio, 2007). The gas bubbles will continue to grow as long as the partial pressure is lower in the gas phase compared to the liquid phase and may coalesce with neighbouring bubbles (Rawlins and Ly, 2012). Depending on the volume of the bubble relative to the oil droplet (and the spreading coefficient), full or partial encapsulation may occur, similar to mechanism (a).

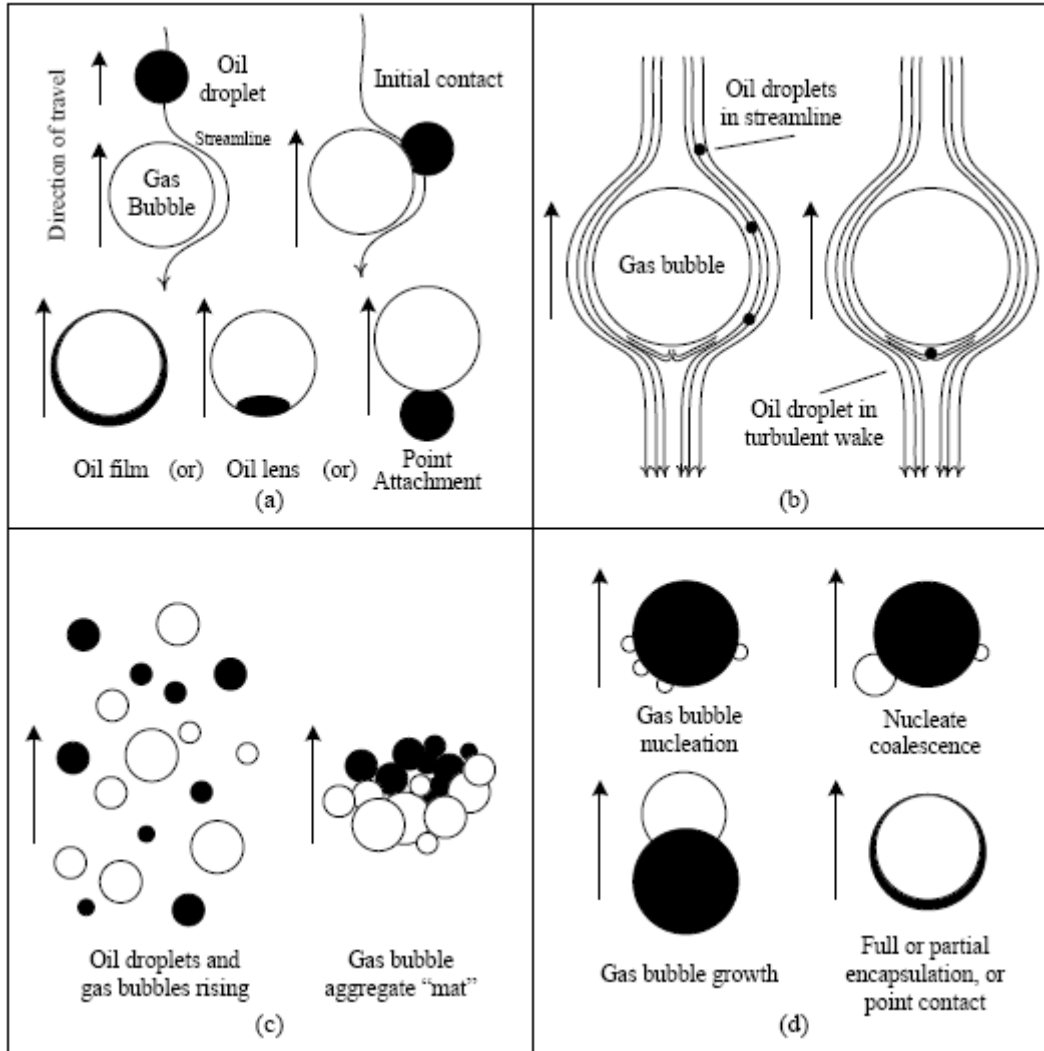


Fig. 2.5. Mechanisms for gas bubble capture of oil droplets suspended in water: (a) direct impingement with full or partial encapsulation by chemical adhesion, (b) hydrodynamic capture of oil droplets in the wake of a rising gas bubble (c) clustering of gas bubbles to form a buoyant mat, and (d) gas bubble nucleation, coalescence, and growth on the surface of an oil droplet to result in full or partial encapsulation. (Reprinted with permission from Rawlins and Ly (2012), Society for Mining, Metallurgy and Exploration, Inc. (SME)).

2.4.5 Air-Assisted Solvent Extraction (AASX)

Chen et al. (2003) first described the use of solvent-coated bubbles in solvent extraction. Termed air-assisted solvent extraction (AASX), the method involved spreading of a kerosene-based solvent over a bubble by carefully passing air through a thin plug of solvent replenished from a reservoir. Spreading was shown to be thermodynamically favoured.

Tarkan and Finch (2005) further developed AASX, generating a stream of solvent-coated bubbles from solvent foam which was forced through an orifice. Coating thickness was estimated at ca. $3 \mu\text{m}$ on a 0.44 cm diameter bubble giving a solvent specific surface area of ca. $3000 \text{ cm}^2/\text{cm}^3$, equivalent to a solvent droplet of ca. $20 \mu\text{m}$. Their setup is shown in Figure 2.6. The foam was generated in chamber A (illustrated at lower right) and injected through a capillary (internal diameter, 2.5 mm) to release coated bubbles at orifice B (top right). Fresh solvent input (C) was regulated by an autoburette. The air readily disengaged at the surface of the solution to leave a layer of solvent (D). They demonstrated good phase separation with a/o volume ratio approaching 150. Compared with conventional solvent extraction, it appeared that AASX had the potential to significantly reduce the amount of solvent needed thus opening the way for treatment of dilute streams, such as AMD.

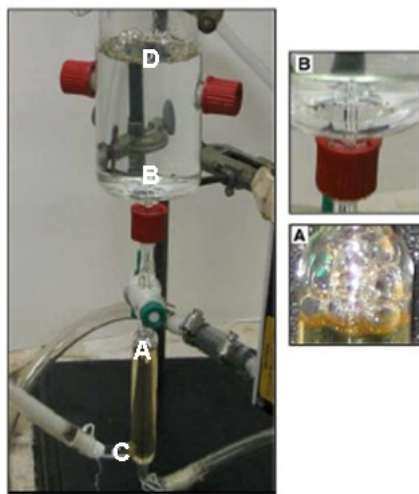


Fig. 2.6. Experimental setup of AASX to produce a stream of solvent-coated bubbles (Reprinted with permission from Tarkan and Finch (2005), Elsevier).

Using the same setup to inject solvent droplets (ca. 3.5 mm diameter), Tarkan and Finch (2005) demonstrated the efficiency of the coated bubble (AASX). For the same 25% extraction, approximately 70 ml of solvent as droplets was required compared to about 1 ml in the AASX case (Figure 2.7). This means that the resulting Cu content in the organic phase in the AASX experiment is significantly increased, revealing the concentration enrichment capability of AASX. To illustrate the efficiency of phase separation, Tarkan and Finch (2005) showed that using a 75:1 a/o ratio, a conventional shake test took some 24 hours for the phases to disengage, while in AASX disengagement was essentially instantaneous (governed by residence time of bubble.)

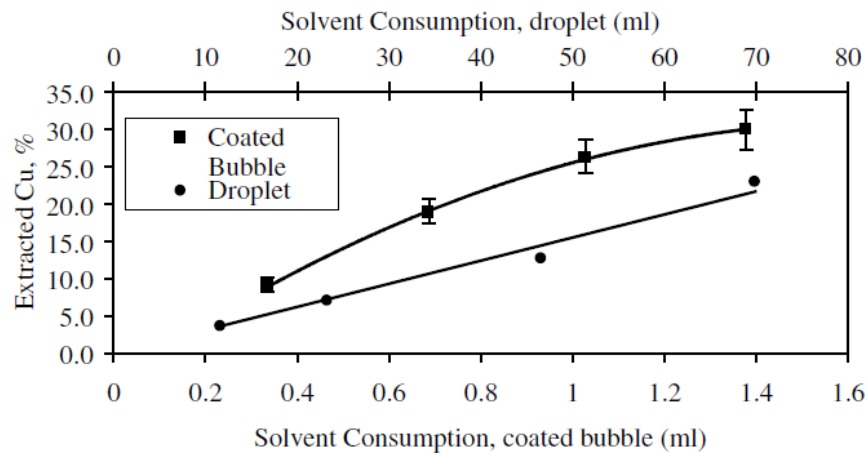


Fig. 2.7. Comparison of extraction as function of solvent volume using solvent droplet and solvent coated bubble (Reprinted with permission from Tarkan and Finch (2005), Elsevier).

2.4.6 Aerosol Technique for Solvent Extraction

Tarkan and Finch (2006) did attempt to scale-up a multi-orifice foam injection setup. However, it did not appear to be practical. Tarkan et al. (2012) then returned to the aerosol coating technique of Maiolo and Pelton (1998) combined with the Venturi bubble generator employed by Gomez et al. (2001). Figure 2.8 shows a general view of that experimental setup.

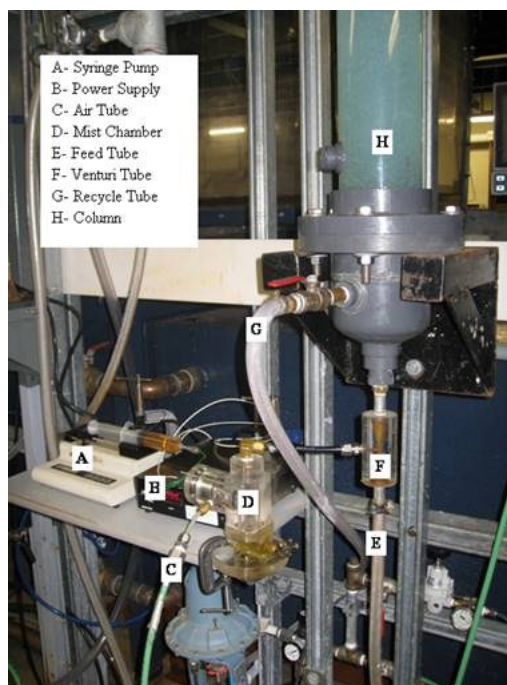


Fig. 2.8. Aerosol technique for solvent coating in AASX (Reprinted with permission from Tarkan et al. (2012), Society for Mining, Metallurgy and Exploration, Inc. (SME)).

In the chamber D, an atomizer nozzle produces a mist of solvent, with air coming from C. The mist was carried by the air through the tubing to the Venturi (F), where the aqueous feed and solvent aerosol/air made contact and coated bubbles were produced. This bubble-liquid phase then discharges to the column (H) where the extraction occurs by the solvent-coated bubbles. The bubbles disengaged (burst) on the surface to leave a metal loaded solvent layer (the solvent was less dense than water). The technique showed excellent extraction results as a function of solvent consumption (Figure 2.9). The initial concentration (3.5 mg/L) reduced to ca. 1.5 mg/L (ca. 60% recovery to solvent) with ca. 50 mL solvent representing an a/o ratio ca. 450/1. However, the delivery rate of aerosol by the ultrasonic generator was only ca. 80 mL/h and thus the extraction time was long (> 1 hour). In this regard the ultrasonic aerosol generator approach did not meet the ‘scale up to large volumes’ criterion. This prompted a look at using the Venturi as the coating ‘reactor’.

Various configurations of Venturi tube were attempted including drawing both air and solvent through the same suction port (Tarkan et al., 2012). None have been successful so

far, with visible evidence of tramp solvent droplets in suspended in solution. It was inferred that the contact time to coat bubbles was not adequate in the Venturi throat, bubble/droplet contact experiments suggesting at least 1s (i.e. induction time) was required (Chen et al., 2003). This in turn suggested that a downcomer might provide the conditions for coating, i.e., be the ‘coating reactor’.

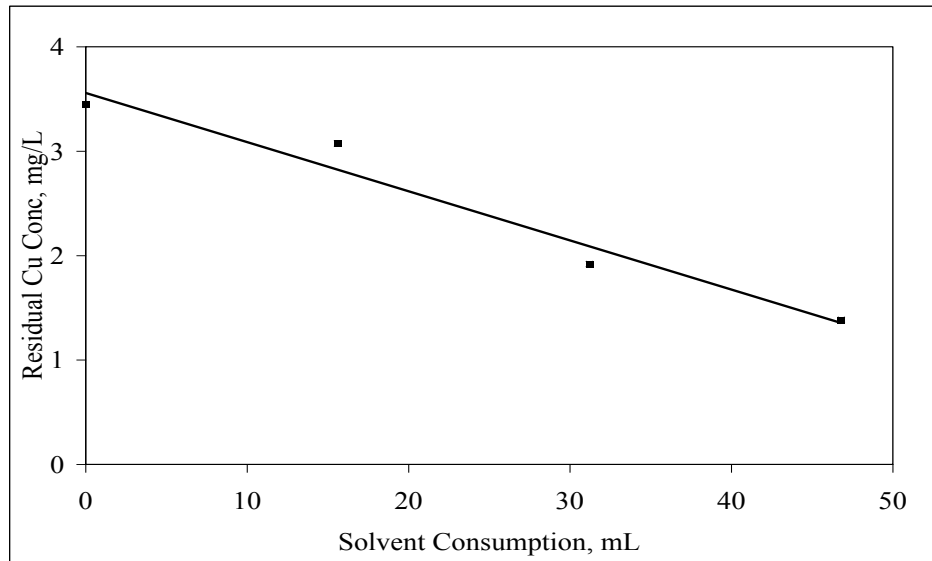


Fig. 2.9. Example extraction experiment (Reprinted with permission from Tarkan et al. (2012), Society for Mining, Metallurgy and Exploration, Inc. (SME)).

2.5 The Downcomer

The use of this device is perhaps best typified in the Jameson Cell. Conceived by Professor Jameson of the University of Newcastle, Australia, the technology was commercialized by Mount Isa Limited (now Xstrata). The attractive feature in the present context is the downcomer provides for close bubble-solvent contact for a few seconds which may be ideal for the coating process. The eventual set up had many of the features of a Jameson Cell. Taking its application in flotation as a starting point, the Cell can be divided into three main zones as in Figure 2.10:

1. The downcomer where primary contacting with bubbles occurs. Feed is pumped into the downcomer through an orifice plate, resulting in a high-pressure jet. The liquid jet entrains air creating a low pressure that simultaneously supports liquid in the downcomer and aspirates air. The aspirated air is sheared into bubbles as the jet plunges into the liquid. Forcing air bubbles down against their buoyancy creates high gas holdup (i.e., high volumetric fraction of gas phase or high bubble concentration). The region of high gas holdup in the downcomer is referred to here as the 'bubble bed'.
2. The separation tank where secondary contacting of bubbles and particles occurs and also where bubbles disengage.
3. The froth zone where entrained materials are removed through froth drainage and/or froth washing.

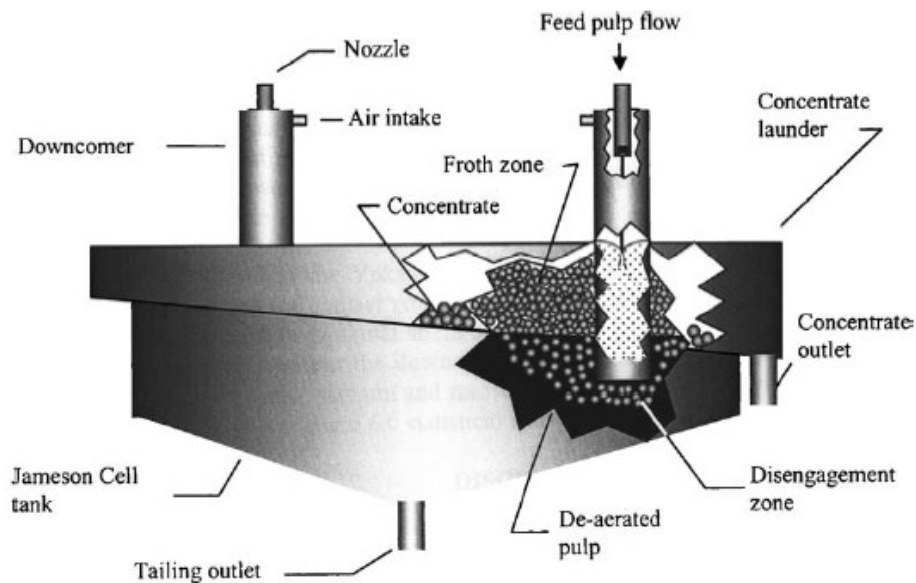


Fig. 2.10. Jameson cell operation (Reprinted with permission from Harbort et al. (2003), Elsevier).

Compared to conventional flotation, the crowded bubbles in the downcomer provide intense bubble-particle contact resulting in a high flotation rate and thus high productivity per unit of floor area. Since its invention in 1986, over 200 Jameson Cells have been installed in a variety of applications including coal and base metal flotation, and of some

relevance to the intended use here, the removal of oil (petroleum) droplets from refinery effluents and the removal of organics from raffinate and electrolyte streams in solvent extraction/electrowinning (SX/EW) circuits (Miller et al., 1997; Young, et al., 2006).

2.6 Surfactant and salt action on bubble size reduction

The Jameson Cell requires agents (e.g. surfactants and/or salts) to produce the small bubbles necessary for the downcomer to operate within the high gas holdup range (> 45% according to Summers et al., 1995). For discussion purposes these agents will be referred to as ‘coalescence inhibitors’.

Frothers (non-ionic surfactants) are typically used to modulate the size, number and thus bubble surface area flux in flotation. Some salts are likewise able to modulate bubble size, sometimes obviating the need for frother (Quinn et al., 2007). The mechanism of bubble size control appears to have two aspects: bubble coalescence and bubble break-up.

2.6.1 Coalescence prevention

Coalescence is the process whereby two or more bubbles come together to generate a new, larger bubble. It occurs in three steps: collision, film thinning, and film rupture (Oolman and Blanch, 1986; Prince and Blanch, 1990; Machon et al., 1997; Tse et al., 1998). In the collision step, bubbles come in contact. Once contact is established, the facing bubble surfaces flatten, leaving an intervening thin film. Initial film thickness is typically 10^{-3} to 10^{-4} cm and for rupture the film must thin to at least 10^{-6} cm and the contact time has to be longer than the time required for the thin film to rupture. For surfactants[†] and salts to act as coalescence inhibitors most emphasis is placed on the thinning step, that it is slowed, the hydrodynamics of the liquid film being controlled by forces associated with surface tension gradients and/or surface visco-elastic effects.

[†] Surfactants discussed are non-ionic surfactants e.g. frothers.

One characteristic of surfactants is their ability to impart elasticity to liquid films, related to the increase in surface (interfacial) tension during stretching. The elasticity is called Gibbs elasticity if the mechanism of increasing tension involves redistribution of components in the film as in the case of surfactants. Gibbs elasticity is a measure of the ability of a liquid film to adjust its surface tension under the action of an external force. If the liquid is stretched, the local surface concentration of surfactant decreases and consequently, the local surface tension increases creating a restoring force that protects the film against rupture (Adamson, 1990). The surface tension gradients are counterbalanced by a shearing stress that generates liquid counter flow along the surface into the film, known as the Marangoni effect, which further protects the film from rupture. Figure 2.11 shows the process: (a) initially at rest with a uniform distribution of surfactant; (b) film stretching causes depletion of surface concentration of surfactant; and consequently creating an opposing surface tension gradient-generated force (depicted by the arrows).

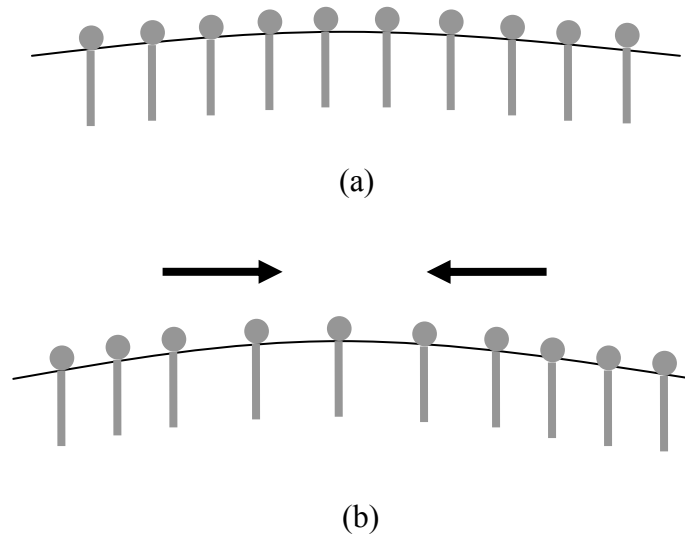


Fig. 2.11. a) Before stretching, surfactant molecules distributed uniformly at interface b) After stretching, local surface tension increases as a consequence of lower surface concentration of surfactant (surfactant decreases surface tension) which induces surface tension gradient and force directed towards the depleted area (the arrows)

The magnitude of surface tension gradients generated during film stretching depends on factors such as deformation rate and the rate of diffusion and adsorption of surfactant from the adjacent liquid (Lucassen and Van Den Tempel, 1972). When the deformation rate is high, the system has no time to respond and the effect is purely elastic. For slower deformation rates, where surface tension gradients are reduced compared to the pure elastic case, visco-elastic properties appear (Lucassen and Van Den Tempel, 1972). At extremely slow deformation rates, the surface maintains equilibrium and the surface tension gradient approaches zero (Monroy et al., 1998).

The situation with salts is less clear and no definitive mechanism has been proposed so far. Salts do alter the surface tension, usually increasing it, thus surface tension gradient effects could be at play. Weissenborn and Pugh (1996) observed that surface tension/electrolyte concentration gradients generated at their transition concentration[‡] (i.e., at and above where bubble coalescence is inhibited) are significantly smaller ($d(\Delta\gamma)/dc$ range of 1.83 to 4.06) than those generated in presence of surfactants ($d(\Delta\gamma)/dc$ of a 'typical' surfactant exceeds -200). This suggested that the surface tension gradients produced in electrolyte solutions are too weak to cause any significant Gibbs-Marangoni effects but does not rule it out entirely.

Lessard and Zieminski (1971) reviewed previous work by Foulk (1929), Schnurman (1929), Foulk and Miller (1931), Marrucci and Nicodemo (1967), and Zieminski and Whittemore (1971) and concluded that the mechanism by which inorganic ions hinder coalescence of bubbles in water is unresolved. They attributed the mechanism to a charge-viscosity combination effect, though favouring viscosity over charge to explain the temperature dependence observed.

The inference made from a charge-viscosity dependence of coalescence inhibition is that the role of salts may possibly revolve around their effect on the water molecules near the surface of bubbles. This effect may be through the hydration associated with inorganic

[‡] The salts involved were MgSO₄, MgCl₂, CaCl₂, Na₂SO₄, LiCl, NaCl, NaBr and KCl and the transition concentrations ranged from 0.032 M to 0.23 M.

ions. The end result is that the properties of the water layer differ from the bulk and influence drainage rate. Surfactant also influences the water molecules at the bubble surface through hydrogen bonding via the hydrophilic groups (e.g. OH) and, again as with surface tension gradients, there may be some similarity in the action with salts.

Craig et al. (1993) described simple combining rules that predict bubble coalescence behavior of electrolytes based on assigned properties of the ions. The ions were empirically assigned a type, α or β , and the combination of ions present in the electrolyte determined if the solution would inhibit coalescence. Thus for NaCl, the Na^+ is assigned an α cation and the Cl^- , an α anion, the combination ($\alpha \alpha$) would lead to coalescence inhibition. Craig (2004) further stressed the importance of the combination of the two ions of an electrolyte rather than the absolute behavior of a single ion in predicting their bubble coalescence inhibition effect.

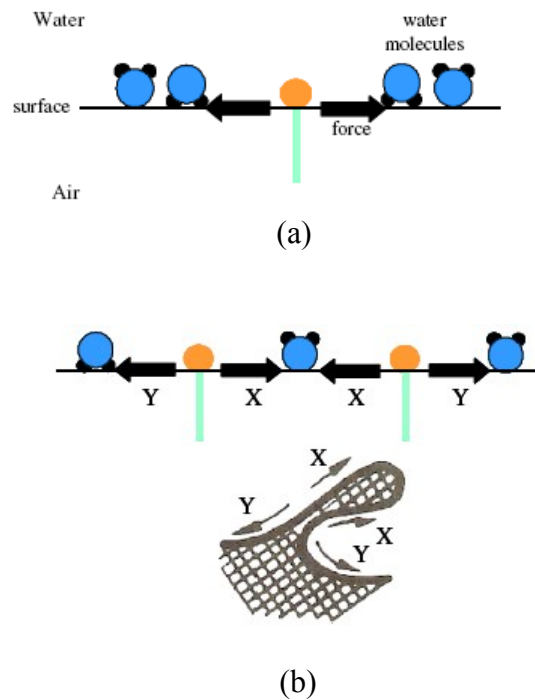
Regardless of the mechanism coalescence prevention has been argued as the origin of bubble size reduction leading to the hypothesis that small bubbles are generated by the machine and preserved by the addition of coalescence inhibitors (Cho and Laskowski, 2002). This notion is exemplified in the term ‘critical coalescence concentration’ (CCC), which, initially applied to frothers, is the concentration producing the minimum bubble size (Cho and Laskowski, 2002; Grau and Laskowski, 2006). Coalescence inhibition may not be the full answer, however.

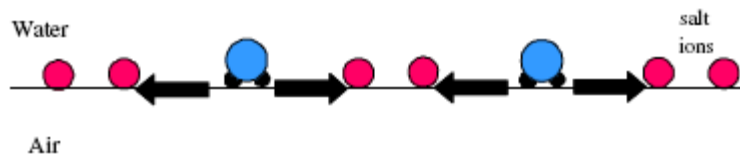
2.6.2 Break-up

Finch et al. (2008) presented a case for and against a ‘coalescence prevention’ mechanism. The case against was made based on three arguments: a) the frequency of coalescence events for small bubbles to combine to become large bubbles was hard to envisage (the example described was a total of sixty four 1 mm bubbles has to coalesce to form a 4 mm bubble); b) extrapolating bubble size (Sauter mean diameter, D_{32}) to zero gas velocity resulted in a notional creation size (D_0) that was a function of frother dosage implying that frother is involved in creating the starting size, not just preserving it (Nesset

at al., 2007); and c) the fact that many frothers are not strong anti-coalescence agents on their own as evidenced by being poor at building froth (in the absence of particles). If not coalescence prevention, then frothers (and salts) must induce bubble (or at least ‘air mass’) break-up.

The break-up mechanism proposed by Finch et al. (2008) has its origin in the dynamic nature of the surface forces caused by uneven concentration of surfactant over the bubble surface coupled with the deformations due to energy dissipation associated with the injection of air. It was speculated that the force resulting from the surface tension gradients could grow the surface deformations to result in break-away of a bubble. The mechanism allows for the effect of increasing frother concentration (frother molecules in the surface are closer together accommodating smaller deformations, resulting in a smaller break-away bubble) and the action of salts whereby the water molecules provide the low surface tension site and force is generated away from the water molecules (i.e. the water molecule has taken the role of the frother in the former case), as shown in Figure 2.12.





(c)

Fig. 2.12. a) Break-up mechanism in surfactant system: force is away from the frother molecule producing a local stress at the interface; b) Opposing forces from nearby frother molecules grow the deformation resulting in break-away of the lobe to form a bubble (lower diagram based on Miller and Neogi, 1985) (the forces X and Y are translated from the upper diagram); c) Break-up mechanism in salt system: force is away from the water molecule, generating a local stress at the interface (i.e., forces X and Y in (b)) (Reprinted with permission from Finch et al. (2008), Elsevier).

2.7 References

Adamson, A.W., 1990. *Physical Chemistry of Surfaces*. 5th edition. Wiley-Interscience Publication, New York.

Chen, F., Finch, J.A., Distin, P.A., Gomez, C.O., 2003. Air assisted solvent extraction. *Canadian Metallurgical Quarterly* 42, 277–280.

Cho, Y.S., Laskowski, J., S., 2002. Effect of flotation frothers on bubble size and foam stability. *International Journal of Mineral processing* 64. 69-80.

Craig, V.S.J., Ninham, B.W., Pashley, R.M., 1993. Effect of electrolytes on bubble coalescence. *Nature*, 364: 317-9.

Craig, V.S.J., Ninham, B.W., Pashley, R.M., 1993. The effect of electrolytes on bubble coalescence in water. *The Journal of Physical Chemistry*, 97: 10192-7.

Craig, V.S.J., 2004. Bubble coalescence and specific-ion effects, *Current Opinion in Colloid and Interface Science* 9, 178-184.

Davies, J., Rideal, E., 1963. *Interfacial Phenomena*, Chapter 8, Academic Press, New York.

Evangelou, V.P., 1995. *Pyrite oxidation and its control*, CRC Press, Boca Raton, Florida.

Finch, J.A., Nasset, J.E., Acuna, C., 2008. Role of frother on bubble production and behaviour in flotation. *Minerals Engineering* 21, 949-957.

Foulk, C., 1929. A theory of liquid film formation, *Industrial and Engineering Chemistry* 21, 815.

Foulk, C.W., Miller, J.N., 1931. Experimental evidence in support of the balanced-layer theory of liquid film formation, *Industrial and Engineering Chemistry* 23, 1283-8.

Fuerstenau, M.C., Jameson, G., Yoon, R.H., 2007. Froth flotation – A century of innovation. Society for Mining, Metallurgy, and Exploration, Inc., Littleton, CO, 357-358.

Gomez, C.O., Acuna, C., Finch, J.A., Pelton, R., 2001. Aerosol enhanced flotation deinking of recycled paper. *Pulp & Paper Canada* 102, 28–30.

Grattoni, C., Moosai, R., Dawe, R.A., 2003. Photographic observations showing spreading and non-spreading of oil on gas bubbles of relevance to gas flotation for oily wastewater cleanup. *Colloids and Surfaces A: Physicochemical and Engineering Aspects* 214: 151- 155.

Grau, R.A., Laskowski, J.S., 2006. Role of frothers in bubble generation and coalescence in a mechanical flotation cell. *The Canadian Journal of Chemical Engineering* 84. 170-182.

Gu, G., Sean Sanders, R., Nandakumar, K., Xu, Z., Masliyah, J., 2004. A novel experiment to study single bubble-bitumen attachment in flotation. *International Journal of Mineral Processing* 74 (1-4), 15-29.

Harbort, G., De Bono, S., Carr, D., Lawson, V., 2003. Jameson Cell fundamentals – a revised perspective. *Minerals Engineering* 16, 1091-1101.

Kentish, S.E., Stevens, G.W., 2001. Innovations in separations technology for the recycling and re-use of liquid waste streams. *Chemical Engineering Journal* 84, 149–159.

Kracht, W., 2008. Effect of frother on bubble coalescence, break-up and initial rise velocity. PhD thesis, McGill University, Montreal, Canada.

Laskowski, J., Iskra, J., 1970. Role of capillary effects in bubble-particle collision in flotation. *Transactions of the Institution of Mining and Metallurgy* 79, C6-C10.

Lekki, J., Laskowski, J., 1971. On the dynamic effect of frother-collector joint action in flotation. *Transactions of the Institution of Mining and Metallurgy* 80, 174-180.

Lessard, R. L., Zieminski, S.A., 1971. Bubble coalescence and gas transfer in aqueous electrolytic solutions, *ind. Eng. Chem. Fundam.* 10 (2), 260-269.

Liu, J., Mak, T., Zhou, Z., Xu, Z., 2002. Fundamental study of reactive oily-bubble flotation. *Minerals Engineering* 15, 667–676.

Lucassen, J., Van Den Tempel, M., 1972. Dynamic measurements of dilational properties of a liquid interface. *Chemical Engineering Science* 27. 1283 – 1291.

Machon, V., Pacek, A.W., Nienow, A.W., 1997. Bubble sizes in electrolyte and alcohol solutions in a turbulent stirred vessel. *Transactions of Institution of Chemical Engineers* 75(A), 339-348.

Maiolo, J., Pelton, R., 1998. Aerosol-enhanced flotation—a possible approach to improved flotation deinking. *Journal of Pulp and Paper Science* 24, 324–328.

Marrucci, G., Nicodemo, L., 1967. Coalescence of gas bubbles in aqueous solutions of inorganic electrolytes, *Chemical Engineering Science* 22, 1257-1265.

Miller, C.A., Neogi, P. 1985. Interfacial phenomena: equilibrium and dynamic effects. In: *Surfactant Science*, vol. 17, Chapter VI: Transport Effects on Interfacial Phenomena, 240-298.

Miller, G.M., Readett, D. J., 1992. The Mount Isa Mines Limited copper solvent extraction and electrowinning plant. *Minerals Engineering* 5 (10-12), 1335-1343.

Miller, G.M., Readett, D.J., Hutchinson, P., 1997. Experience in operating the Girilambone copper SX-EW plant in changing chemical environments. *Minerals Engineering* 10(5), 467-481.

Misra, M., Anazia, I., 1987. Ultrafine coal flotation by gas phase transport of atomized reagents. *Minerals and Metallurgical Processing* (November), 233–236.

Moosai, R., Dawe, R., 2003. Gas attachment of oil droplets for gas flotation for oily wastewater cleanup, *Separation and Purification Technology* 33, 303-314.

Monroy, F., Giermanska, Kahn, J., Langevin, D., 1998. Dilational viscoelasticity of surfactant monolayers. *Colloids and Surfaces A: Physicochemical and Engineering Aspects* 143, 251-260.

Nesset, J.E., Finch, J.A., Gomez, C.O., 2007. Operating variables affecting the bubble size in forced-air mechanical flotation machines. *AusIMM, Proceedings of the 9th Mill Operators Conference*, 55-65.

Niewiadomski, M., Nguyen, A.V., Hupka, J., Nalaskowski, J., and Miller, J.D., 2007. Air bubble and oil droplet interactions in centrifugal fields during air-sparged hydrocyclone flotation. *International Journal of Environment and Pollution* 30.2: 313-331.

Oliveira, R.C.G., Gonzalez, G., Oliveira, J.F., 1999. Interfacial studies on dissolved gas flotation of oil droplets for water purification, *Colloids and Surfaces A: Physicochemical and Engineering Aspects* 154, 127-135.

Oolman, T.O., Blanch, H.W., 1986. Bubble coalescence in stagnant liquids. *Chemical Engineering Communications* 43. 237-261.

Peng, F., 1996. Surface energy and induction time of fine coals treated with various levels of dispersed collectors and their correlation to flotation responses. *Energy Fuels* 10, 1202-1207.

Peng, F.F., Li, H.R., 1991. Oil-coated air bubble flotation to improve coal flotation rate and recovery. *Soc. Mining, Metal., Exploration, Inc., Preprint Number 91-77*, pp. 1-9.

Prince, M.J., Blanch, H.W., 1990. Bubble coalescence and break-up in air-sparged bubble columns. *American Institute of Chemical Engineers Journal* 36 (10) 1485-1499.

Quinn, J.J., Finch, J.A., 2007. Comparing the effect of salts and frother (MIBC) on gas dispersion and froth properties. *Minerals Engineering* 20, 1296 – 1302.

Rawlins, C.H., Ly, C., 2012. Mechanisms for flotation of fine oil droplets. *Separation Technologies for Minerals, Coal, and Earth Resources. Society for Mining, Metallurgy and Exploration, Inc. (SME), Colorado*, pp. 307-315.

Reed, B.E., 1998. Waste water treatment: Heavy metals. *Environmental Analysis and Remediation* 8, 5220-5225.

Ritcey, G.M., Ashbrook, A.W., 1978. *Solvent Extraction: Principles and Application to Process Metallurgy*. Elsevier Scientific, Amsterdam, New York.

Ritcey, G.M., 1989. *Tailings management: Problems and solutions in the mining industry*. Elsevier, Amsterdam.

Rodrigues, R.T., Rubio, J., 2007. DAF – Dissolved air flotation: potencial applications in the mining and mineral processing industry, *International Journal of Mineral Processing* 82, 1-13.

Rydberg, J., Cox, M., Musikas, C., Choppin, G.R., 2004. *Solvent extraction principles and practice*. Marcel Dekker, New York, Basel.

Schnurmann, R., 1929. The size of gas bubbles in liquid, *Z. Phys. Chem.* 143(5-6), 456.

Strickland, W.T., 1979. Laboratory results of cleaning produced water by gas flotation. SPE Paper 7805, SPE 1979 Production Operators Symposium, February 25-27, Oklahoma City, Oklahoma, Unites States.

Su, L., Xu, Z., Masliyah, J., 2006. Role of oily bubbles in enhancing bitumen flotation. *Minerals Engineering* 19, 641-650.

Summers, A.J., Manqiu, X., Finch, J., 1995. Technical note: Effect of level in separation tank on downcomer behaviour in a Jameson Cell, *Minerals Engineering* 8 (12), 1607 – 1613.

Sylvester, N.D., Byeseda, J.J., 1979. Oil/water separation by induced-air flotation. *International Symposium on Oilfield and Geothermal Chemistry*, January 22-24, Houston, TX.

Taggart, A.F., 1927. *Handbook of Ore Dressing*. John Wiley & Sons, New York.

Tarkan, H. M., Finch, J.A., 2005. Air-assisted solvent extraction: towards a novel extraction process. *Minerals Engineering* 18, 83-88.

Tarkan, H.M., Finch, J.A., 2006. Multi-bubble production in the air-assisted solvent extraction process. In: XXIII. *International Mineral Processing Congress*, September 3-8, Istanbul, Turkey, 1340-1345.

Tarkan, H.M., Kuan, S.H., Finch, J.A., 2012. Studies on Air-assisted solvent extraction. Separation technologies for minerals, coal and earth resources. Society for Mining, Metallurgy and Exploration, Inc. (SME), 317-324.

Tse, K.L., Martin, T., McFarlane, C.M., Niewnow, A.W., 1998. Visualisation of bubble coalescence in a coalescence cell, a stirred tank and a bubble column. Chemical Engineering Science 53 (23), 4031-4036.

Wang, Z.N., Wang, H.F., Qiao, G.L., 1988. High selective coal flotation by gasfication of hydrocarbon collector, 13th International Conference on Coal & Slurry Technology, April 12–15, Denver, USA.

Weissenborn, P.K., Pugh, R.J., 1996. Surface tension of aqueous solutions of electrolytes: relationship with ion hydration, oxygen solubility, and bubble coalescence. Journal of Colloid and Interface Science 184: 550-563.

Ye, Y., Khandrika, S., Miller, J., 1989. Induction-time measurements at a particle bed. International Journal of Mineral Processing 25, 221-240.

Yoon, R., Yordan, J., 1991. Induction time measurements for the quartz-amine flotation system. Journal of Colloid and Interface Science 141 (2), 374-382.

Young, M.F., Barnes, K.E., Anderson, G.S., Pease, J.D., 2006. Jameson Cell: The ‘comeback’ in base metal applications using improved design and flow sheets. Proceedings, 38th Annual Meeting of the Canadian Mineral Processors, January 17-19, 2006, Ottawa, Canada, 311-332.

Zieminski, S. A., Whittemore, R.C., 1971. Behavior of gas bubbles in aqueous electrolyte solutions, Chemical Engineering Science. 26, 509-520.

Chapter 3 - Collapsing bubble bed in the downcomer with the introduction of solvent

3.1 Introduction

An established process, solvent extraction is generally restricted to concentrated solutions (> 500 mg/L) and requires an aqueous to solvent (a/o) ratio of ca. 1 (Kentish and Stevens, 2001). When applied to dilute solutions, solvent losses, high capital costs, phase disengagement difficulties and large solvent inventory count among some of the disadvantages of SX. The interest was to extend SX to dilute streams, such as acid mine drainage which led to the concept of using solvent-coated bubbles (Chen et al., 2003).

Organic-coated bubbles have been studied to promote the flotation of hydrophobic particles such as coal. Various methods have been used to produce coated bubbles over the years (Misra and Anazia, 1987; Wang et. al., 1988; Peng and Li, 1991; Maiolo and Pelton, 1998; Gomez et. al., 2001; Liu et. al., 2002; Chen et. al., 2003; Tarkan and Finch, 2005; Li et. al., 2008). Chen et. al. (2003) first described the use of solvent-coated bubbles in solvent extraction. Termed air-assisted solvent extraction (AASX), the method involved spreading of a kerosene-based solvent over a bubble by carefully passing air through a thin plug of solvent replenished from a reservoir. Spreading was shown to be thermodynamically favored. Tarkan and Finch (2005) gave further proof of concept by exploiting the foaming properties of kerosene-based solvents to inject foam through an orifice to produce solvent-coated bubbles. Metal recovery and ease of phase separation were demonstrated but scale up using multiple orifices did not appear feasible (Tarkan and Finch, 2006).

Tarkan et al. (2012) returned to the aerosol coating technique of Maiolo and Pelton (1998) combined with the Venturi bubble generator employed by Gomez et al. (2001). The technique however was limited by the delivery rate of aerosol using the ultrasonic generator (which was only ca. 80mL/h) and thus the extraction time was long (about 2

hours in the example quoted). In this regard the ultrasonic aerosol generator approach did not meet the ‘scale up’ criterion. As alternative coating methods, various configurations of Venturi tube were attempted including drawing both air and solvent through the same suction port (Tarkan et al., 2012). None have been successful so far, with visible evidence of tramp solvent droplets in the aqueous phase. It was inferred that the contact time to coat bubbles was not sufficient in the Venturi throat, bubble/droplet contact experiments suggesting at least 1s (i.e. induction time) was required (Chen et al., 2003).

This led to the present work whereby a downcomer, familiar from the Jameson Cell, was tested as a ‘coating reactor’. In a downcomer, the feed stream is introduced vertically downwards through an orifice to mix with and shear air into bubbles. Since the bubbles tend to rise against the down-flowing liquid this creates a high gas holdup (over 45% as measured by Summers et al., 1995) inside the downcomer. This high gas holdup region will be referred to as the ‘bubble bed’. This bubble bed was anticipated as ideal for solvent to contact and coat bubbles, the typical retention time in the downcomer of a few seconds exceeding the estimated 1s induction time needed for solvent to coat bubbles. In addition, the high gas holdup in the downcomer suggested fast extraction by the solvent coated bubbles. Some encouragement for this use of a downcomer is the fact that Jameson Cells are employed to recover solvent droplets from electrolyte in SX plants suggesting ready attachment of bubbles and solvent (Miller and Readett, 1992; Miller et al., 1997; Young et al., 2006).

3.2 Experimental

3.2.1 General setup

The test rig is shown in Figure 1. The downcomer dimensions are 2.54 cm in diameter and 122 cm in length. The test solution was prepared and put in the feed tank (N in Figure 3.1). The feed pump (I) delivers the solution from the feed tank to the top of the downcomer. The solution goes through the orifice into the downcomer and a jet is produced. The jet hits the pool of water in the downcomer tube (J) to form and entrain

bubbles. Three techniques of solvent injection into the downcomer were explored: into the bubble bed, into the feed solution, and as aerosol into the air inlet. The bubbles exit the downcomer into the separation tank (K) where they rise and burst on top. The loaded solvent overflows with some solution into the launder and accumulates on top as a thin film. The depleted solution (raffinate) in the separation tank flows back to the feed tank through the underflow hose (M). The depleted solution in the launder flows via the overflow hose (L) into the feed tank. The process is semi-batch (batch in aqueous but continuous in air and solvent injection).

Vacuum pressure was measured online using a pressure transmitter (U in Figure 3.3) connected to a laptop (A in Figure 3.1). Gas holdup in the separation tank was measured online with a differential pressure transmitter (F in Figure 3.1), also connected to the laptop. The McGill Bubble Size Analyzer (Figure 3.1 (D) and Figure 3.2) was used to capture bubble images (Nesset et al., 2006). The device was placed on top of the separation tank. Bubble images were analyzed using available software. Feed flow rate was measured with a flow meter (E and G in Figure 3.1). An air valve (S in Figure 3.3) was installed to control air rate into the downcomer. The air rate was monitored using the vacuum pressure transmitter initially and using a manual air flowmeter in later experiments. Air is self-aspirated, therefore no exterior air supply is required.

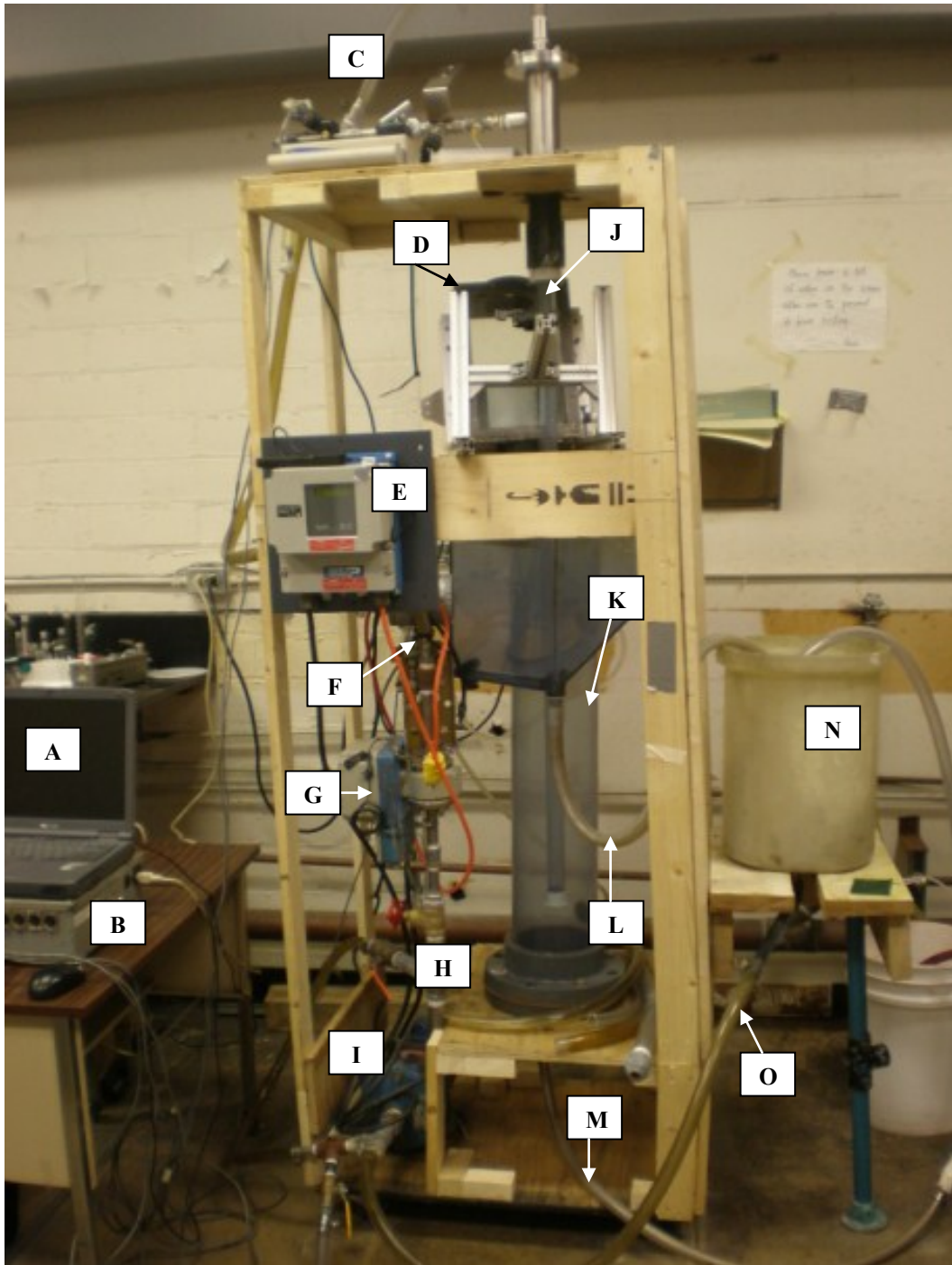


Fig. 3.1. General setup: A – Laptop, B – Electrical box, C – Feed to downcomer, D – Bubble size analyzer, E – Flow meter reader, F – Gas holdup differential pressure transmitter, G – Flow meter sensor, H – Feed pipe, I – Feed pump, J – Downcomer pipe, K – Separation tank, L – Overflow hose, M – Underflow hose, N – Feed tank, O – Feed hose to pump

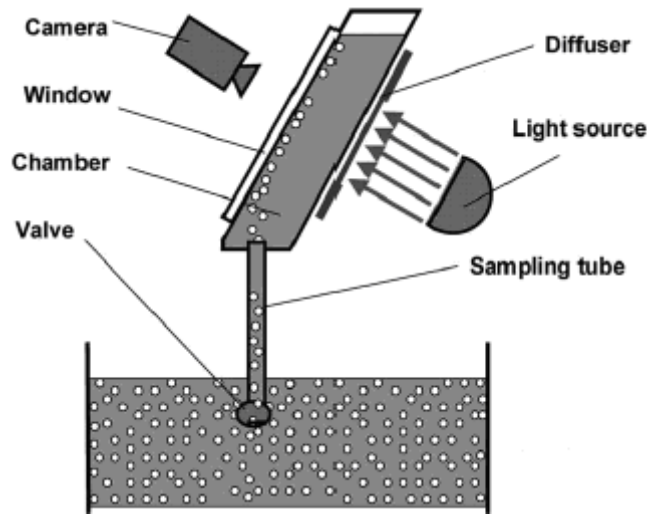


Fig. 3.2. McGill Bubble Size Analyzer. (Reprinted with permission from Nasset et al., (2006), Elsevier).

3.2.2 Solvent injection

Three techniques of solvent injection into the downcomer were devised, namely: Method 1 - into the bubble bed in the downcomer (Figures 3.3 and 3.4), Method 2 - into the feed solution (Figure 3.5), and Method 3 - as aerosol into the air inlet (Figure 3.6). In Method 1, solvent was injected via a syringe pump (Q in Figure 3.3) with the syringe (T) connected to a small tube (ID = 2.5 mm) that went into the downcomer (Figure 3.4). The tube end was positioned to introduce solvent directly into the bubble bed. The solvent flow rate was controlled by the syringe pump.

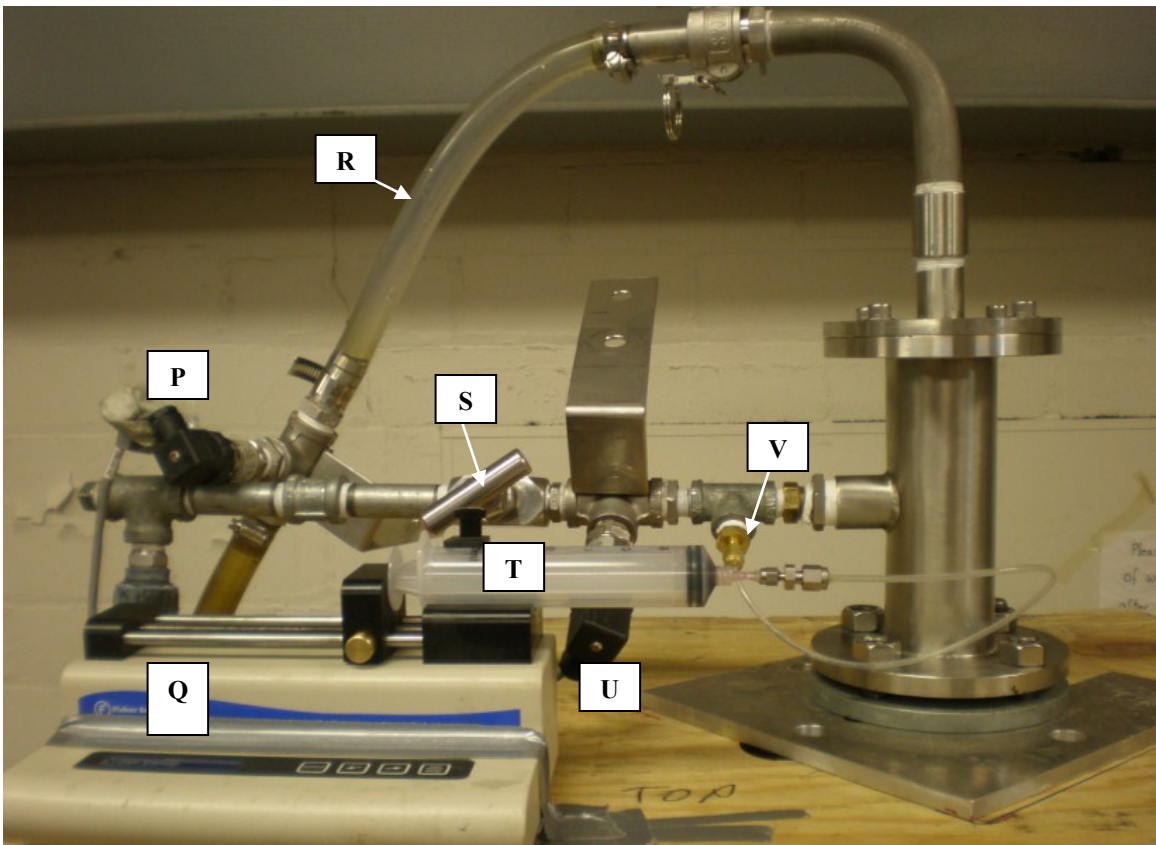


Fig. 3.3. Method 1: Experimental setup for solvent injection: P – Feed pressure transmitter, Q – Syringe pump, R – Feed to downcomer, S – Valve, T – Syringe, U – Vacuum pressure transmitter, V – Solvent inlet into downcomer

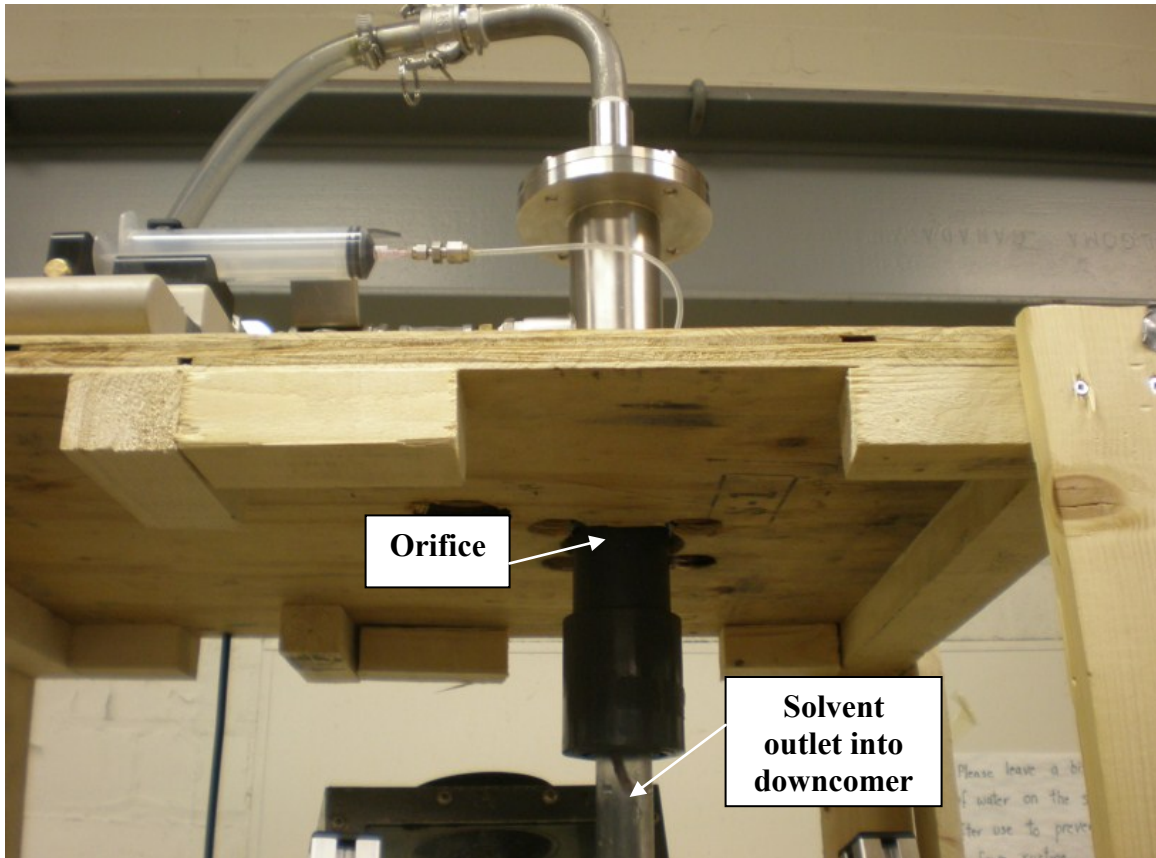


Fig. 3.4. Method 1: Point of solvent discharge

Figure 3.5 shows solvent injection method 2. This involves solvent injection into the feed solution via a syringe and a syringe pump (D and E in Figure 3.5).

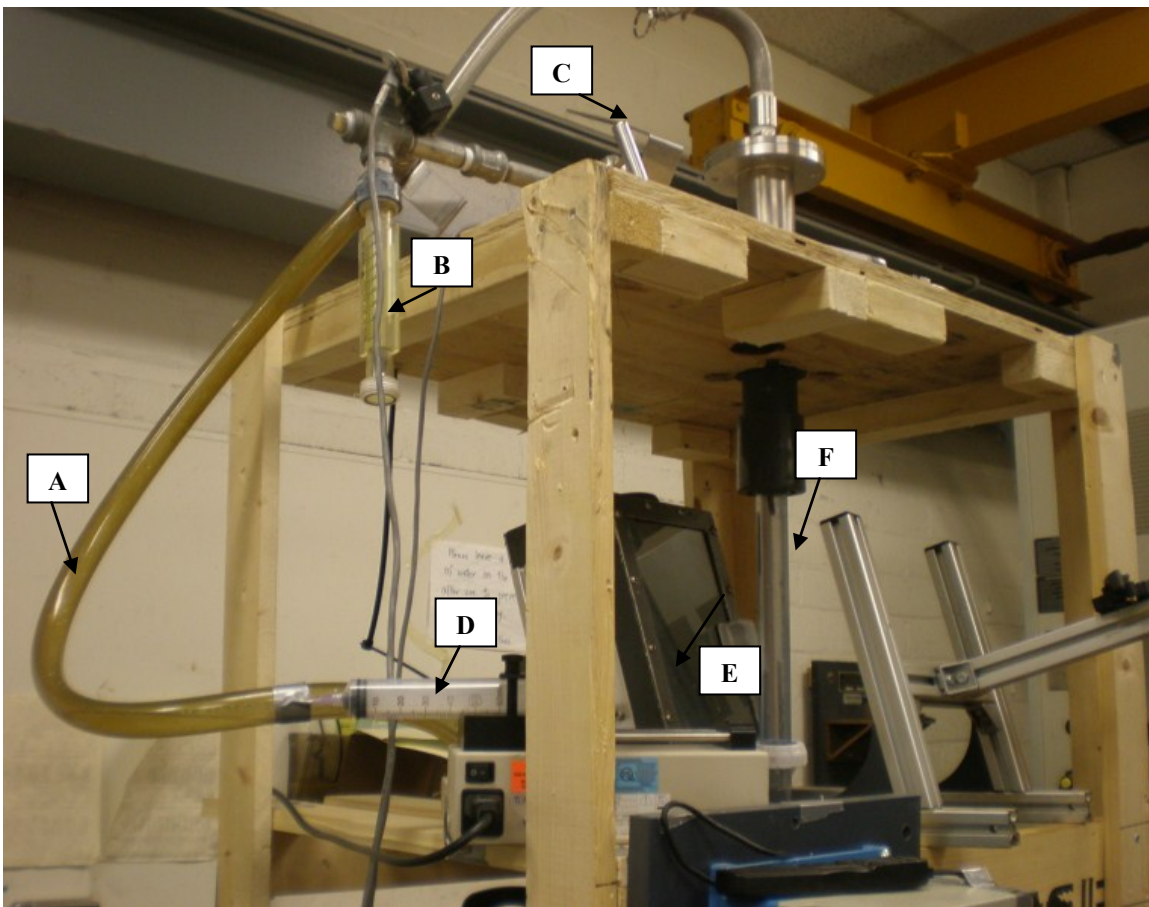


Fig. 3.5. Method 2: Experimental setup for introduction of solvent into solution: A – Feed to downcomer, B – Air flowmeter, C – Air valve, D – Syringe , E – Syringe pump, F – Downcomer pipe.

Figure 3.6 shows solvent injection Method 3, which involves introducing the solvent as an aerosol into the air inlet of the downcomer. The syringe pump (A) injects solvent into the ultrasonic nozzle (E) via syringe (B). The nozzle is controlled by a broadband generator (D) to produce solvent aerosol or mist. Air is drawn in through the air suction hose (J) and enters the mist chamber (F) at the air inlet (G) and carries the solvent mist into the downcomer (H). A steel clamp (I) was used to control the amount of air entering the mist chamber. The aerosol-bearing air then mixes with the plunging jet inside the downcomer to form bubbles. The broadband generator was manufactured by Sono-Tek as was the ultrasonic nozzle, Model 8700-48. The arrangement (Figure 3.6) required a

certain suction (negative pressure) to carry the aerosol droplets generated by the nozzle into the downcomer. As such, to keep the negative pressure, aspirated air flow rate in this method is controlled at a lower rate than in Methods 1 and 2.

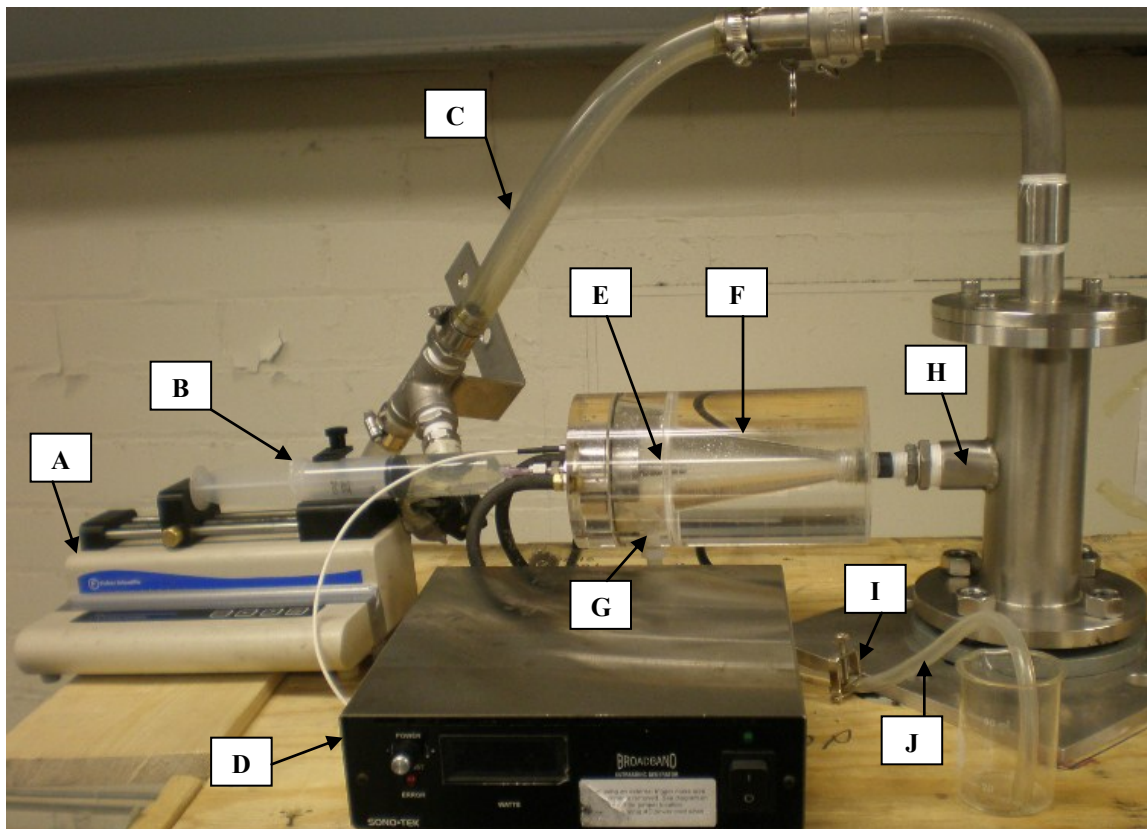


Fig. 3.6. Method 3: Experimental setup for introduction of solvent as aerosol into the air inlet: A – Syringe pump, B – Syringe, C – Feed hose, D – Broadband ultrasonic generator, E – Ultrasonic nozzle, F – Mist chamber, G – Air inlet into mist chamber, H – Air inlet into Jameson cell, I – Steel clamp for air control, J – Air suction hose.

3.2.3 Materials and methods

Reagent grade $\text{CuSO}_4 \cdot 5\text{H}_2\text{O}$ (American Chemicals Limited) was used to prepare 6 ppm Cu test solution. Two frothers (MIBC and PPG 425) and one salt (NaCl) were chosen to help create small bubbles and correspondingly high gas holdup in the downcomer. The frothers represent the two major classes, alcohol (MIBC) and polyglycol (PPG 425). The NaCl not only produces small bubbles but simulates the ionic strength frequently found in metal-bearing effluents such as AMD. Some properties of the frothers and salt are given in Table 3.1.

Table 3.1. The frothers/salt used.

Frother/Salt	Type	Formula	Mol. Wt. g/gmol	Supplier
MIBC	Methyl isobutyl carbinol	$\text{C}_6\text{H}_{13}\text{OH}$	102	Sigma Aldrich
PPG 425	Polypropylene glycol	$\text{H}(\text{OC}_3\text{H}_6)_7\text{OH}$	425	Flottec
NaCl	Table salt	NaCl	58.4	Fisher Scientific

The solvent was the chelating type extractant LIX 973N (supplied by BASF) diluted in reagent grade kerosene (supplied by Sigma Aldrich). The chemical composition of the extractant is given in Table 3.2. The density of the extractant is 0.95 g/cm^3 . The density of the diluent is 0.8 g/cm^3 with a flash point of $82 \text{ }^\circ\text{C}$.

Table 3.2. Chemical composition of the extractant (MSDS of LIX 973N)

Extractant	X (%)	Y (%)	Pet. Distill. (%)	Alcohols (%)	Nonylphenol (%)
LIX 973N	< 46	< 18	> 30	-	< 6

X: Benzaldehyde, 2-hydroxy-5-Nonyl Oxime; Y: 5-T-Nonyl-2-Hydroxyacetophenone, Oxime.

Samples of the solution were collected from the feed tank and analyzed for copper content and turbidity (as indication of tramp solvent droplet (emulsion) formation). Turbidity was measured by turbidimetry (HF Scientific, inc. Micro 1000 IR Turbidimeter) and Cu assay by Atomic Absorption (AA) spectrometry (Varian AA240 FS).

3.2.4 Estimating solvent rate

The solution feed rate to the downcomer was set at 16.5 LPM, the maximum for the orifice diameter of 5mm to promote high gas holdup in the downcomer. The solvent rate was estimated based on the amount of solvent needed to coat the surface of the bubbles produced. The calculation is based on the bubble surface area flux (S_b), derived by Finch and Dobby (1990) as six times the gas superficial velocity (J_g) divided by the Sauter mean bubble diameter (D_{32}):

$$S_b = 6 \frac{J_g}{D_{32}} \quad (3.1)$$

The gas superficial velocity (J_g) is the volumetric air flow rate (Q_g) divided by the cross-sectional area of the downcomer ($A_{downcomer}$):

$$J_g = \frac{Q_g}{A_{downcomer}} \quad (3.2)$$

Then the solvent rate needed to coat the bubbles produced is given by:

$$Solvent\ rate = S_b \times A_{Downcomer} \times film\ thickness \quad (3.3)$$

Taking the water case, substituting the volumetric flowrate of aspirated air, $Q_g = 0.5$ LPM = $8.3 \text{ cm}^3/\text{s}$, and $A_{downcomer} = 5.1 \text{ cm}^2$ into Equation 3.2, $J_g = 1.64 \text{ cm/s}$ and substituting J_g and $D_{32} = 3.9 \text{ mm}$ (in water alone) into Equation 3.1, $S_b = 25.3 \text{ s}^{-1}$. Substituting S_b , $A_{Downcomer}$ and film thickness of ca. $3 \mu\text{m}$ (Tarkan et al., 2006) in Equation 3.3, the solvent rate is calculated to 0.04 mL/s .

The other important factor is the amount of solvent needed to extract the copper from solution. This calculation was based on a copper loading of 2.7 g/L Cu (LIX:Kerosene 1:9) provided by the supplier. The calculation is as follows. The feed solution was 30L containing 6 ppm of Cu^{2+} for a total of 0.18 g Cu. Dividing the amount of copper in the feed by the copper loading produced a solvent requirement of 66.7 mL. Setting target extraction at 50% to start, therefore 33.3mL of solvent was needed. This produces an aqueous/organic ratio of 30L / 33.33mL or 900. Using a density of 0.815 g/cm^3 for the solvent, the concentration is 27164 mg / 30L or ca. 900 ppm. At the solvent rate of 0.04 mL/s this gives an experimental time of ca. 12 min.

When frothers and salt were used, the bubble size decreased and the amount of air entrained increased, i.e. the bubble surface area flux increased. Figure 3.7 shows the amount of solvent needed to coat the surface of the bubbles produced in the case of water alone ($D_{32} = 3.9 \text{ mm}$), as calculated above and with frothers or salt (D_{32} ranging from 0.58 to 0.99 mm) for a solvent coating thickness of $3 \mu\text{m}$.

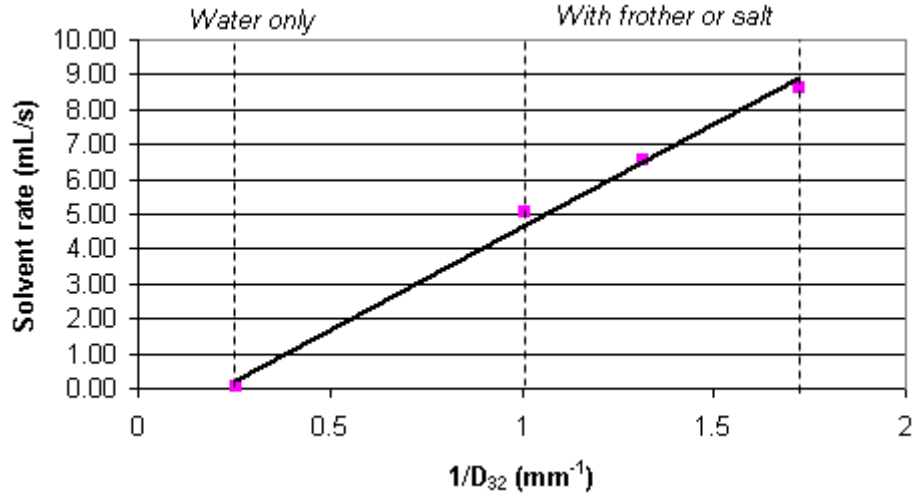


Fig. 3.7. Solvent rate versus $1/D_{32}$ simulating conditions from water to frother or salt solutions

Figure 3.7 shows that higher solvent rates in the presence of frother or salt are possible compared to water alone but this would reduce the experiment time to a few seconds. This short time frame was judged unrealistic for the various measurements to be performed (gas holdup, bubble size, turbidity and copper assay). For this reason, the more conservative solvent rate of 0.04 mL/s calculated for water was retained.

3.3 Results

3.3.1 Extraction and turbidity

Attempts to run without coalescence inhibitors[§] to simplify the process gave unstable downcomer operation and no bubble bed. Thus all subsequent data is in presence of frother or salt.

Initial tests were conducted at a LIX:kerosene ratio of 1:29. The extraction (Figure 3.8) appears divided into two groups: 50 ppm MIBC, 90 ppm MIBC and 0.8 M NaCl having

[§] The term “coalescence inhibitors” is used for simplicity and does not assume coalescence prevention is the sole mechanism for bubble size reduction. As elaborated in Section 2.6, there are two possible mechanisms for bubble size control of surfactants and salts: coalescence prevention and break-up.

higher kinetics (higher slopes), and 0.4 M NaCl, 10 ppm PPG 425 and 30 ppm PPG 425 having lower kinetics. Final extraction levels usually exceeded the targeted 50% Cu (the exception being with PPG 425).

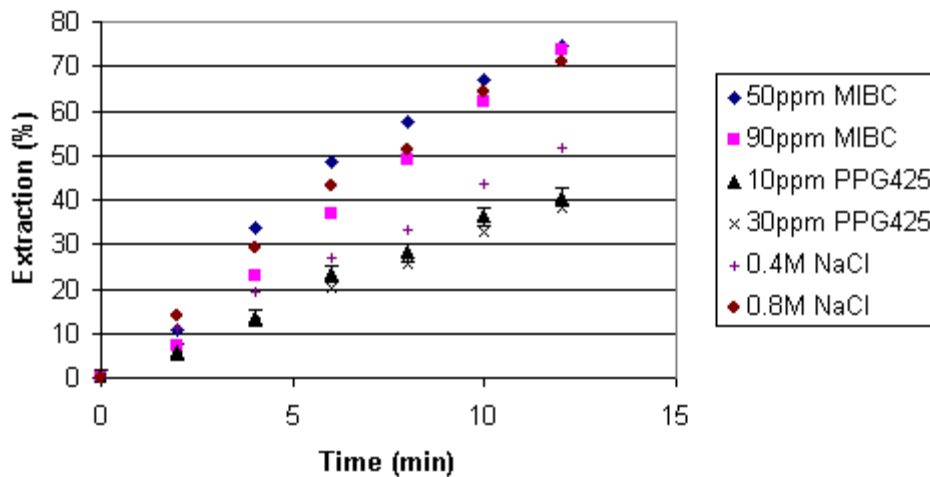


Fig. 3.8. Extraction as a function of solvent addition in presence of MIBC, PPG 425 and NaCl. The error bars here and throughout the thesis correspond to the 95% confidence interval (see Appendix C).

The turbidity (Figure 3.9) increased with solvent addition at a rate dependent on the system, slowest for 0.8 M NaCl and highest for 30 ppm PPG 425. The turbidity data suggest that tramp droplet (emulsion) formation is occurring. Results from Figures 3.8 and 3.9 imply that high ionic strength (0.8 M NaCl) can replace the function of frother in driving up extraction while lowering solution turbidity.

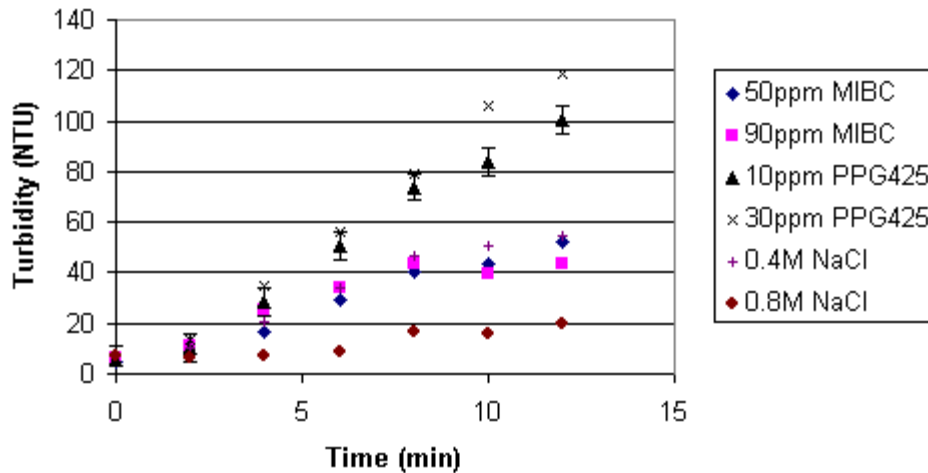


Fig. 3.9. Turbidity as a function of solvent addition in presence of MIBC, PPG 425 and NaCl.

3.3.2 Collapsing bubble bed

3.3.2.1 LIX:Kerosene 1:29

3.3.2.1.1 Gas holdup and air rate

Before solvent introduction, gas holdup readings were stable for all systems. Once solvent was introduced, however as Figure 3.10 shows, gas holdup decreased continuously with solvent additions up to 33.3 mL. This was accompanied by visual observation of the bubble bed ‘collapsing’: the bed level dropped, the jet lengthened, and air slugs were seen in the downcomer towards the end of the experiment. The gas holdup re-stabilises once solvent injection is stopped (at 33.33 mL of solvent or after 12 minutes), as seen in Figure 3.11.

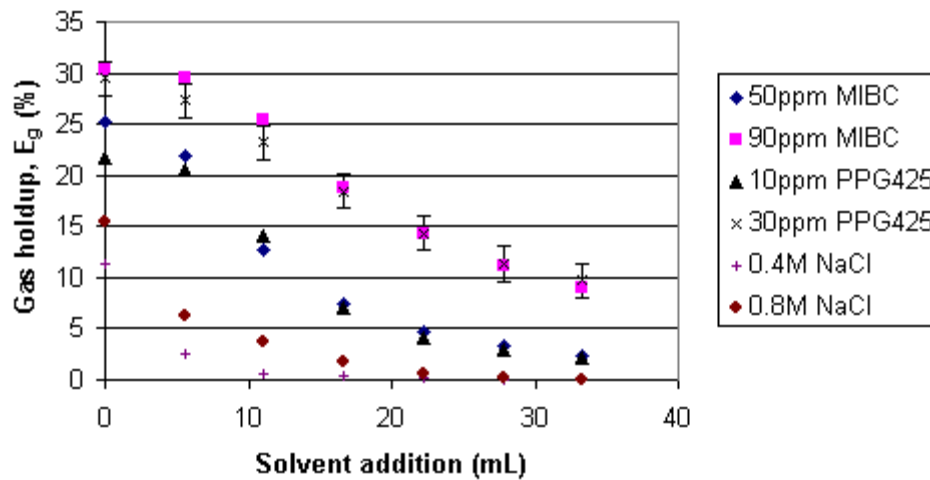


Fig. 3.10. Gas holdup in separation tank as a function of solvent addition in presence of MIBC, PPG 425 and NaCl.

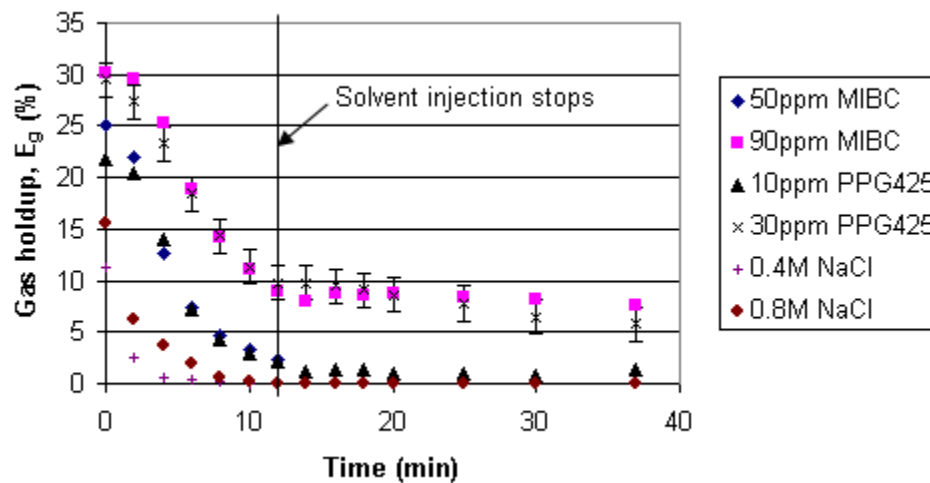


Fig. 3.11. Gas holdup in separation tank as a function of time in presence of MIBC, PPG 425 and NaCl illustrating stabilisation of gas holdup when solvent injection is stopped at 12 minutes.

The aspirated air superficial velocity (shown in Figure 3.12 as ‘air rate’) into the downcomer showed a similar pattern to the gas holdup, decreasing with progressive solvent addition.

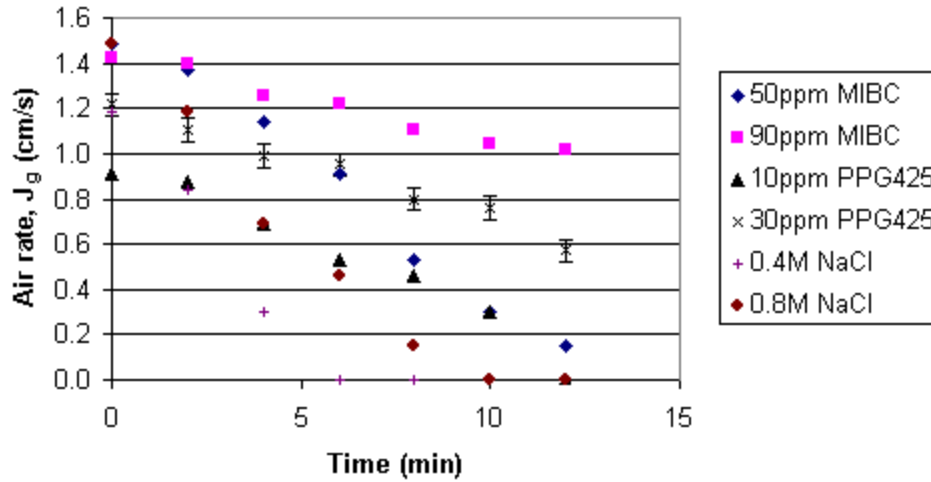
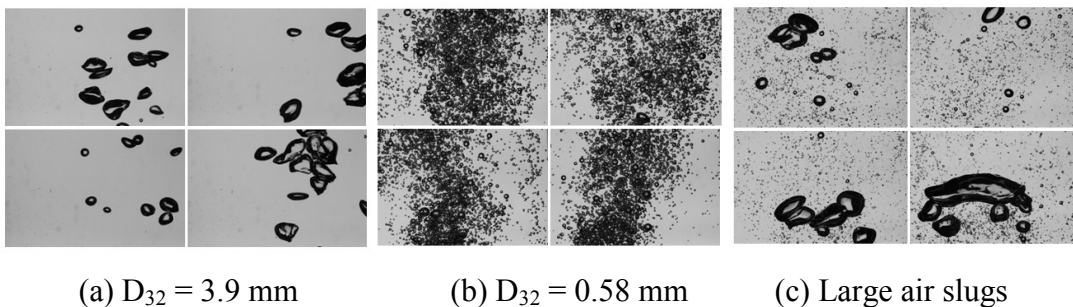


Fig. 3.12. Air rate as a function of solvent addition in presence of MIBC, PPG 425 and NaCl. Note that gas rate was calculated based on the cross sectional area of the separation tank.

3.3.2.1.2 Bubble size

Bubble size gives another indication of bubble bed collapse. From Figures 3.13 to 3.15, in water alone (a), bubbles produced in the downcomer were few and large ($D_{32} = 3.9$ mm); when frother or NaCl was added (b), bubble size reduced and bubble counts increased, as expected and commonly attributed to coalescence inhibition; and upon subsequent addition of solvent (LIX:kerosene 1:29) (c), in concert with the collapsing bed, large air slugs formed regardless of the coalescence inhibitor used.



(a) $D_{32} = 3.9$ mm

(b) $D_{32} = 0.58$ mm

(c) Large air slugs

Fig. 3.13. (a) Bubbles in water. (b) Bubbles with addition of 50 ppm MIBC. (c) Bubbles after 33.33 mL solvent injection in presence of 50 ppm MIBC.

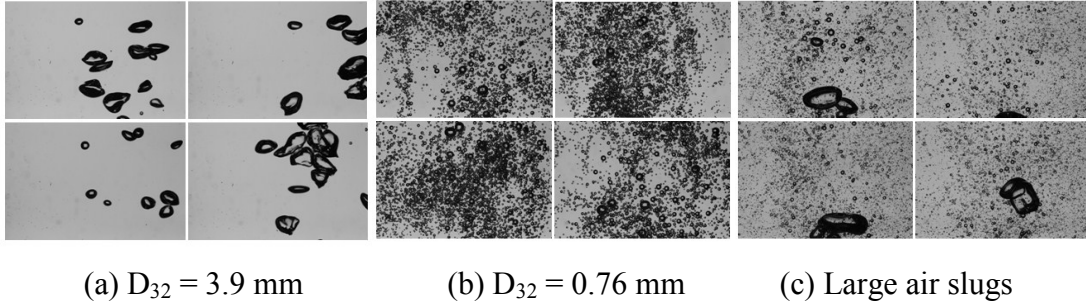


Fig. 3.14. (a) Bubbles in water. (b) Bubbles with addition of 10 ppm PPG 425. (c) Bubbles after 33.33 mL solvent injection in presence of 10 ppm PPG 425.

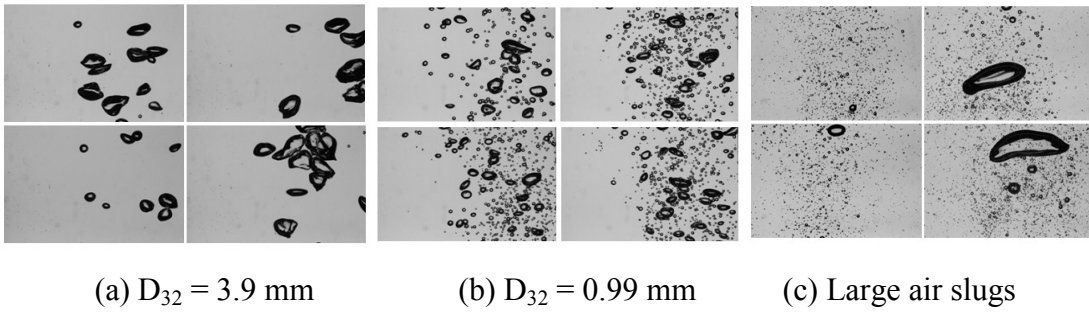


Fig. 3.15. (a) Bubbles in water. (b) Bubbles with the addition of 0.4 M NaCl. (c) Bubbles after 33.33 mL solvent injection in presence of 0.4 M NaCl.

3.3.2.2 Effect of LIX to kerosene ratio

One way to counter bed collapse may be through control of solvent properties. The obvious first attempt is to vary the LIX content. Since the 0.8M NaCl yielded the lowest turbidity of the tested conditions (implying the least loss of solvent as droplets) and had one of the highest extraction rates, it was chosen to test the effect of LIX to kerosene ratio. Tests were conducted with ratios from 0:1 to 1:0, i.e. from kerosene alone to LIX alone. All tests were conducted with the 6 ppm Cu solution.

Figure 3.16 shows that when no solvent was added, gas holdup was about 14% and stayed constant throughout the experiment. Figure 3.17 shows that when kerosene (alone) was injected, gas holdup dropped to about 7% after 33.3 mL addition. The rate of gas holdup reduction increased with the addition of LIX, the higher the LIX to kerosene ratio

the higher the gas holdup reduction rate. At a LIX to kerosene ratio of 1:1 and 1:0 (i.e. just LIX), gas holdup dropped to zero with about 10 mL solvent addition.

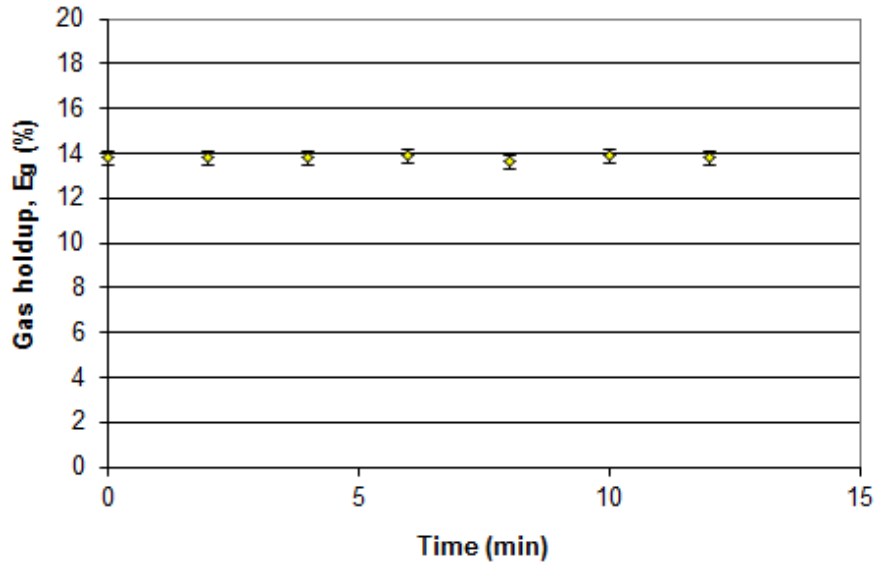


Fig. 3.16. Gas holdup before solvent addition with 0.8M NaCl

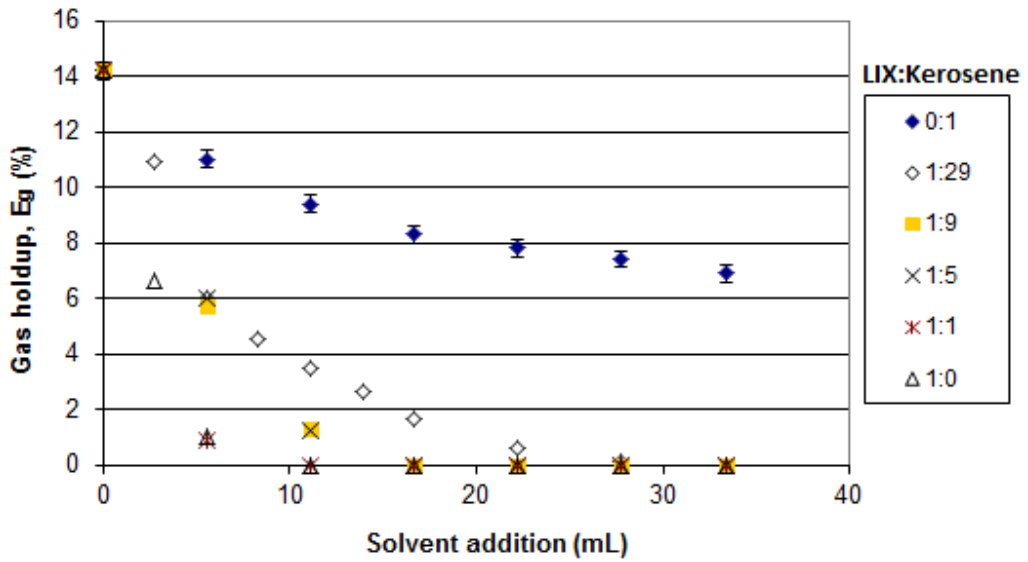


Fig. 3.17. Gas holdup as a function of solvent addition and LIX to kerosene ratio

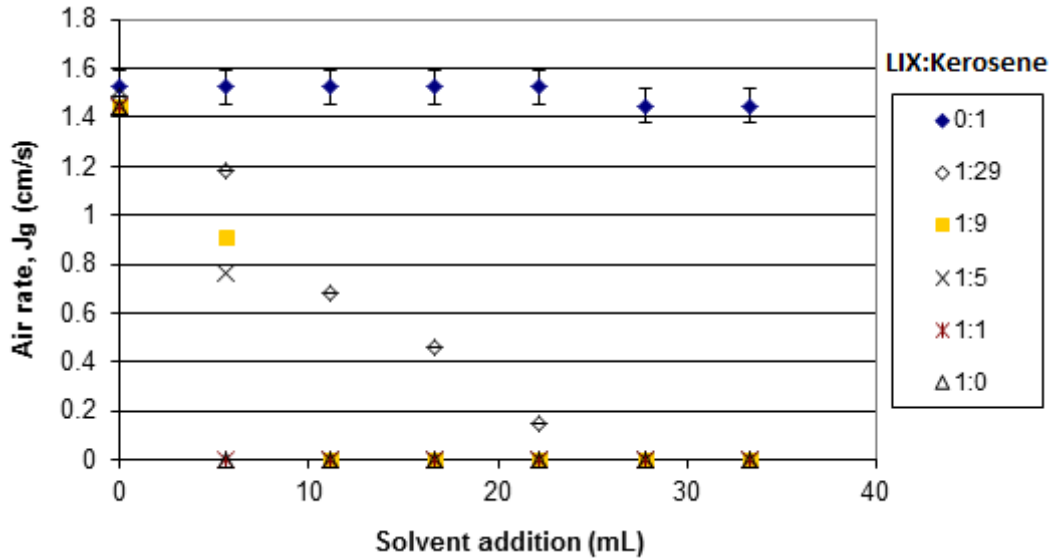


Fig. 3.18. Air rate as a function of solvent addition and LIX to kerosene ratio. Note that gas rate was calculated based on the cross sectional area of the separation tank.

The change in aspirated air rate followed the gas holdup trend. The air rate stayed constant at 1.45 cm/s (based on separation tank) when no solvent was added. The addition of kerosene induced a small drop in air rate after about 22 mL (Figure 3.18). The addition of solvent at LIX:kerosene ratio of 1:29 dropped the gas rate to zero after 28 mL and the rate of reduction increased as LIX to kerosene ratio was increased.

3.3.2.3 Effect of injection method

Another possibility to counter bed collapse was to alter the injection method. Figure 3.19 (for MIBC) shows that regardless of how solvent is injected, gas holdup decreases progressively with the introduction of solvent. The same was found for PPG 425 (Figure 3.20) and NaCl (Figure 3.21).

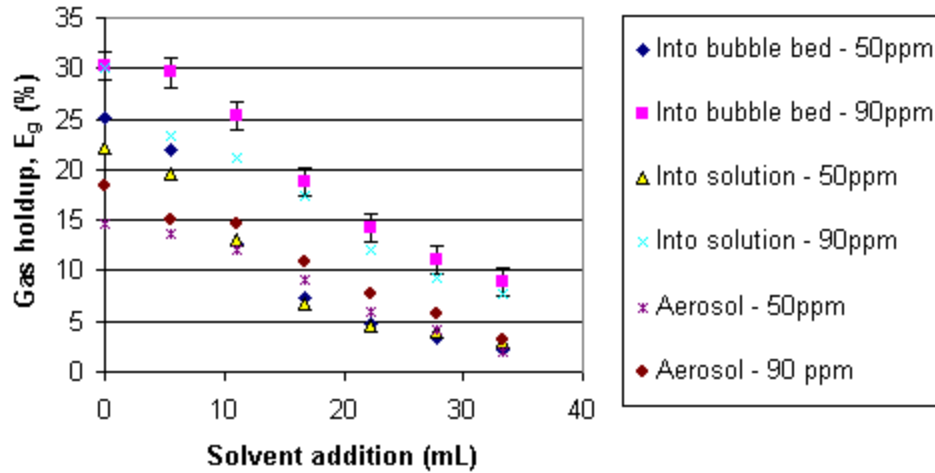


Fig. 3.19. Comparison of gas holdup data for the three solvent introduction techniques (into bubble bed, into solution and aerosol) for MIBC systems. (Note, the gas holdup starts lower for the aerosol method than the other two because the air flowrate was reduced to create a higher suction (more negative vacuum pressure) to carry the aerosol droplets into the downcomer.)

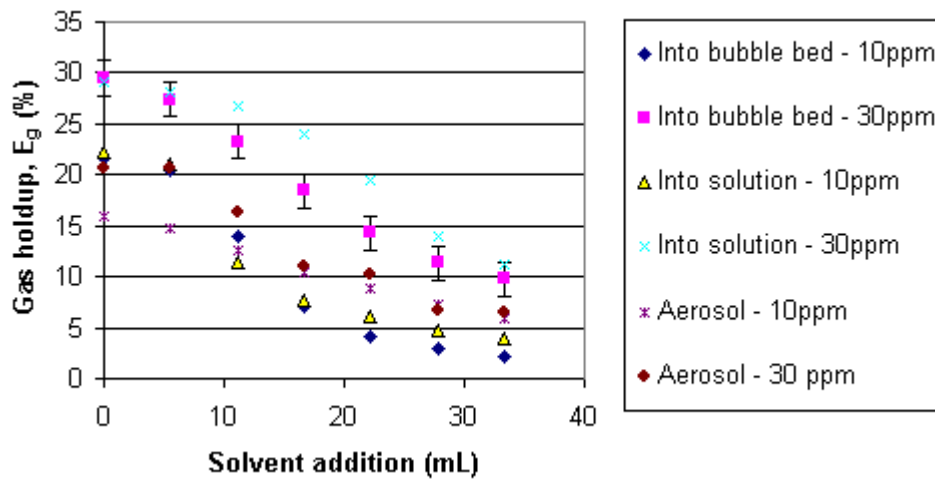


Fig. 3.20. Comparison of gas holdup data for the three solvent introduction techniques for PPG 425 systems.

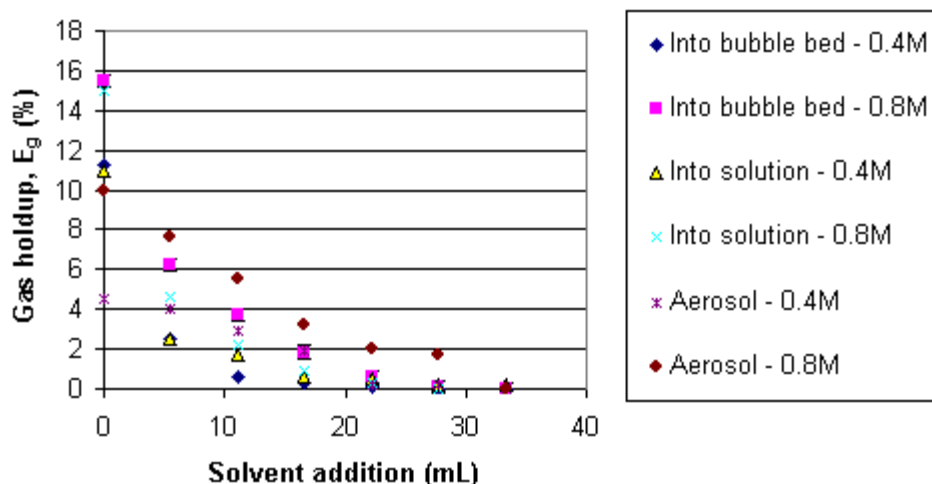


Fig. 3.21. Comparison of gas holdup data for the three solvent introduction techniques for NaCl systems.

3.3.3 Effect of aeration after stopping solvent injection

When solvent injection was stopped at 12 minutes, in some tests operation was continued for a period. As shown in Figure 3.22, the turbidity decreased progressively when MIBC and NaCl were used but fluctuated with PPG 425.

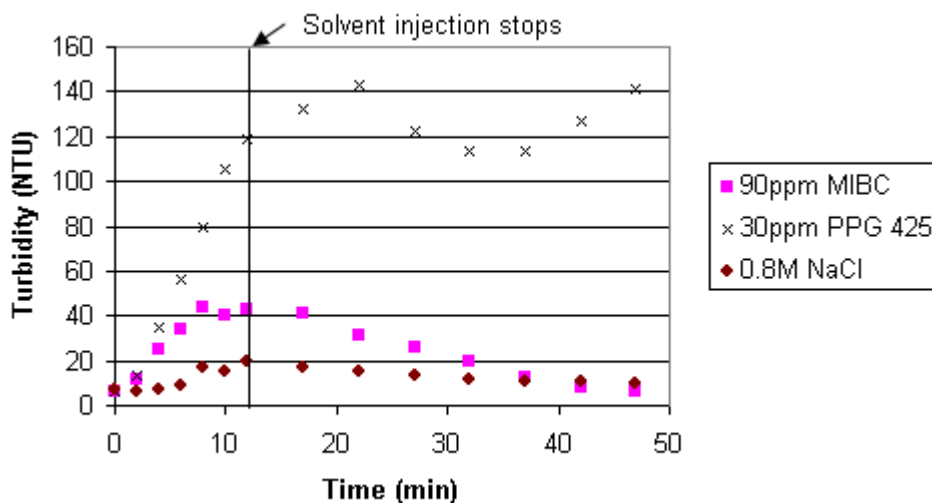


Fig. 3.22. Turbidity as a function of time during and after solvent addition in presence of MIBC, PPG 425 and NaCl.

Figure 3.23 shows that at the same time, extraction increased slowly in all the three systems. Figures 3.22 and 3.23 suggest that the air is removing the tramp droplets held in the solution, but this is a slow process.

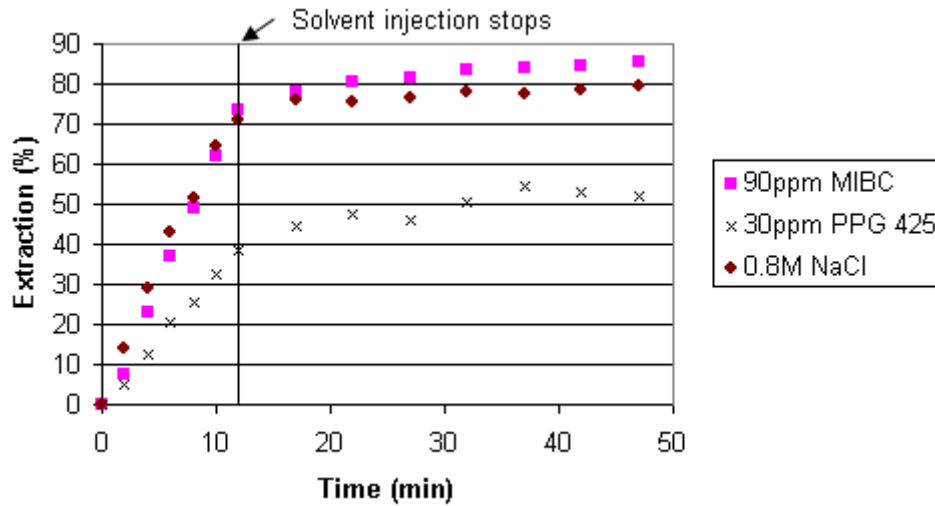


Fig. 3.23. Extraction as a function of time during and after solvent addition in presence of MIBC, PPG 425 and NaCl.

As Figure 3.24 shows, the gas holdup stabilizes after solvent injection is stopped but does not return to the original values, suggesting that not enough solvent is being removed for bubble bed collapse to be reversed.

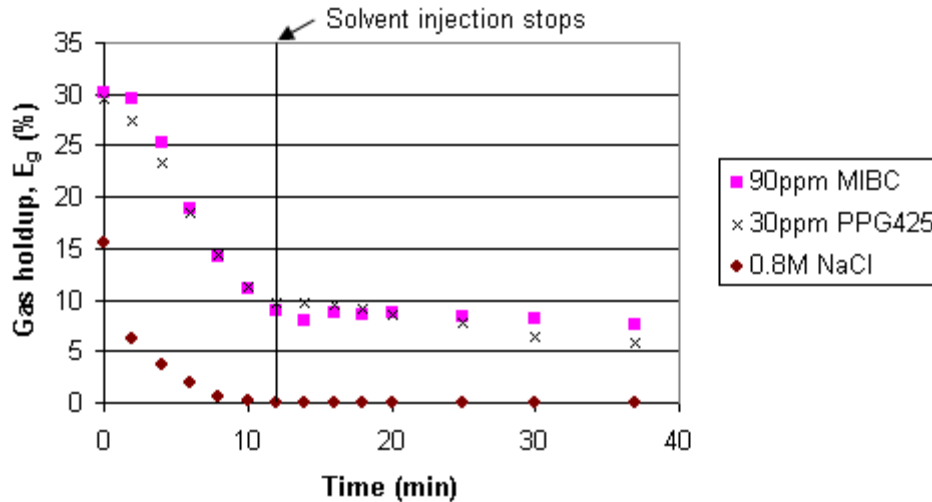


Fig. 3.24. Gas holdup as a function of time during and after solvent addition in presence of MIBC, PPG 425 and NaCl.

3.4 Discussion

The extraction results (Figure 3.8) appear encouraging: extraction is fast and exceeds the targeted 50%. This result, however, masks a problem. First, there is evidence of solvent loss, tramp droplets forming in solution suggested by the turbidity data (Figure 3.9). Second, and more damaging, was the collapse of the bubble bed indicated by the rapid decrease in gas holdup and aspirated air rate. The focus now became to eliminate the bed collapse as this was obviously counter-productive to the goal of coating swarms of bubbles with solvent.

One attempt was to alter the solvent composition by changing the LIX:kerosene ratio. But it was evident that increasing the LIX:kerosene ratio only increased the collapse rate. The appendix (Figure A9) shows another attempt to control through manipulation of solvent composition by adding silicone oil to the solvent, following its use by Tarkan et al. (2005); this also failed to prevent bubble bed collapse. There does not seem much room to control bed collapse through modifying solvent chemistry.

The next attempt to eliminate bed collapse was to alter the solvent injection point as bed collapse may be due to the direct injection of solvent into the bed. The evidence is that regardless of how solvent is introduced (the other two being as droplets in solution and as aerosol in the air), the bed collapses.

The collapse was a surprise especially given the use of the Jameson Cell for recovering solvent droplets (de-oiling) streams in solvent extraction plants (Miller and Readett, 1992; Miller et al., 1997; Young et al., 2006). Attention then turned to understanding the collapse mechanism. An answer does emerge from the literature on the use of oils as antifoaming agents, considering the solvent as the oil and the high gas holdup in the downcomer (> 45%) giving the bubble bed some attributes of foam.

A widely accepted mechanism for antifoaming action with oil separates the process into two steps: first the oil droplet enters the air-water interface (i.e., is hydrophobic), and step 2, begins to spread forcing liquid from the foam film causing rupture (Ross and McBain, 1944). Early attempts to correlate oil properties with foam stability were conducted by Robinson and Woods (1948) using the coefficients introduced by Harkins (1941). They defined an entering coefficient (E) and a spreading coefficient (S) in terms of the corresponding change in free energy:

$$E = \gamma_{W/A} + \gamma_{W/O} - \gamma_{O/A} \quad (3.4)$$

$$S = \gamma_{W/A} - \gamma_{W/O} - \gamma_{O/A} \quad (3.5)$$

where $\gamma_{W/A}$, $\gamma_{O/A}$ and $\gamma_{W/O}$ are the surface tension of the aqueous phase and the oil phase and interfacial tension of the oil - aqueous interface, respectively. The act of oil spreading forces the original aqueous film out replacing it with an oil film that is unstable and ruptures (Figure 3.25). The work of Chen et al. (2003) established for kerosene-based solvents that $S > 0$ and, note, if $S > 0$ then $E > 0$ because $(E - S) = 2\gamma_{O/W} > 0$; i.e., if the oil droplets spreads, it must have overcome the entry barrier to the air-water interface.

Though equations 3.4 and 3.5 give some guide to antifoaming action, they do not consider the geometry of the system (i.e., dimensions of the bubbles and oil droplets) or the influence of interfacial interactions within the thin film (Pugh, 1996). Also, there is a difference in magnitude between values of the initial entry coefficient (when the components are pure) and the equilibrium values (after each component contaminates the other). Denkov and Marinova (2006) distinguish the initial spreading coefficient, S_{IN} (defined using $\gamma_{A/W}$ in the absence of oil on the solution surface) from the equilibrium spreading coefficient, S_{EQ} ($\gamma_{A/W}$ in presence of oil). Negative values of S_{IN} mean the oil does not spread on the surface; positive values of S_{IN} mean the oil would spread. The S_{EQ} provides information about the thickness of the equilibrium layer: when $\gamma_{A/W} = \gamma_{O/W} + \gamma_{O/A}$ (i.e. $S_{EQ} = 0$), the oil would spread as a thick layer (or ‘duplex film’) compared to a thin equilibrium layer when $S_{EQ} < 0$ and $S_{IN} > 0$.

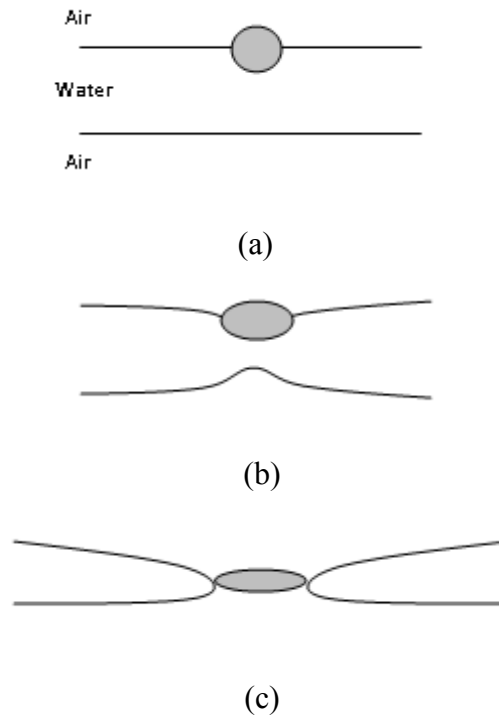


Fig. 3.25. Film rupture caused by spreading of oil droplet. Droplet enters air-water interface (a) and begins to spread (b) causing adjacent liquid to flow out of the film until film ruptures (c). (adapted from Dickenson, 1992)

Ross (1950) found that most of the oils with noticeable antifoam activity had positive spreading coefficients and speculated that the oil droplet should first connect the two foam film surfaces (i.e., form an oil bridge) and then spread to replace a portion of the stable aqueous foam film by an unstable oil bridge so that the film rupture can occur. Garrett (1980) defined a bridging coefficient, B , denoted by:

$$B \equiv \gamma_{W/A}^2 + \gamma_{W/O}^2 - \gamma_{O/A}^2 \quad (3.6)$$

where positive values of B mean positive entry coefficient (E) though the reverse is not always true (Aveyard et al., 1993; Kralchevsky and Nagayama, 2001). Garrett's analysis predicts that oils with $B > 0$ would form unstable bridges and oils with $B < 0$ ** would form stable bridges. Foam film rupture through oil bridge formation is possible at negative values of S (Garrett, 1993; Garrett et al., 1994), which means there is no specific requirement for spreading of oil; i.e., oil spreading is not a necessary condition for antifoam action. That said, spreading could facilitate the foam destruction process due to the correlation between the spreading ability of oils and their antifoam activity which has been observed in many systems (Denkov and Marinova, 2006).

Putting together the literature, the following three scenarios are established:

1. When the entry coefficient (E) is negative, i.e., $E < 0$, the droplet does not enter the air-water interface and remains in the aqueous phase (Figure 3.26b). When the entry coefficient (E) is positive, i.e., $E > 0$, the droplet enters the air-water interface (Figure 3.26b). If the spreading coefficient (S) is positive, i.e., $S > 0$, then the droplet spreads at the air-water interface (Figure 3.26c).

** Denkov (1999) concluded that oil bridges could acquire equilibrium shapes for both positive and negative values of B . The equilibrium shapes include a certain deformation of foam film surfaces not accounted in Garrett's model. Therefore, Denkov's model suggests that while only stable bridges exist at $B < 0$, both stable and unstable equilibrium bridges can be formed at $B > 0$.

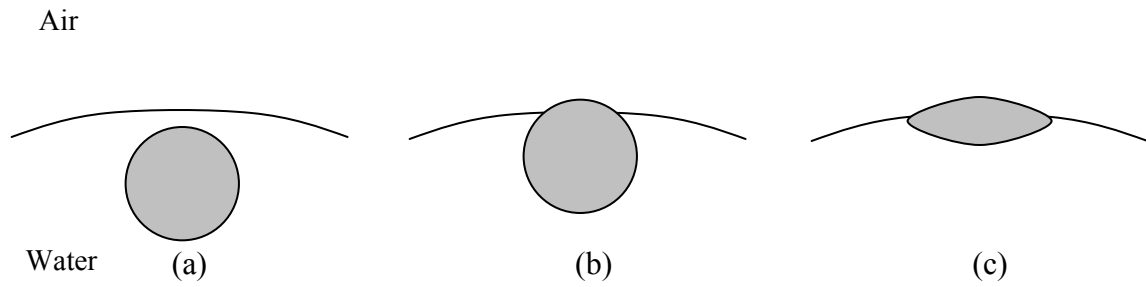


Fig. 3.26 (a) Droplet does not enter interface when $E < 0$; (b) Droplet enters interface when $E > 0$; (c) Droplet spreads at interface when $S > 0$

2. When the bridging coefficient (B) is negative, i.e., $B < 0$, and the contact angle $\Theta_{A/W} < 90^\circ$ a stable oil bridge is formed (Figure 3.27a). When the bridging coefficient (B) is positive, i.e. $B > 0$ and the contact angle $\Theta_{A/W} > 90^\circ$ then a unstable oil bridge is formed (Figure 3.27b). This bridge can deform to reach equilibrium and if it does not rupture, the bridge is thus deemed 'stable' at equilibrium (Figure 3.27c).

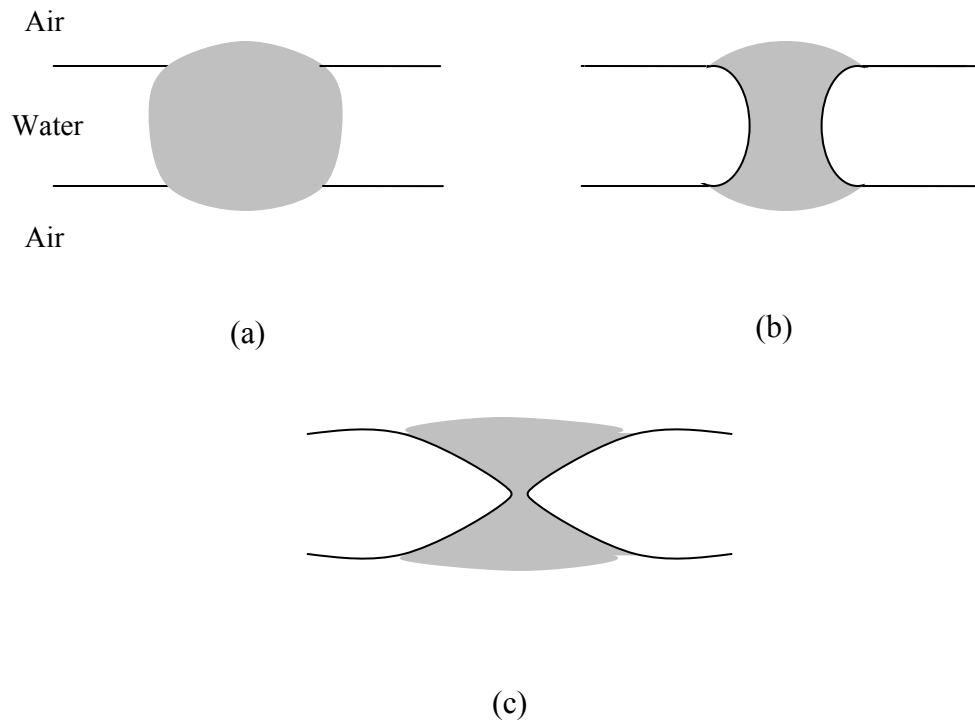


Fig. 3.27. (a) Stable oil bridge formation $B < 0$, $\Theta_{A/W} < 90^\circ$; (b) Unstable oil bridge formation $B > 0$, $\Theta_{A/W} > 90^\circ$; (c) Stable oil bridge at equilibrium after deformation

3. When the entry coefficient (E) is positive, i.e. $E > 0$, bridging coefficient (B) is positive, i.e., $B > 0$, and the spreading coefficient (S) is positive, i.e. $S > 0$, the oil droplet enters the air-water interface (Figure 3.28a), forms an oil bridge (Figure 3.28b) which stretches with time until a thin, unstable oil film is formed (Figure 3.28c) and finally ruptures, i.e., bubbles coalesce. This mechanism, called the bridging-stretching mechanism (Denkov and Marinova, 2006) is similar to that proposed by Ross and McBain (1944) shown in Figure 3.25.

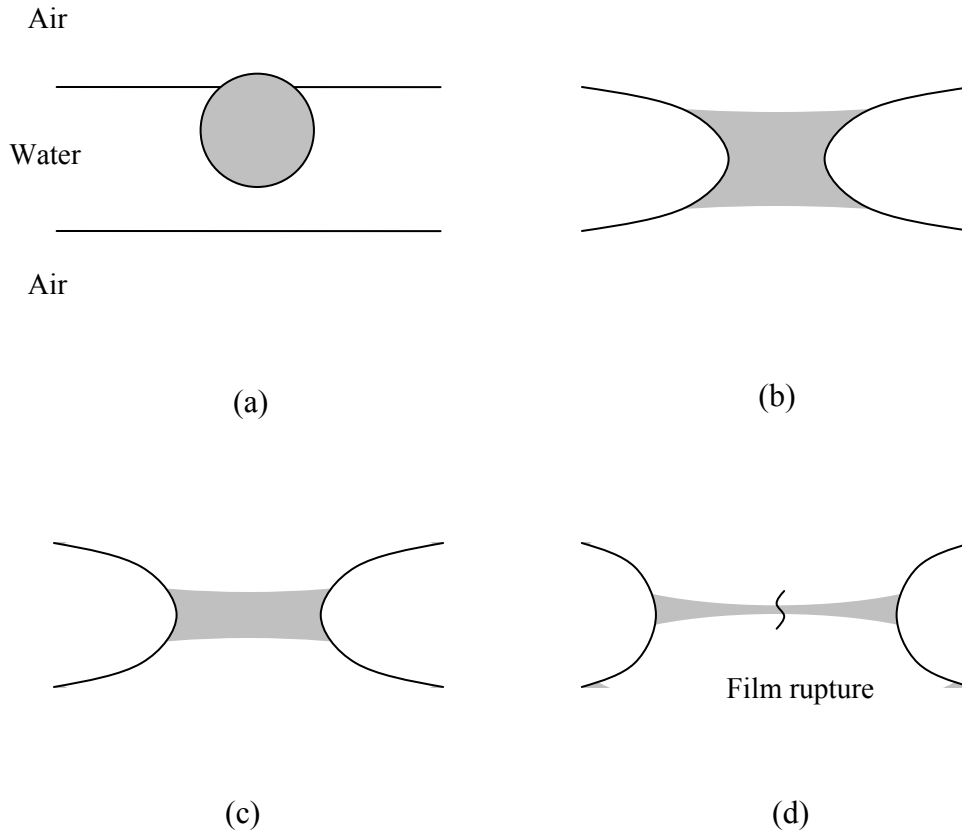


Fig. 3.28 (a) Oil droplet enters interface; (b) Oil bridge formation; (c) Oil bridge is stretched with time; (d) Film ruptures.

The high gas holdup in the downcomer ($> 45\%$ (measured by Summers et al. (1995) using conductivity rings installed in the downcomer) makes the condition of the bubble bed in the downcomer approach that of a foam and thus invites the de-foaming mechanisms described to explain bed collapse. Based on the mechanisms proposed by Ross and McBain (1944) and Denkov and Marinova (2006), it can be argued that the very act of solvent spreading onto the bubbles required for AASX inadvertently also collapses the bubble bed. The extent of collapse varies according to frother/salt type and concentration which must be affecting one or other of the sub-processes: droplet attachment, bridge formation, spreading, and stability of the solvent film.

The mechanisms described depend on antifoaming properties of solvent (oil). It is known that small amounts of strongly hydrophobic solid particles can de-stabilize foam (or froth) (Dippenaar, 1982). This raises the question of how stable is the downcomer bubble bed in the presence of hydrophobic solids and whether such a study might reveal something about the collapse mechanism, which is examined in the next chapter.

3.5 Conclusions

1. The downcomer was selected as 'coating reactor' for the AASX process based on the high gas holdup bubble bed created.
2. Copper extraction approached 70% with 50 ppm MIBC, 90 ppm MIBC and 0.8M NaCl used to reduce bubble size.
3. Turbidity measurements indicated some loss of solvent which depended on the frother or salt used.
4. For both frothers and the salt, gas holdup and aspirated air rate decreased and large bubbles formed with introduction of solvent, i.e. the bubble bed 'collapsed'. The collapse occurred with all three solvent injection techniques (into the bubble bed, into the feed solution, and as aerosol into the air).
5. The rate of bubble bed collapse increased with increase in LIX content in solvent.
6. The mechanism of bed collapse appears to be related to the de-foaming properties of oil droplets, considering the solvent as the oil and the high gas holdup in the bubble bed approximating foam.

3.6 References

Aveyard, R., Binks, B.P., Fletcher, P.D.I., Peck, T.G., Garrett, P.R., 1993. *J. Chem. Soc. Faraday Trans.*, 89, 4313.

Chen, F., Finch, J.A., Distin, P.A., Gomez, C.O., 2003. Air assisted solvent extraction. *Canadian Metallurgical Quarterly* 42, 277–280.

Dickenson, E., 1992. *Introduction to Food Colloids*. Oxford University Press.

Denkov, N.D., 1999. Mechanisms of action of mixed solid-liquid antifoams 2. Stability of oil bridges in foam films, *Langmuir* 15, 8530 – 8542..

Denkov, N. D., Marinova, K.G., 2006. Antifoam effects of solid particles, oil drops and oil-solid compounds in aqueous foams. *Colloidal particles at liquid interfaces*. Cambridge University Press.

Dippenaar, A., 1982. The destabilization of froth by solids. I. The mechanism of film rupture, *International Journal of Mineral Processing* 9, 1-14.

Finch, J.A., Dobby, G.S., 1990. *Column flotation*. Pergamon Press, Oxford.

Garrett, P.R., 1980. Preliminary considerations concerning the stability of a liquid heterogeneity in a plane-parallel liquid film. *Journal of Colloid and Interface Science* 76, 587.

Garrett, P.R., 1993. *Defoaming: Theory and industrial applications*, Surfactant science series, Vol. 45, Marcel Dekker, New York.

Garrett, P.R., Davis, J., Rendall, H.M., 1994. An experimental study of the antifoam behavior of mixtures of a hydrocarbon oil and hydrophobic particles. *Colloids and Surfaces A, Physicochemical and Engineering Aspects* 85(2-3), 159-197.

Gomez, C.O., Acuna, C., Finch, J.A., Pelton, R., 2001. Aerosol enhanced flotation deinking of recycled paper. *Pulp & Paper Canada* 102, 28–30.

Harkins, W.D., 1941. A general thermodynamic theory of the spreading of liquids to form duplex films and of liquids or solids to form monolayers, *Journal of Chemical Physics* 9, 552.

Hernandez-Aguilar, J.R., Gomez, C.O., Finch, J.A., 2002. A technique for the direct measurement of bubble size distribution in industrial flotation cells, *Proceedings-34th Annual Meeting of the Canadian Mineral Processors*, January 22-24, Ottawa, Canada.

Kentish, S.E., Stevens, G.W., 2001. Innovations in separations technology for the recycling and re-use of liquid waste streams. *Chemical Engineering Journal* 84, 149–159.

Kralchevsky, P.A., Nagayama, K., 2001. *Particles at fluid interfaces and membranes*, Elsevier, Amsterdam.

Li, C., Chen, Y., Hsiao, S., 2008. Compressed air-assisted solvent extraction (CASX) for metal removal. *Chemosphere* 71, 51-58.

Liu, J., Mak, T., Zhou, Z., Xu, Z., 2002. Fundamental study of reactive oily-bubble flotation. *Minerals Engineering* 15, 667–676.

Maiolo, J., Pelton, R., 1998. Aerosol-enhanced flotation—a possible approach to improved flotation deinking. *Journal of Pulp and Paper Science* 24, 324.

Ross, S., McBain, J.W., 1944. Inhibition of foaming in solvents containing known foamers. *Industrial and Engineering Chemistry* 36(6), 570-573.

Chapter 4 - Effect of hydrophobic material on bubble bed in the downcomer

4.1 Introduction

As seen in the previous chapter, the progressive addition of solvent into the downcomer collapsed the bubble bed regardless of which coalescence inhibitor was used, MIBC, PPG 425 or NaCl, the LIX:kerosene ratio, or how the solvent was introduced, into the bubble bed, into the feed solution, or into the air as aerosol. The collapse mechanism proposed was based on the anti-foaming action of oils, treating the bubble bed as the foam and the solvent as the oil. The mechanism sees solvent attachment at the air-water interface and via bridging and/or spreading causing film rupture and bubble bed collapse. It was noted that solid hydrophobic particles (as opposed to oil, i.e., liquid hydrophobic particles) are also known to de-stabilize foam. The purpose of this chapter is to determine how sensitive the bubble bed is to the presence of small quantities of hydrophobic solids, compared to the obvious de-stabilizing effect of their liquid counterpart. The observations may shed some light on the solvent-related mechanism. To start, the theory of foam destabilization is reviewed.

4.2 Theory of foaming destabilization by hydrophobic material

The theory of foam (film) destabilization by liquid hydrophobic particles (oil droplets) was introduced in Chapter 3. Here we consider hydrophobic solid particles.

Dippenaar (1982) observed the effect of a spherical particle on a thin film of distilled water in a specially designed cell. Hydrophobic particles caused the film to thin and particles with contact angle $\Theta > 90^\circ$ ruptured the film when it was thinned sufficiently for the particle to bridge it. The process can be understood by considering a hydrophobic particle attached at one air-water interface is approached by another air-water interface (Figure 4.1a). The initial contact angle at the second interface is smaller than the

equilibrium contact angle and thus, this boundary moves over the particle to attain the equilibrium contact angle causing the thickness of the film around the particle to thin and, depending on Θ , disappear certainly if $\Theta > 90^\circ$, i.e. the particle is strongly dewetted by the liquid. Using films of distilled water, experiments with a glass bead made strongly hydrophobic ($\Theta = 102^\circ$) confirmed the film destabilization mechanism. For a spherical particle with $\Theta < 90^\circ$, the result was movement of the lower boundary that ceased before it reached the upper boundary and the particle was always surrounded by a liquid film of finite thickness (Figure 4.1b). The film remained stable to the end of the experiment (ca. 1 s), i.e., the particle is not so strongly dewetted by the liquid. It is potentially significant that this work of Dippenaar did not include anti-coalescence agents such as frothers.

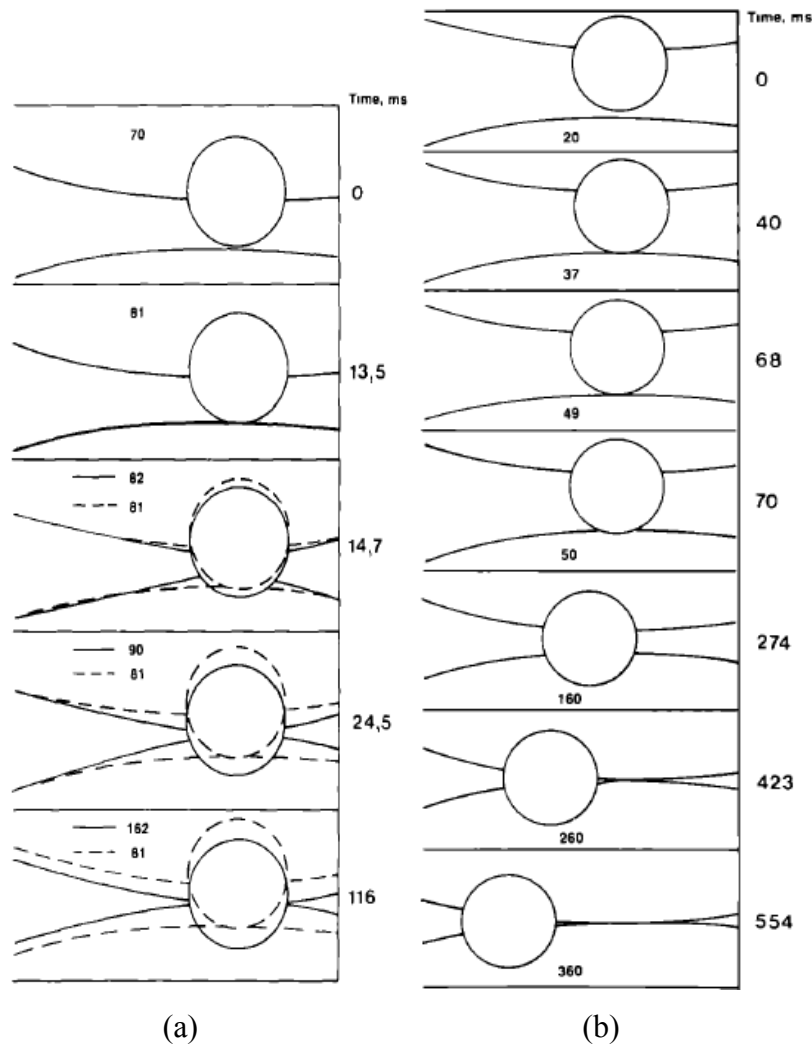


Fig. 4.1. (a) Interaction of a glass bead $\Theta = 102^\circ$ with a film of liquid; (b) Interaction of a glass bead $\Theta = 74^\circ$ with a film of liquid (Reprinted with permission from Dippenaar, (1982), Elsevier)

Pugh (1996) suggested that the antifoaming action of an oil droplet could be similar to that of a hydrophobic particle, particle bridging and oil bridging mechanisms both leading to rupture of thin films. Garrett (1993) also suggested that an oil droplet could break the foam by bridging similar to a solid particle, i.e., without spreading being a factor. Ross and McBain (1944), however, specify that the oil droplet after entering the air-water interface must spread to drive out the original water film, leaving an oil film which is unstable and can easily rupture (Figure 3.25 in Chapter 3).

The depiction in Figure 4.1 is for an isolated hydrophobic particle. Simovic (2004) suggested that small concentrations of hydrophobic particles can dominate film instability. Finch and Dobby (1990), noting periodic instabilities in column flotation froths, argued that stability would be a function of particle loading on the bubble. For interfaces well-loaded with hydrophobic particles the films are stabilized mechanically, which is how most froths in flotation systems appear to form enabling the flotation process to work.

Hunter et al. (2008) reviewed work on foam stabilising effect of particles and found conflicting results. Although ‘bridging-dewetting’ mechanisms (as in Figure 4.1) imply that particles with contact angle below 90° could act as foam stabilizers, subsequent research has shown that particles can begin to act as de-foamers at contact angles much less than 90° . It is understood that for $\Theta < 90^\circ$ the second interface in Figure 4.1b still advances over the particle thinning the film in the vicinity of the particle to a thickness that may induce rupture depending on the properties of the film. Hunter et al. concluded that foam stability could be increased if a high concentration of small (nanosized) particles of moderate hydrophobicity are used and suggested de-stabilisation is increased with the presence of even a small concentration of larger more hydrophobic particles.

The fact that hydrophobic solid particles can destabilize foam and the same bridging mechanism suggested for oil droplets could be at play, prompted examination of the effect of hydrophobic solids on the bubble bed in the downcomer compared to that of the solvent. Would hydrophobic solids as well as hydrophobic liquids have a similar effect or would they be different? What if both were added to the system? Would they have a synergistic effect? Or would one counter the effect of the other? The experiments were planned to address these points.

4.3 Experimental

4.3.1 General setup

The test rig was described in Chapter 3 (Figure 3.1). As shown in that chapter, how solvent is injected does not matter, and Method 3, introducing the solvent as an aerosol into the air inlet of the downcomer was selected (Figure 3.6 in Chapter 3).

4.3.2 Materials and methods

Water was used instead of copper sulfate solution (since extraction was no longer the focus). As previously, the two frothers (MIBC and PPG 425) and NaCl were used as coalescence inhibitors to help create small bubbles and corresponding high gas holdup bubble bed in the downcomer.

Talc powder (supplied by Fisher Scientific) and graphite powder (supplied by Sigma Aldrich) were chosen as the model hydrophobic solids. The molecular formula for talc is $3\text{MgO}_4\text{SiO}_2\text{H}_2\text{O}$. The specific gravity is 2.5 - 2.8 with an average particle size of 2.5 μm . The graphite specific gravity is 1.9 and average particles size is ca. 1 - 2 μm . Graphite was added only when NaCl was used due to the fact that frothers are adsorbed by graphite. Graphite serves as a 'purer' hydrophobic material than talc, which has hydrophilic sites. The solids were weighed with an analytical balance (Mettler AJ100) and mixed with the solution in the feed tank by stirring.

The first series of tests used the hydrophobic solids only (no solvent). In case of talc, amounts were added progressively up to 0.07 % w/w or 700 ppm (comparable to the total of 900 ppm of solvent added to solution in the previous chapter), then further increased up to 1 % w/w. Graphite was also added (to NaCl solution) progressively up to 0.07 % w/w, and subsequently up to 1%. In the second test series, solvent was added (up to 900 ppm) to solutions containing 0.07 %, 0.5 % and 1 % w/w talc or graphite to gauge possible interaction effects. Some properties of the solvent used were given in Table 3.2 of the previous chapter. The solvent used here was LIX:kerosene 1:29.

4.4 Results

4.4.1 Effect of hydrophobic liquid (solvent)

Figure 4.2 reminds the situation with solvent addition (Chapter 3), the bed collapses (gas holdup decreases) regardless of whether frother or salt was used as coalescence inhibitors.

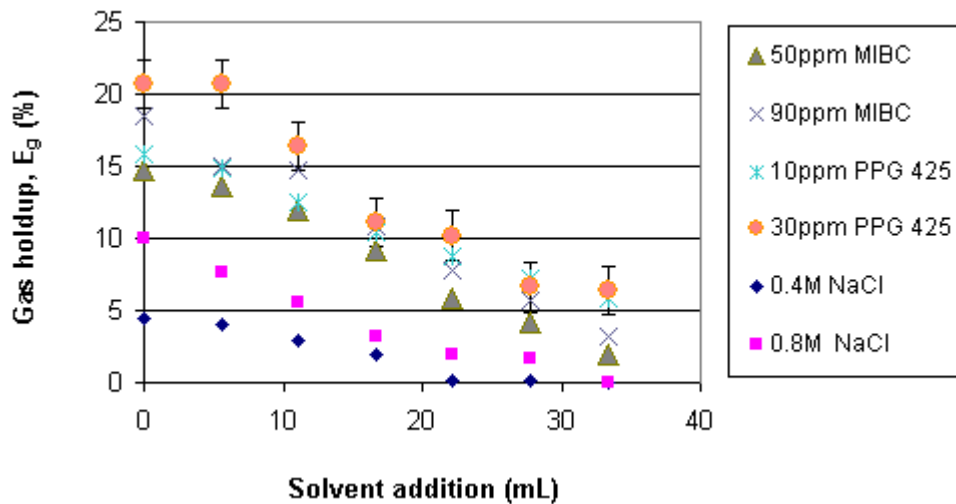


Fig. 4.2. The gas holdup in separation tank as a function of solvent addition in presence of MIBC, PPG 425 and NaCl (solvent introduced as aerosol in the air inlet- Method 3).

4.4.2 Effect of hydrophobic solids

4.4.2.1 Talc

When small amounts of talc were added, the system reacted differently depending on the coalescence inhibitor used. Figure 4.3 shows that with 50 ppm MIBC solution or 10 ppm PPG 425, the addition of talc up to 0.07 % w/w (700 ppm) had no effect on gas holdup or on bubble size. The addition of talc up to 0.07 % w/w in the 0.4 M NaCl solution, however, caused a significant increase in gas holdup from ca. 4.0 % to 8.8 %. This gas

holdup increase was confirmed by a decrease in bubble size, D_{32} decreasing from 0.99 mm to 0.86 mm.

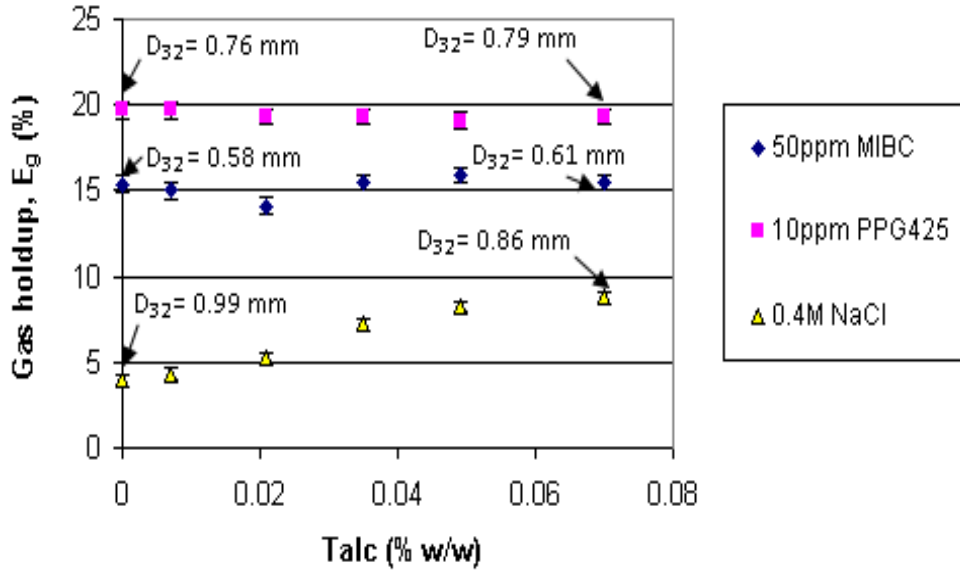


Fig. 4.3. The effect of talc up to 0.07 % w/w on gas holdup and bubble size in presence of MIBC, PPG 425 and NaCl

When further amounts of talc were added up to 1 % w/w, for the MIBC case, gas holdup stayed constant as well as the bubble size (Figure 4.4). With PPG 425, in contrast, gas holdup decreased significantly from 20 % to 5 %, accompanied by a progressive increase in bubble size, as shown in Figure 4.5. Figure 4.6 shows that in the case of NaCl the initial increase in gas holdup up to 0.07 % w/w (700 ppm) was not continued but reached a plateau at around 10 % gas holdup up to the 1 % talc w/w addition. The bubble size data confirmed that no further change occurred.

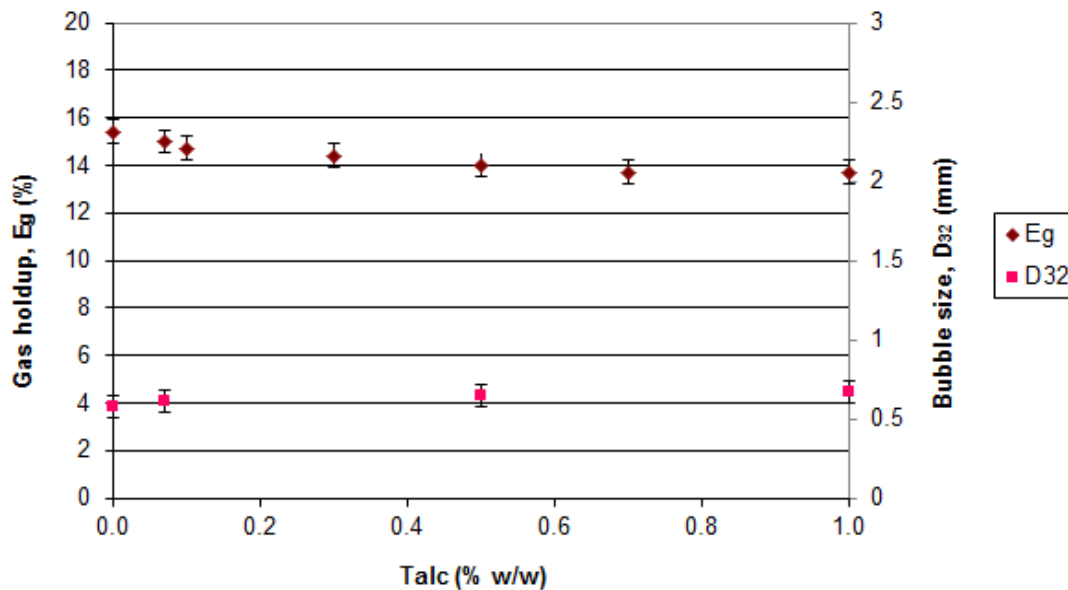


Fig. 4.4 Effect of talc up to 1 % w/w on gas holdup and bubble size in presence of 50 ppm MIBC

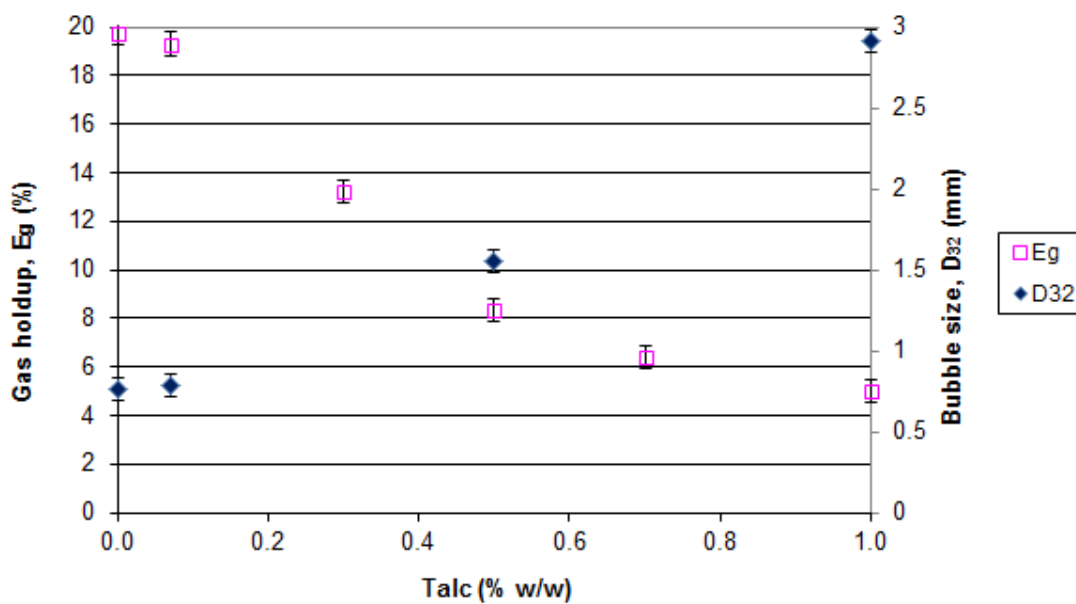


Fig. 4.5. Effect of talc up to 1 % w/w on gas holdup and bubble size in presence of 10 ppm PPG 425

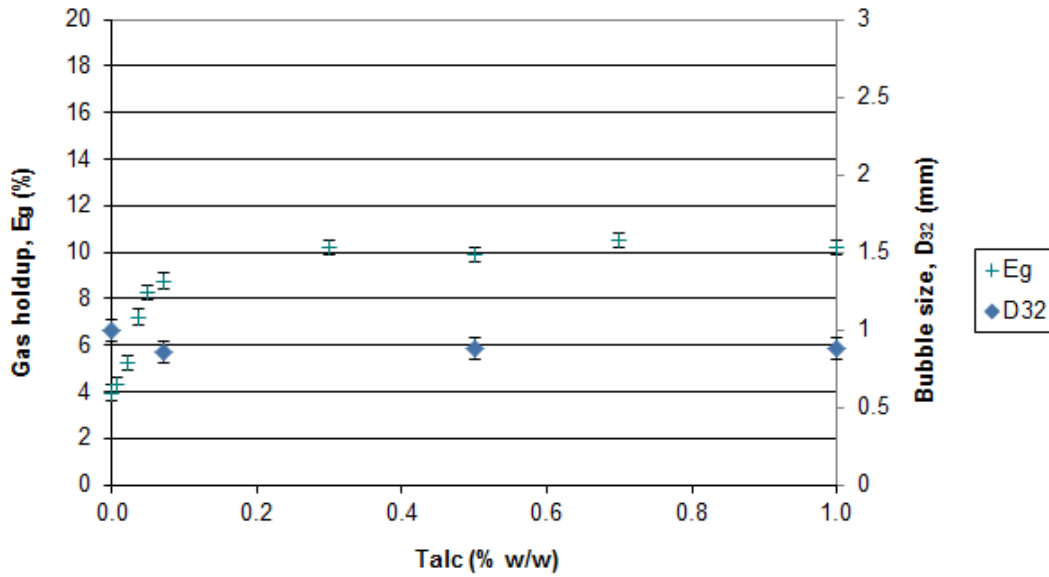


Fig. 4.6. Effect of talc up to 1 % w/w on gas holdup and bubble size in presence of NaCl

4.4.2.3 Graphite

Figure 4.7 shows that when 0.07 % w/w graphite was added to the NaCl solution, gas holdup increased from 4 % to 8 % accompanied by a decrease in bubble size (D_{32}) from 0.99 mm to 0.79mm, i.e. a similar outcome as with talc. The gas holdup, however, returned to the original value at 0.3 % w/w addition and remained steady up to 1 % w/w graphite; in contrast, the bubble size data indicated no change. A new observation in the bubble size analyzer chamber when graphite concentration was increased above 0.07 % w/w was camera shutter speed had to be increased which indicates an increase in bubble rise velocity.

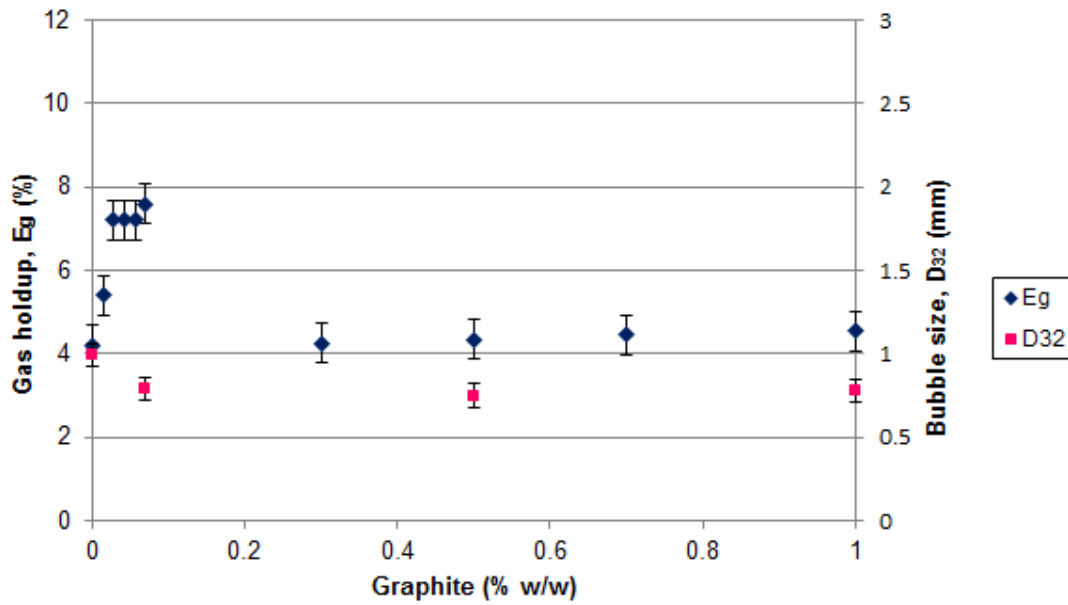


Fig. 4.7. Effect of graphite up to 1 % w/w on gas holdup and bubble size in presence of NaCl

4.4.3 Effect of hydrophobic solids and solvent

4.4.3.1 Gas holdup

Figure 4.8 shows that in the 50 ppm MIBC system, the presence of talc (0.07 % to 1 % w/w) preserves the gas holdup at around 14% in contrast to the known decrease in the absence of talc (zero talc included for reference).

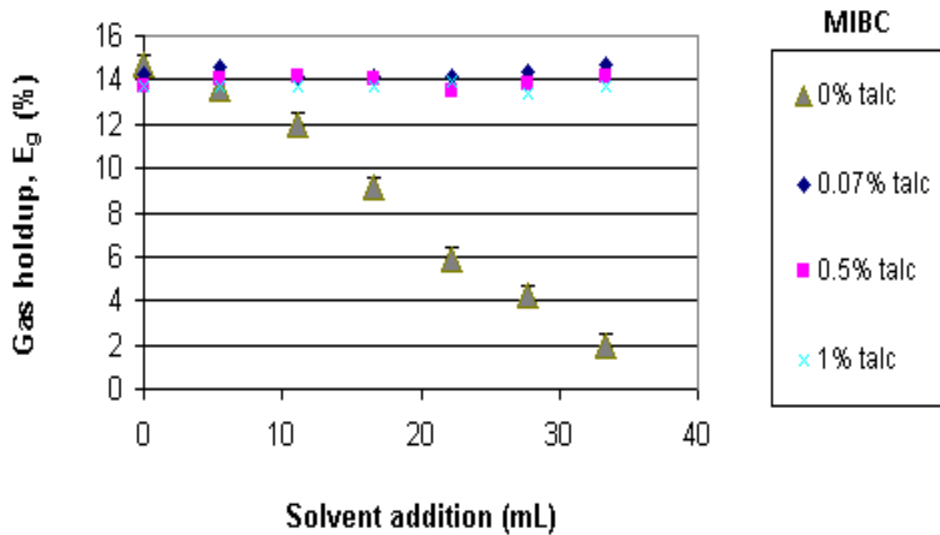


Fig. 4.8. Combined effect of talc and solvent on gas holdup in presence of 50 ppm MIBC

Figure 4.9 shows that in presence of 10 ppm PPG 425 preservation of gas holdup was not achieved: gas holdup dropped progressively with the introduction of solvent for all talc concentrations. Note that the gas holdup starts at different values at zero solvent addition for the different talc concentrations due to the fact that the presence of talc decreases the gas holdup, as seen in Figure 4.5. The lower initial gas holdup for 0% talc than for 0.07% talc is because the air rate for the former was inadvertently set lower.

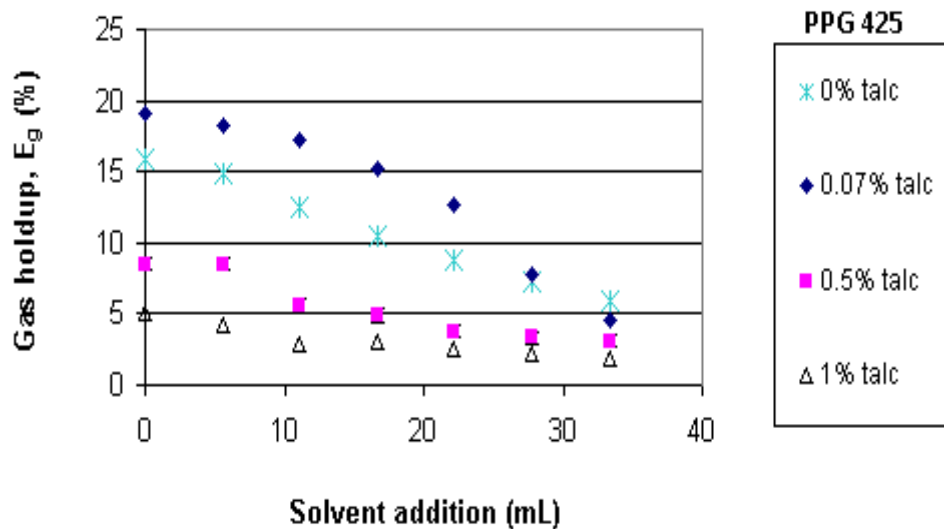


Fig. 4.9. Combined effects of talc and solvent on gas holdup in presence of 10 ppm PPG 425

In 0.4M NaCl solution, the results were similar to PPG 425: gas holdup decreased (Figure 4.10) progressively with the advent of solvent regardless of the talc concentration. The gas holdup started at different points at zero solvent addition due to the fact that addition of talc increases the gas holdup, as seen in Figure 4.6.

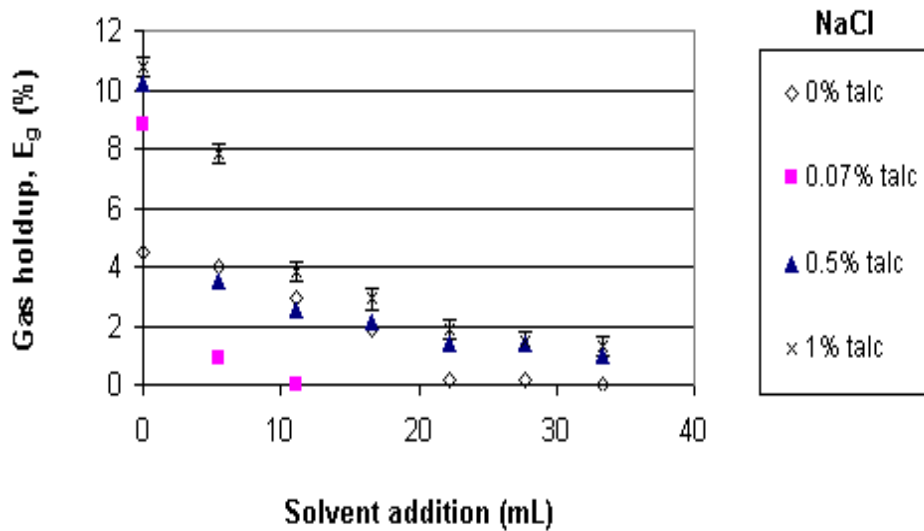


Fig. 4.10. Combined effect of talc and solvent on gas holdup in presence of 0.4M NaCl

In the graphite 0.4 M NaCl case, gas holdup also decreased (Figure 4.11) reaching zero with less than 6 mL solvent added (less than 2 minutes). The gas holdup started at different points at zero solvent addition due to the fact that addition of graphite changes the gas holdup, as seen in Figure 4.7.

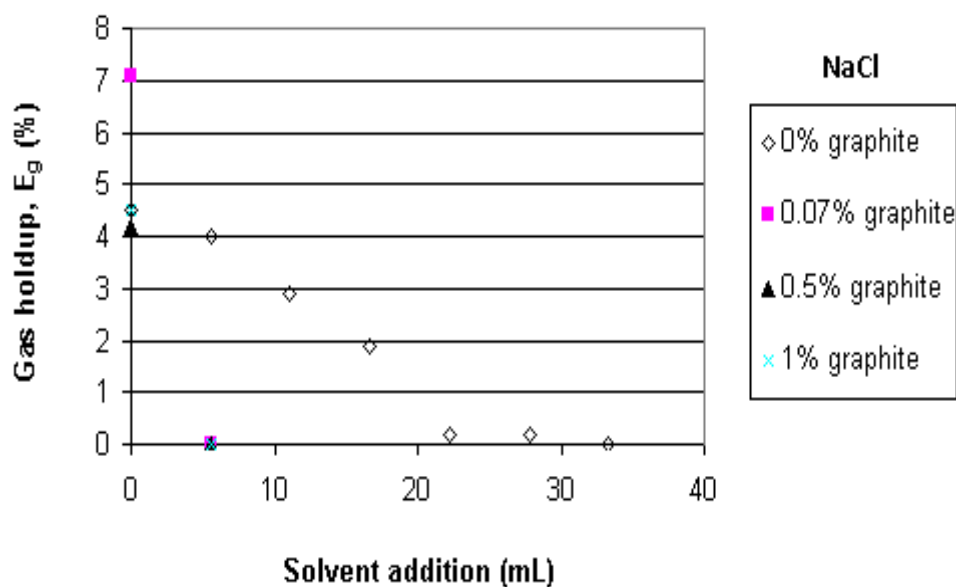


Fig. 4.11. Combined effect of graphite and solvent on gas holdup in presence of 0.4M NaCl

4.4.3.2 Bubble images

The bubble images supported the gas holdup results. Figure 4.12 shows the evolution of the bubble swarm when MIBC, talc and solvent were added sequentially. Bubble size decreased with MIBC alone (b), remained small with addition of talc up to 1% (c – e), and remained at this size with subsequent addition of solvent up to 33.33 mL (a/o 900) (f).

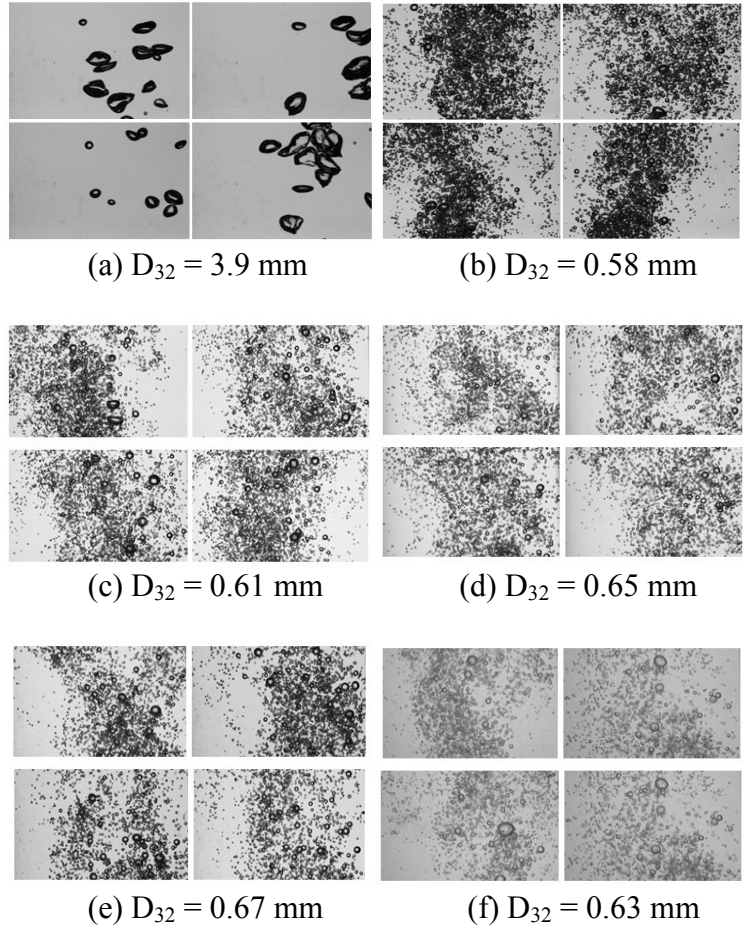


Fig. 4.12. Bubble images for the following sequence: (a) Water alone; (b) After addition of 50 ppm MIBC; (c) After addition of 0.07 % w/w talc; (d) After addition of 0.5 % w/w talc; (e) After addition of 1 % w/w talc; (f) After addition of 33.3 mL solvent (A/O 900).

Figure 4.13 shows swarm evolution when PPG 425, talc and solvent were added sequentially. Bubble size decreased when PPG 425 was added (b), then increased progressively with addition of talc up to 1% (c – e), and increased further on addition of 33.3 mL solvent (A/O 900) where large air slugs formed (f).

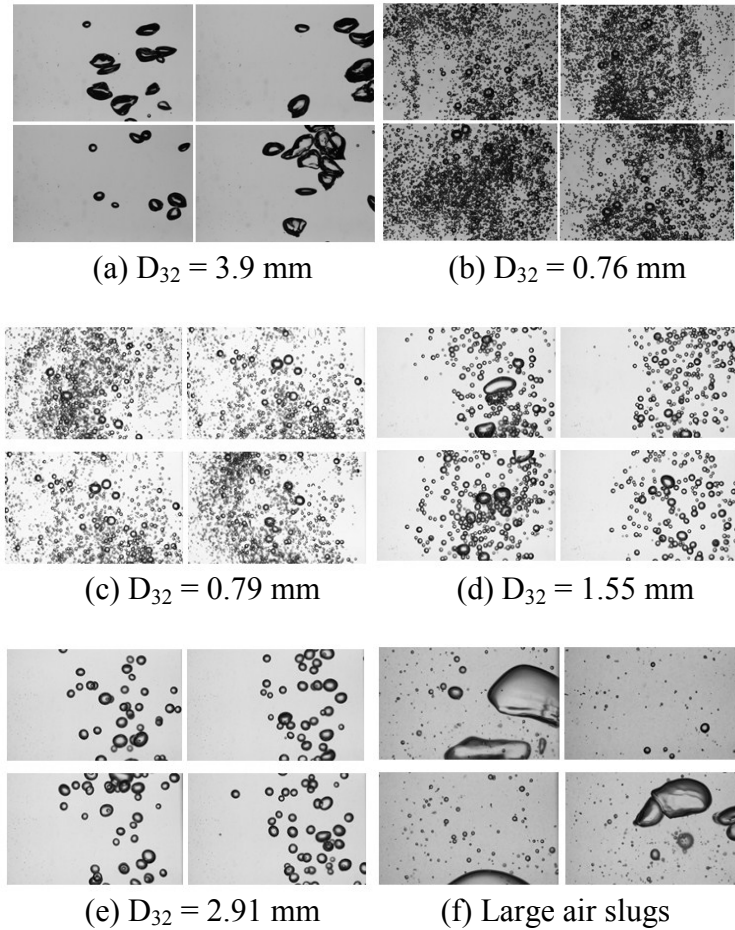


Fig. 4.13. Bubble images for the following sequence: (a) Water only; (b) After addition of 10 ppm PPG 425; (c) After addition of 0.07 % w/w talc; (d) After addition of 0.5 % w/w talc; (e) After addition of 1 % w/w talc; (f) After addition of 33.3 mL solvent (A/O 900).

Figure 4.14 shows the evolution when NaCl, talc and solvent were added sequentially. Bubble size decreased when NaCl was added (b), decreased further with addition of talc up to 0.07% (c), then remained constant with further talc additions up to 1% (d – e). Addition of solvent up to 33.3 mL at the 1% talc level increased the bubble size and large air slugs were formed (f).

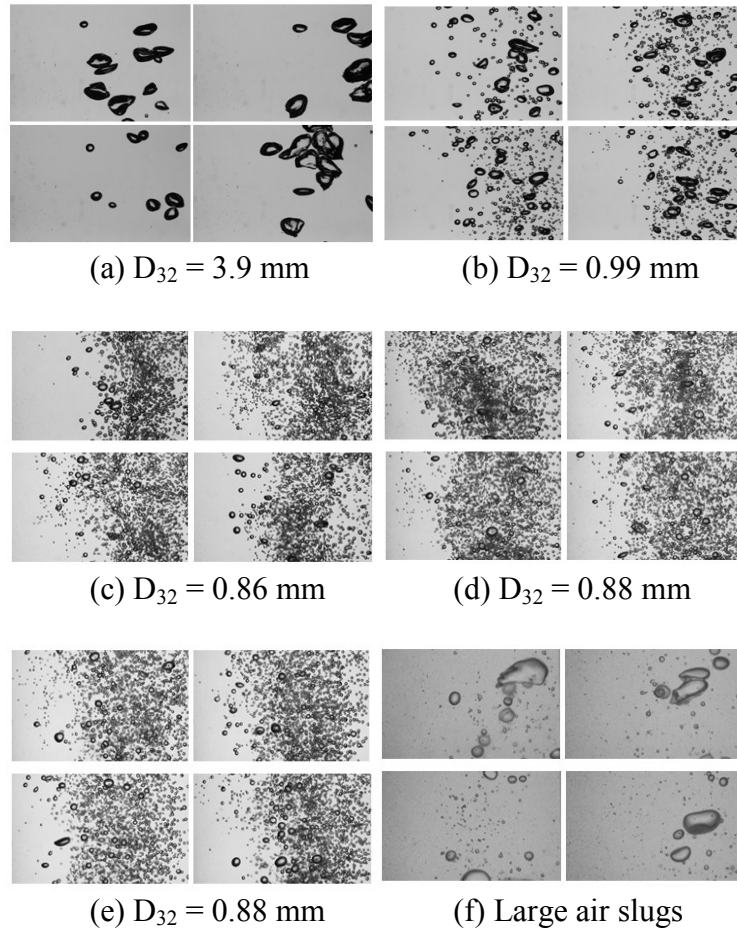


Fig. 4.14. Bubble images for the following sequence: (a) Water only; (b) After addition of 0.4M NaCl; (c) After addition of 0.07 % w/w talc; (d) After addition of 0.5 % w/w talc; (e) After addition of 1 % w/w talc; (f) After addition of 33.3 mL solvent (A/O 900).

The evolution of the bubble size when NaCl, graphite and solvent were added sequentially followed the same trend as that when talc was used (Figure 4.15). Bubble size decreased when NaCl was added (b), decreased further with addition of graphite up to 0.07% (c), then remained constant with further graphite additions up to 1% (d – e). Addition of solvent up to 33.3 mL at 1% graphite increased the bubble size where large air slugs were formed (f).

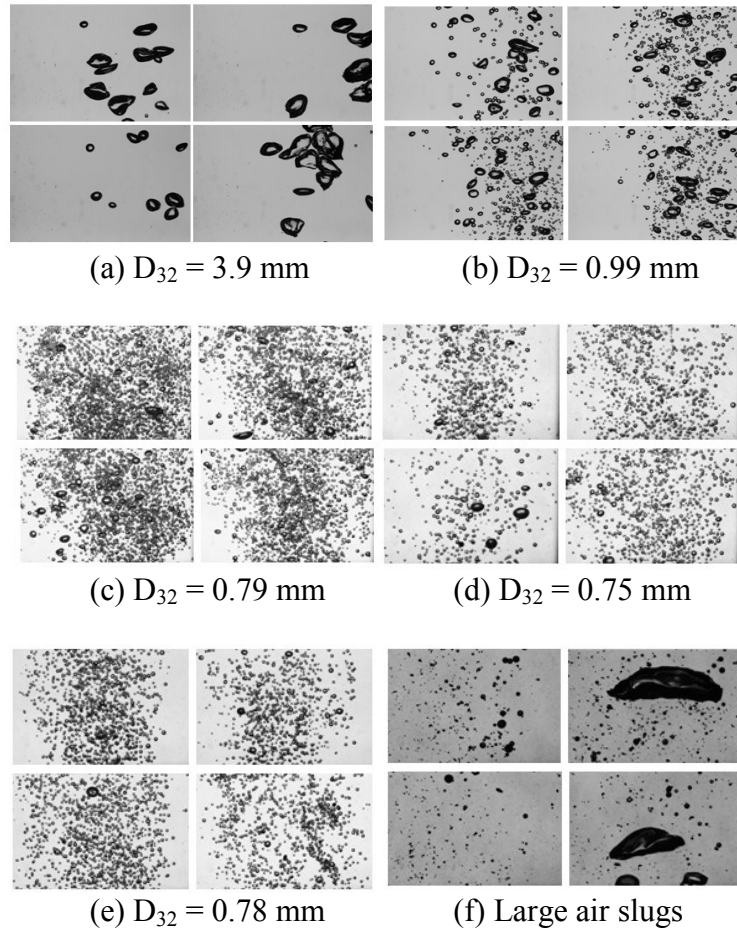


Fig. 4.15. Bubble images for the following sequence: (a) Water only; (b) After addition of 0.4M NaCl; (c) After addition of 0.07 % w/w graphite; (d) After addition of 0.5 % w/w graphite; (e) After addition of 1 % w/w graphite; (f) After addition of 33.3 mL solvent (A/O of 900).

4.4.3.3 Froth buildup in the presence of solids

Another notable effect of adding solids was froth build-up in the launder, especially in the talc/MIBC and talc/NaCl systems even to the extent of overflowing the launder in some cases (Figures 4.16 and 4.17). The subsequent addition of solvent collapsed the froth formed in presence of NaCl but not in presence of MIBC. With PPG 425, evidence of froth build-up was noticeable at talc additions of 1 %. Subsequent addition of solvent collapsed the froth. With graphite/NaCl, similar observations were observed as with

talc/NaCl: froth buildup with addition of solids and subsequent collapse with advent of solvent.

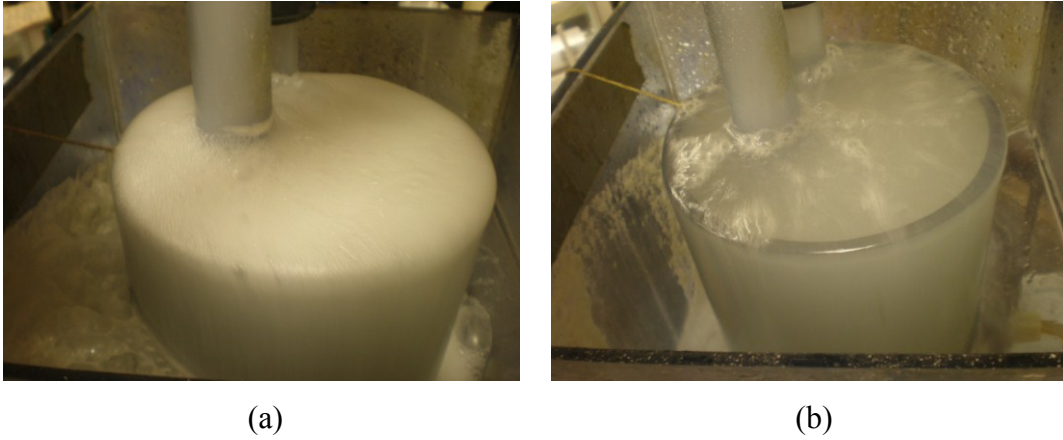


Fig. 4.16. In presence of 0.4 M NaCl: (a) Froth build-up in launder after the addition of 0.5 % w/w talc; (b) Froth collapse after subsequent solvent addition



Fig. 4.17. In presence of 0.4 M NaCl: (a) Froth build-up in launder after the addition of 1 % w/w talc; (b) Froth collapse after subsequent solvent addition

4.5 Discussion

4.5.1 In MIBC system

When MIBC was used as coalescence inhibitor, upon addition of solvent gas holdup decreased and bubble size increased (as seen in Chapter 3). The collapse of the bubble bed was attributed to solvent droplets bridging and/or spreading at the air-water interface causing inter-bubble film thinning and subsequent rupture (Figure 3.25 in Chapter 3). This mechanism implies that the de-stabilizing effect of the solvent overrides the coalescence inhibiting effect of the MIBC adsorbed at the air-water interface.

The addition of hydrophobic solid particles, talc and graphite, did not collapse the bubble bed. This may indicate that bridging alone does not cause the bed collapse but rather it is related to a spreading mechanism available only to the liquid solvent. The talc and graphite in fact appeared to add stability, amounts up to 0.07 % w/w increasing gas holdup, decreasing bubble size, and causing foam (froth) to form in the separation tank. The theory indicated that hydrophobic solids can stabilize foam depending on loading at the air-water interface. In Kuan and Finch (2010) froth stabilization by addition of similar amounts of talc as here was observed, notably with alcohol type frothers. Blonde and Finch (2012), in their work on visualization of flow in froth, found that frothers required talc to produce a stable and transportable froth.

In the MIBC system, the presence of talc, even as little as 0.07 % w/w and up to 1 % w/w, stabilized the bubble bed against collapse upon subsequent introduction of solvent. This is plausibly due to the presence of two stabilizing entities, the frother molecules and the talc particles which appear to reinforce each other. How they reinforce is not immediately clear. Frother molecules and talc particles may pack together to cause adhesive bonding (Pugh, 1996) sufficient to counter the antifoaming solvent spreading mechanism because foam drainage rate is decreased through the increased surface viscosity and surface elasticity due to the mixed packing. Figure 4.18 is an impression of the coalescence inhibiting effect due to the combination of talc and MIBC at the air-water interface. The packing of the MIBC molecules and talc particles at the interface may both

hinder the droplet from entering the air-water interface and if it does enter may oppose spreading.

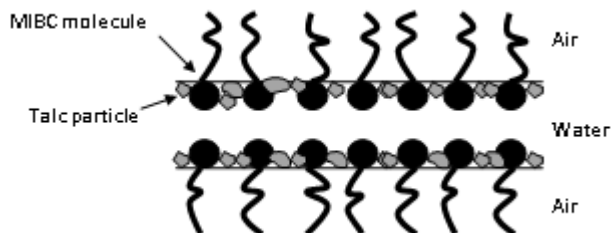


Fig. 4.18. Coalescence inhibiting effect due to packing of talc particles and MIBC molecules at the air-water interface.

4.5.2 In PPG 425 system

In this system, unlike with MIBC gas holdup decreased upon addition of talc above 0.07 % w/w. Kuan and Finch (2010) observed that PPG 425 (in their case the commercial version F150) is adsorbed by talc whereas alcohol frothers (e.g. MIBC) were not. This removal (loss) from solution is one factor reducing the anti-coalescence action of PPG 425 contributing to the decrease in gas holdup and the increase in bubble size. Kuan and Finch went further to speculate on a talc action in competition with PPG 425 adsorbed on the bubble surface (i.e., air-water interface). The mechanism emphasizes the manner in which the PPG 425 molecule sites (orients) at the air-water interface due to its two OH groups. Rather than having the hydrocarbon chain extend into the air (as in the case of the frothers with one OH group such as MIBC), the PPG 425 molecule sits flatter on the interface to accommodate the two OH groups' affinity for water (Figure 4.19). This orientation exposes the hydrophobic chain of the molecule to the hydrophobic face of the talc, opening an adsorption mechanism through hydrophobic interaction. Thus, it was speculated that the talc could detach PPG 425 molecules from the interface further retarding the PPG 425 coalescence inhibiting action. The same effect in the present case would make the talc/PPG 425 system less able to counter the antifoaming action of the solvent compared to the talc-MIBC system, as found. In the talc/MIBC system, the two

combine to counter the solvent effect; but in the talc/PPG 425 system, they interfere to reduce the counteraction and the solvent destabilization effect dominates.

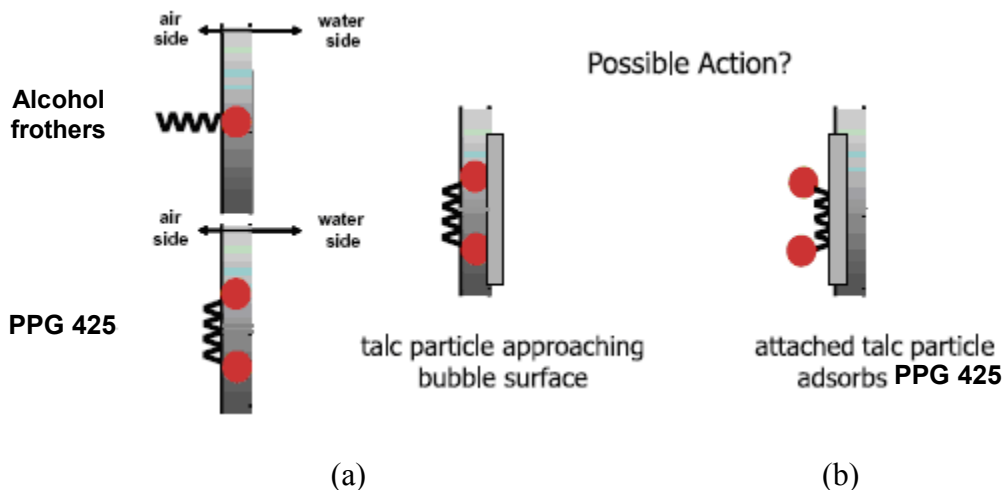


Fig. 4.19. (a) Frother orientation at air-water interface comparing PPG 425 with two OH end groups to frothers with one OH end group (i.e., alcohols, e.g. MIBC); (b) Removal of PPG 425 from interface by adsorption on talc (Adapted and reprinted with permission from Kuan and Finch (2010), Elsevier).

4.5.3 In the NaCl system

4.5.3.1 Talc

Addition of talc increases the gas holdup initially (up to 0.07 % w/w talc) but it stabilizes thereafter (at least up to 1 % w/w talc). The bubble size data are in concert with this trend, decreasing when gas holdup increased and becoming constant when gas holdup stabilized. If coalescence inhibition is the origin of small bubbles, then talc appears to reinforce the effect of salt, but it does leave open the possibility that the effect is on the bubble formation process. The literature is largely silent on any effect of particles on bubble size but the salt/talc (and salt/graphite) system may be the one to study the impact, noting in the present work that talc did not alter bubble size in the presence of MIBC (talc/PPG 425 is a different matter as already discussed). Regardless of this apparent increase in bubble bed stability (also indicated by foam formation in the separation tank),

subsequent introduction of solvent nevertheless collapses the bubble bed as before. The salt/talc combination is not as effective as the MIBC/talc combination in opposing the action of solvent.

4.5.3.2 Graphite

The graphite behaves in a similar fashion to talc at concentrations up to 0.07 % w/w: gas holdup increases and bubble size decreases. At concentrations above 0.07 % w/w up to 1 % w/w, gas holdup was seen to drop though bubble size remained the same. This appears to correspond to the observation in the bubble size analyzer that there was an apparent increase in bubble rise velocity. An increase in bubble velocity in turn decreases gas holdup (the faster bubbles rise the less accumulation of bubbles in a given section in a vessel). If there was a change in bubble velocity when talc was added to the NaCl system, this was not significant enough to be noticed and the camera shutter speed was maintained at the same setting throughout the talc tests. An effect of solid particles decreasing gas holdup with no apparent change in bubble size was reported by Banisi et al. (1995), who also explained it by an effect on bubble velocity, which was later confirmed (Shen et al., 1996).

While outside the intended scope, it is interesting to ponder the difference in behaviour between the two hydrophobic solids. One possibility lies in the fact that graphite is more hydrophobic than talc which has hydrophilic sites. Perhaps the answer lies in the bubble wake mechanism proposed by Banisi et al. (1995): that graphite being more hydrophobic has a higher probability of attaching to a rising bubble and ending up in the bubble wake, increasing the viscosity of the wake and consequently the velocity of the trailing bubbles and hence, the velocity of the bubble swarm.

For our purposes the most important observations is that, like for salt/talc case, subsequent introduction of solvent also collapsed the bubble bed in the salt/graphite case, indeed at a rate faster than the salt/talc combination. Whether this difference in ‘collapse rate’ between talc and graphite in the presence of salt is due to differences in

hydrophobicity or physical properties (particle shape, size) is beyond the data to inform. In comparison to frother (at least MIBC which does not interact with talc) it can be surmised that salt is a less powerful bubble bed stabilizer (a judgment reinforced by the fact that only a few ppm of MIBC is needed while at least 0.2 M salt is required to form the bubble bed in the first place). Being less stabilizing salts cannot take advantage of additional stabilization from talc or graphite compared to MIBC.

4.5.3 Bubble bed collapse and industrial practice of organic removal using Jameson Cells

As noted the Jameson Cell is used for recovering solvent droplets from streams in solvent extraction (SX) plants (Miller and Readett, 1992; Miller et al., 1997; Young et al., 2006). The observation of bubble bed collapse in the presence of solvent in this work leads to the question: Does bubble bed collapse in the downcomer occur when it is used for solvent recovery?

The successful application of the Jameson Cell in SX plants may be related to low organic concentrations. Actual levels are difficult to find, but, for example, Miller et al. (1997) reported levels of 37 ppm being treated by a Jameson Cell. We might reasonably expect levels ranging from 50 to 200 ppm whereas in the present work solvent concentration reached 900 ppm. From the current experience, at concentrations up to 200 ppm, gas holdup was not lost completely suggesting the operation would continue without the effect necessarily being noticed (Figure 4.20). Even in the present work it was noted that when solvent injection was stopped and air was continued turbidity decreased (Figures 3.22 in Chapter 3) implying that droplets are being removed even though gas holdup is low (Figure 3.24). This is evidence that solvent recovery still occurs even after considerable bed collapse.

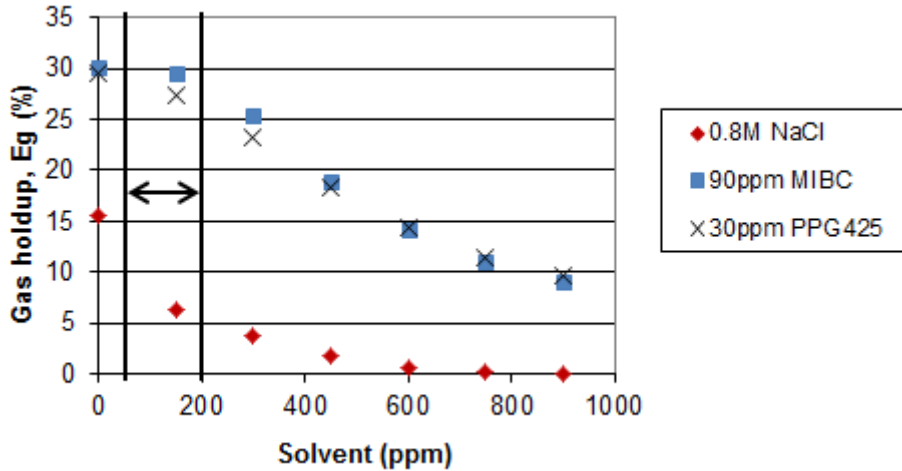


Fig. 4.20. Gas holdup as a function of solvent concentration in presence of MIBC, PPG 425 and NaCl.

4.6 Conclusions

1. Whereas there was a rapid bubble bed collapse with introduction of small amounts of solvent, with the two hydrophobic solids, talc and graphite, the bed did not collapse.
2. The effect of solid addition depended on the system: talc/MIBC - there was no change in gas holdup or bubble size but foam was formed; talc/PPG 425 - gas holdup decreased above 0.07 % w/w talc attributed to adsorption of PPG 425 by talc; talc/NaCl and graphite/NaCl - gas holdup increased and bubble size decreased for additions up to 0.07 % w/w.
3. The effect of subsequent addition of solvent showed one major division: in the talc/MIBC system the bubble bed was stabilized with up to 900 ppm solvent but in all other systems the bubble bed collapsed upon solvent addition.
4. The stability of the bubble bed in the talc/MIBC/solvent system is tentatively attributed to enhanced foam stabilization due to packing of talc particles and MIBC molecules at the air-water interface.
5. The eventual loss of bed stability in the talc/PPG 425 case is attributed to adsorption of the frother by the talc.

6. In presence of NaCl, both talc and graphite showed an initial increase in gas holdup with addition of small amounts of solid up to 0.07% w/w.

4.7 References

Ata, S., Ahmed, N., Jameson, G. J., 2004. *Minerals Engineering* 17, 897-901.

Aveyard, R., Binks, B.P., Fletcher, P.D.I., Peck, T.G., Rutherford, C.E., 1994. Aspects of aqueous foam stability in the presence of hydrocarbon oils and solid particles, *Advances in Colloid and Interface Science* 48, 93-120.

Banisi, S., Finch, J.A., Laplante, A.R., 1995. Effect of solid particles on gas holdup in flotation columns II. Investigation of mechanisms of gas holdup reduction in presence of solids, *Chemical Engineering Science* 50, 2335-2342.

Blonde, P., Finch, J.A., 2012. Visualization of flow in froth. *Minerals Engineering* 35, 16-19.

Dippenaar, A., 1982. The destabilization of froth by solids. I. The mechanism of film rupture, *International Journal of Mineral Processing* 9, 1-14.

Garrett, P.R., 1993. *Defoaming. Surfactant Science Series, Vol. 45.* Marcel Dekker, Inc., New York.

Grau, R.A., Laskowski, J.S., 2006. Role of frothers in bubble generation and coalescence in a mechanical flotation cell. *The Canadian Journal of Chemical Engineering* 84, 1700-182.

Hunter, T.N., Pugh, R.J., Franks, G.V., Jameson, G.J., 2008. The role of particles in stabilizing foams and emulsions, *Advances in Colloid and Interface Science* 137, 57-81.

Kracht, W., 2008. Effect of frother on bubble coalescence, break-up, and initial rise velocity, PhD thesis, McGill University, Montreal, Canada.

Kuan, S.H., Finch, J.A., 2010. Impact of talc on pulp and froth properties in F150 and 1-pentanol frother systems, *Minerals Engineering* 23, 1003-1009.

Miller, G.M., Readett, D. J., 1992. The Mount Isa Mines Limited copper solvent extraction and electrowinning plant. *Minerals Engineering* 5 (10-12), 1335-1343.

Miller, G.M., Readett, D.J., Hutchinson, P., 1997. Experience in operating the Girilambone copper SX-EW plant in changing chemical environments. *Minerals Engineering* 10(5), 467-481.

Nesset, J.E., Hernandez-Aguilar, J.R., Acuna, C., Gomez, C.O., Finch, J.A., 2006. Some gas dispersion characteristics of mechanical flotation machines, *Minerals Engineering*, 19 (6-8), 807-815.

Nesset, J.E., Finch, J.A., Gomez, C.O., 2007. Operating variables affecting bubble size in forced-air mechanical flotation machines, *AusIMM, Proceedings of the 9th Mill Operators Conference*, 55-65.

Neiman, O., Hilscher, B., Siy, R., Secondary recovery of bitumen using Jameson downcomers, 2012. 44th Annual Canadian Mineral Processors Conference, Ottawa, Canada. January 17 -19.

Pugh, R.J., 1996. Foaming, foam films, anti-foaming and defoaming. *Advances in Colloid and Interface Science* 64, 67-142.

Ross, S., McBain, J.W., 1944. Inhibition of foaming in solvents containing known foamers. *Industrial and Engineering Chemistry* 36(6), 570-573.

Shen, G., G, Finch, J.A., 1996. Bubble swarm velocity in a column. *Chemical Engineering Science* 51 (14), 3665-3674.

Simovic, S., Prestidge, C.A., 2004. *Langmuir* 20, 8357-65.

Smith, T., Lin, D., Brigitte, L., Anderson, G., 2008. Removal of organic carbon with a Jameson cell at Red Dog Mine, 40th Annual Canadian Mineral Processors Conference, Ottawa, Canada. January 22 -24.

Summers, A., Xu, M., Finch, J.A., 1995. Technical Note: Effect of level in separation tank on downcomer behaviour in a Jameson Cell, *Minerals Engineering* 8 (12), 1607-1613.

Young, M.F., Barnes, K.E., Anderson, G.S., Pease, J.D., 2006. Jameson Cell: The 'comeback' in base metal applications using improved design and flow sheets. *Proceedings, 38th Annual Meeting of the Canadian Mineral Processors*, January 17-19, 2006, Ottawa, Canada, 311-332.

Chapter 5 – Solvent droplet-bubble contact in presence of frothers, salt and hydrophobic solids

5.1 Introduction

The previous chapter (Chapter 4) compared the effect on bubble bed stability of two hydrophobic solids, talc and graphite, to that of solvent, i.e. a hydrophobic liquid. The results showed that the solids did not affect the bubble bed in the same way as the solvent: rather than destabilize the bubble bed as did the solvent, if anything the solids promoted bed stability. Possible mechanisms in each scenario (combination of coalescence inhibitor, solid, and solid plus solvent) were presented. The purpose of this chapter is to test the mechanisms using a bubble-droplet contact setup.

5.2 Experimental

5.2.1 General setup and procedure

The setup is designed to simulate the bubble-droplet contact environment of the downcomer. Two apparatus were built. The first is shown in Figure 5.1. It comprises a transparent acrylic cell of 7.5 cm by 7.5 cm by 21 cm, two steel capillaries (ID = 1 mm, OD = 3 mm) mounted one on either side to generate air bubbles, with a third vertical capillary to introduce a solvent droplet. Bubbles and droplet were generated using a syringe. A light source was placed behind the cell for illumination. Images were captured using a high speed camera (Fastec Imaging model TSHRMS) at 250 to 500 frames per second. The vertical capillary was held in a removable acrylic top to the cell. The capillary was later replaced with a syringe to reduce the droplet size produced.

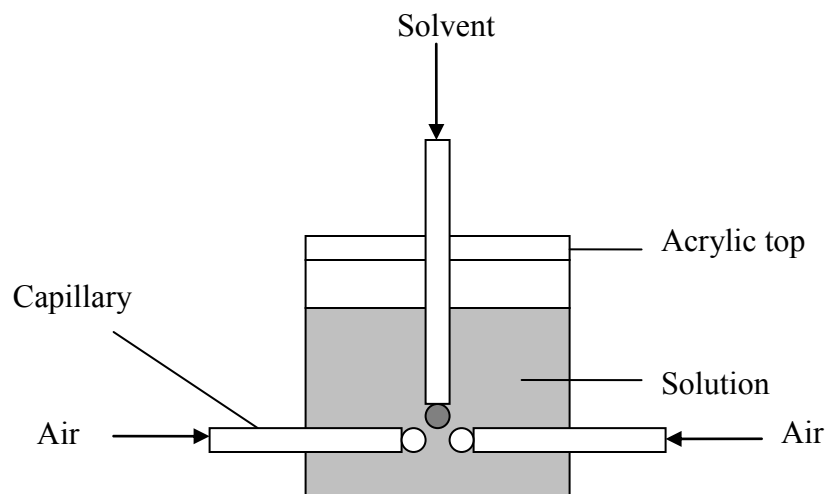


Fig. 5.1. Setup 1: Contacting two bubbles with a solvent droplet

Solution was prepared and placed in the cell. Bubbles were produced, brought close together, ca. 0.4 - 0.6 mm (i.e., not touching), then a solvent drop was introduced and contacted with the bubbles.

The setup did not produce outcomes that helped interpret the results in Chapter 4. The suspected limitation was the size of droplet that could not be made small enough relative to the bubble. The solution (setup 2 in Figure 5.2) was to retain the two capillaries for bubble generation but to introduce solvent as dispersions in a circulating stream. This setup also permitted testing dispersions of solids (talc or graphite). A pump (Masterflex model 7553-50) circulated the dispersion.

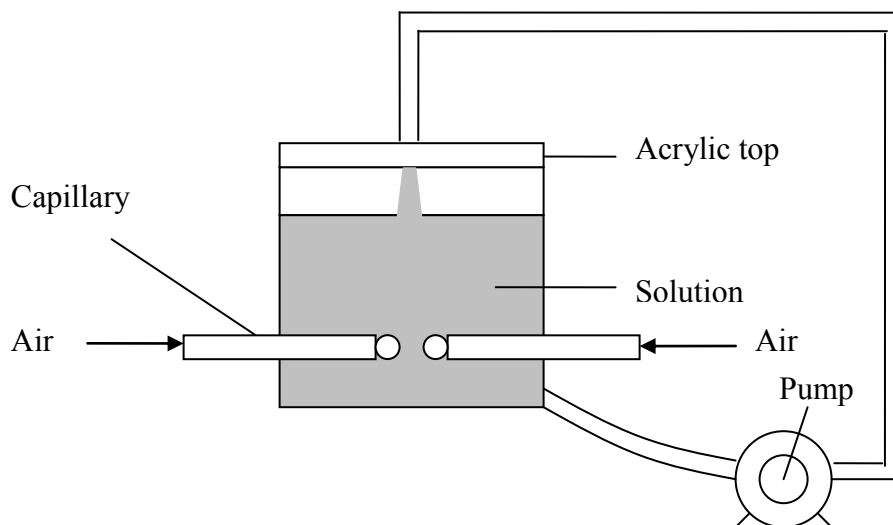


Fig. 5.2. Setup 2: Contacting circulating dispersion past the bubbles.

5.2.2 Materials and methods

The solvent used, unless otherwise stated, was the LIX:kerosene 1:29 (Some properties of the solvent are given in Table 3.2 of Chapter 3). In setup 2 when solvent droplets were circulated, solvent concentrations were varied between 1000 to 5000 ppm. Most tests were conducted at 1600 ppm since at higher concentrations, solvent film build-up was too rapid and at lower concentrations the frequency of solvent droplet-bubble collision was too low. Pump flowrate was set at 375 ml/min, the maximum before bubbles would vibrate too rapidly and dislodge from the capillary.

As in Chapter 4, two frothers (MIBC and PPG 425) and one salt (NaCl) were used. Laboratory grade talc (supplied by Fisher Scientific) was weighed with an analytical balance (Mettler AJ100) and dispersed into the solution by stirring. The specific gravity was 2.5 - 2.8 with an average particle size of 2.5 μ m. About 0.02 % w/w or 200 ppm talc was added, selected to retain good visibility which disappeared completely above 0.04 % w/w talc. Graphite was added only when NaCl was used due to the fact that frothers are

adsorbed by graphite. It served as a stronger hydrophobic counterpart to talc, with no hydrophilic sites. The specific gravity was 1.9 with an average particle size of 1 – 2 μm . About 0.02% w/w or 200 ppm graphite was added, again to preserve visibility.

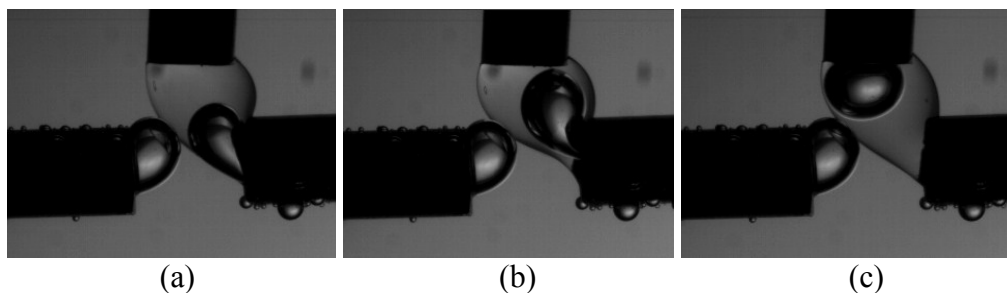
Surface and interfacial tension measurements were made using the plate method with the Kruss K12 tensiometer. The measurements were used in Equations 3.4 to 3.6 (Chapter 3) to predict if the solvent droplet would enter the air-water (aqueous) interface and spread over the bubble.

5.3 Results

5.3.1 Setup 1: Droplet contacting the two bubbles

5.3.1.1 $D_d/D_b \gg 1$

Using the capillary droplet size (diameter ca. 3 mm) was larger than the bubbles (ca. 2.1 mm). Under these conditions the solvent tended to spread on one bubble before the other (Figure 5.3 b). Repeat experiments (up to 10 times) showed that this preference of one bubble over the other was consistent and the choice, left or right bubble, was random. Once solvent had spread over both bubbles, the bubbles did not coalesce after a period of ca. 3 min (Figure 5.3e).



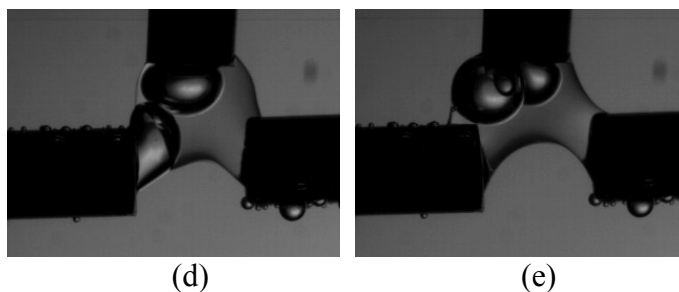


Fig 5.3. Setup 1: Solvent droplet in contact with two bubbles in presence of 50 ppm MIBC: a) Initial contact and spreading of droplet over first bubble; (b)-(c) Displacement of bubble towards the solvent capillary; (d) Spreading of droplet over the second bubble; (d)-(e) Displacement of second bubble towards the solvent capillary; (e) No coalescence after extended time.

Although rare, there were occurrences where the solvent spread simultaneously on both bubbles. The phenomenon is captured in Figure 5.4. Again, the bubbles did not coalesce after an extended time (ca. 3 min).

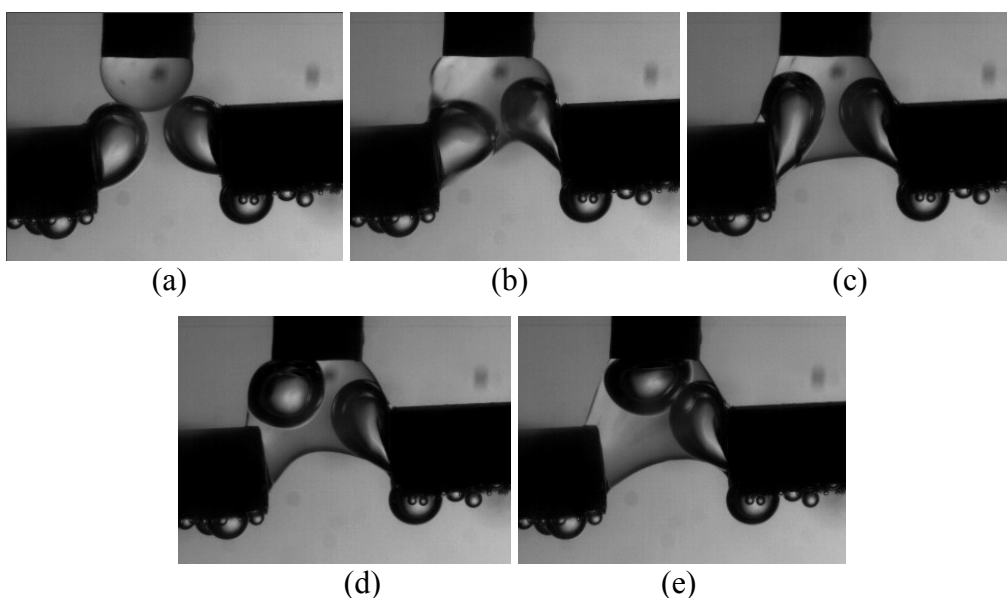


Fig 5.4. Setup 1: Solvent droplet formed at capillary in contact with two bubbles in water: (a) Initial contact of droplet and bubbles; (b) Spreading of droplet over two bubbles;

(c)-(d) Bubbles displaced towards solvent capillary; (e) No coalescence observed after extended time.

The observation common to Figures 5.3 and 5.4 is that the bubbles are virtually immersed in solvent, i.e., the inter-bubble solvent film is quite thick. The experiment was modified to try to reduce the volume of solvent retained on the bubbles by retreating the droplet back into the capillary to leave a thinner film of solvent between the two bubbles. Under these conditions coalescence was observed (Figure 5.5).

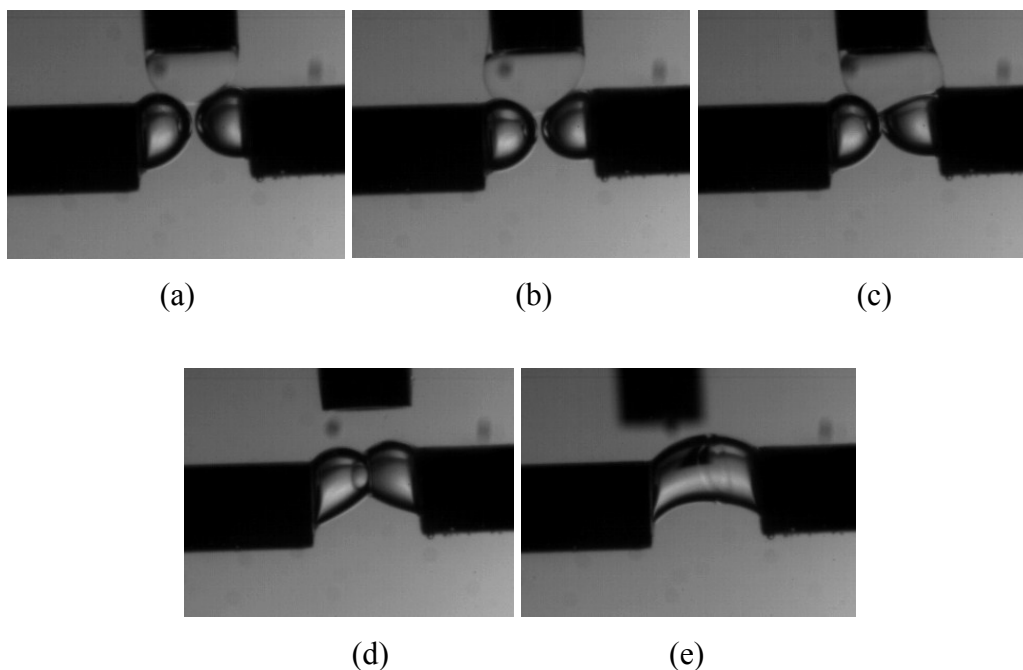


Fig 5.5. Setup 1: Solvent droplet formed at capillary in contact with two bubbles in presence of 10 ppm PPG 425: (a) Initial contact of droplet with bubbles; (b) Spreading of solvent droplet over one bubble; (c) Spreading of droplet over the second bubble; (d) Droplet receded back into capillary; (e) Coalescence occurs.

Figures 5.3 and 5.4 indicate that large solvent droplets relative to the bubble ($D_d / D_b = 1.4$) did not induce bubbles to coalesce. Figure 5.5 showed that when the solvent amount (film) was reduced, bubble coalescence was observed. This prompted use of the syringe to produce a droplet size smaller than the bubble size.

5.3.1.2 $D_d/D_b < 1$

In the case where the droplet (1.5 mm) was smaller than the bubbles (2.1 mm) or $D_d / D_b = 0.7$, again the droplet spread on one bubble before the other (Figure 5.6). After a certain time (ca. 50 s starting from the initial contact between the droplet and bubbles), the bubbles coalesced, forming a larger bubble engulfed in a solvent film (Figure 5.6). The same phenomenon was observed with PPG 425 (Figure 5.6), MIBC and NaCl (refer to Appendix: Figures A10 and A11).

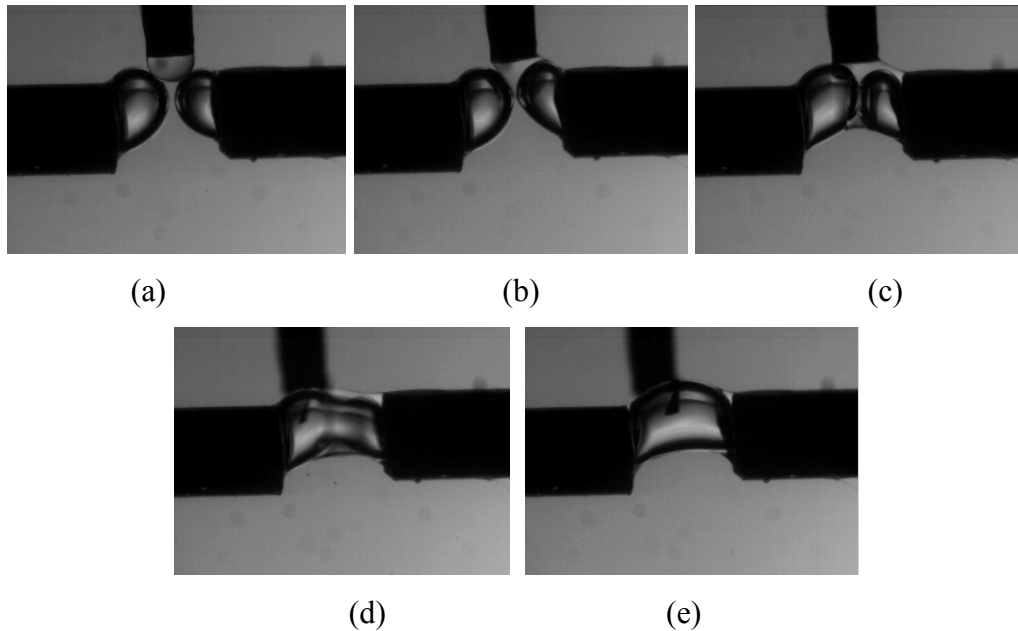


Fig 5.6. Setup 1: Solvent droplet formed with syringe in contact with two bubbles in presence of 10 ppm PPG 425: (a) Initial contact of droplet with bubbles; (b) Spreading of solvent droplet over one bubble; (c) Spreading of droplet over the second bubble; (d) Coalescence occurs; (f) Solvent film stabilizes.

5.3.2 Setup 2: Circulating dispersions

5.3.2.1 Water only

In water alone when the bubbles were held at a separation distance of ca. 0.04 – 0.06 mm, no coalescence occurred after a period of ca. 3 min (Figure 5.7).

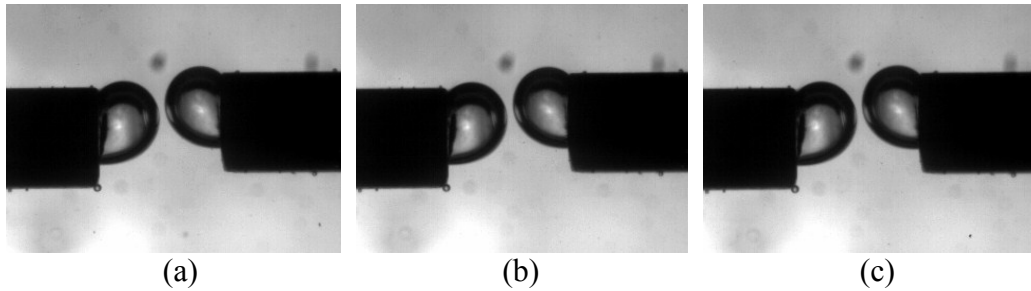
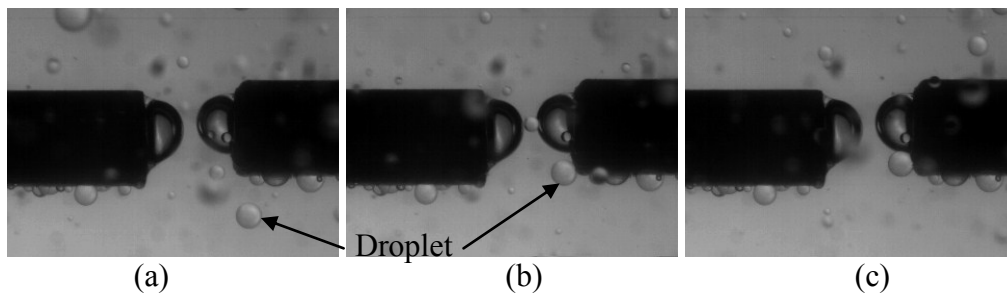


Fig. 5.7. Setup 2: Two bubbles in water only

5.3.2.1.1 Water and solvent

When solvent droplets were circulated, the droplets would collide with and spread on the bubbles (Figure 5.8 b - e). This event repeated over a period of time (typically ca. 3 s was allowed) building up a solvent layer on the bubble. Figure 5.9 shows the build-up of solvent layer on one bubble over time and subsequent spreading over the other bubble (Figure 5.9 e - f).



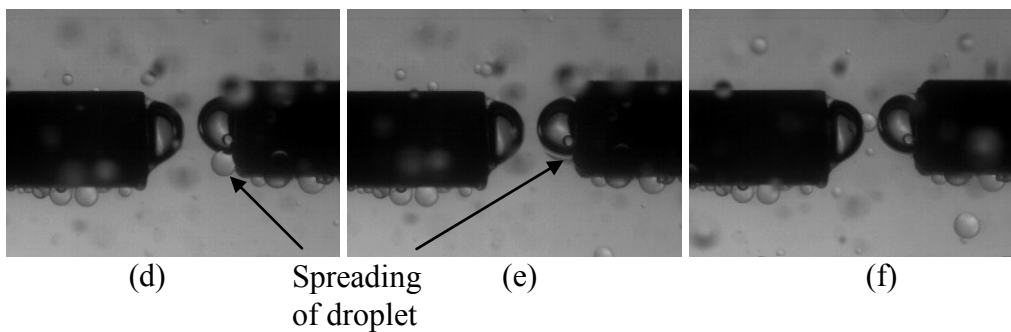


Fig. 5.8. Setup 2: Solvent droplet colliding with bubble and spreading (ca. 3 s).

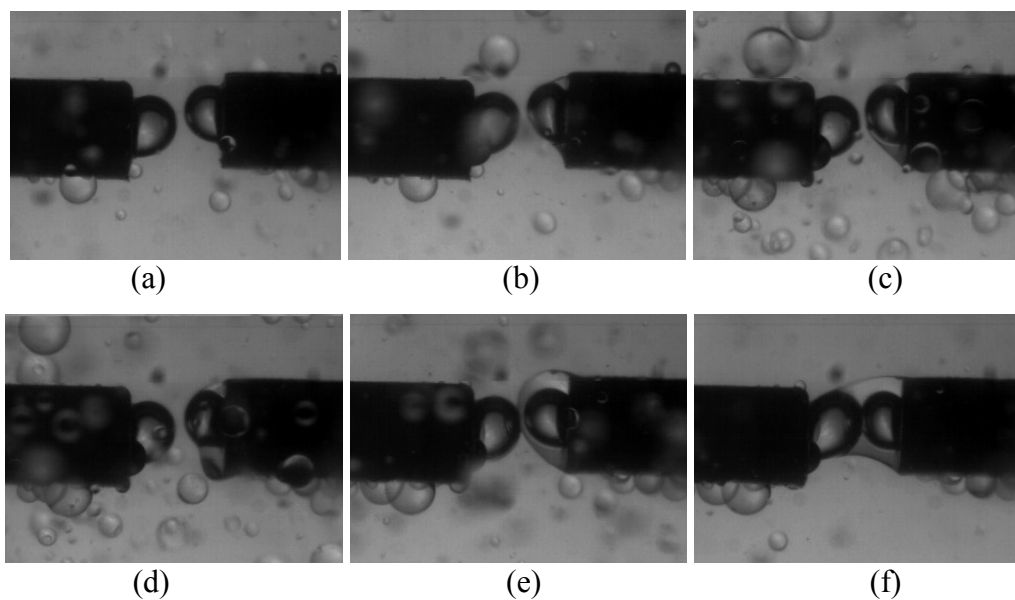


Fig. 5.9. Setup 2: Build-up of solvent layer through time (ca. 37 s).

5.3.2.2.2 *Water and talc or graphite*

In presence of talc (Figure 5.10) or graphite (Figure 5.11), coalescence was observed after a certain time measured from the start of circulation (ca. 65 - 70 s).

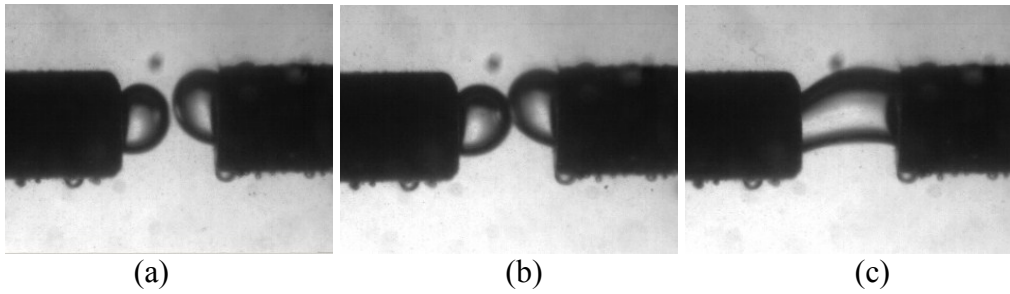


Fig. 5.10. Setup 2: Water and 0.02 % w/w talc, time from a to c, ca. 65-70 s.

In presence of graphite, coalescence of the bubbles was also observed after a certain elapse of time (ca. 65 - 70 s), as shown in Figure 5.11.

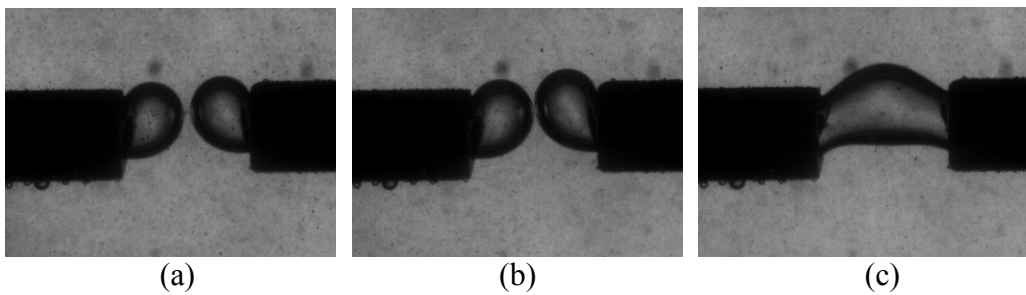


Fig. 5.11. Setup 2: Water and 0.02 % w/w graphite, time from a to c, ca. 65-70 s.

5.3.2.2 *In presence of MIBC*

5.3.2.2.1 *MIBC alone*

When 50 ppm MIBC solution was circulated, coalescence did not occur after a period of ca. 3 min (Figure 5.12).

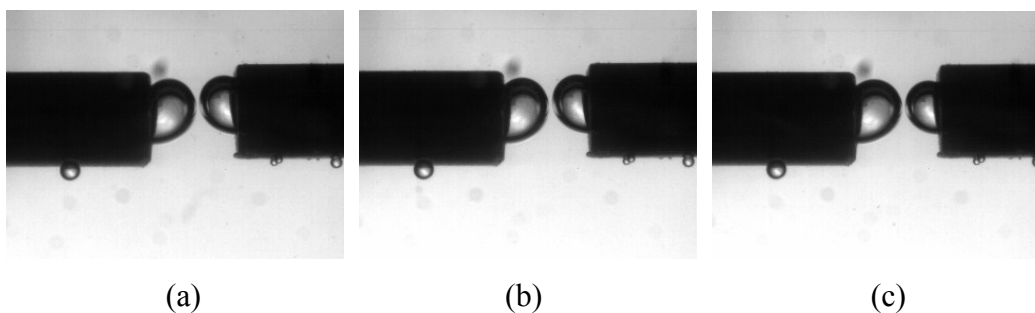


Fig. 5.12. Setup 2: 50 ppm MIBC.

5.3.2.2.2 MIBC and solvent

When solvent droplets were circulated with the 50 ppm MIBC solution, the bubbles coalesced after ca. 65 – 75 s (again measured from the start of circulation), as shown in Figure 5.13. The bubbles seem to be drawn closer to each other until coalescence occurs.

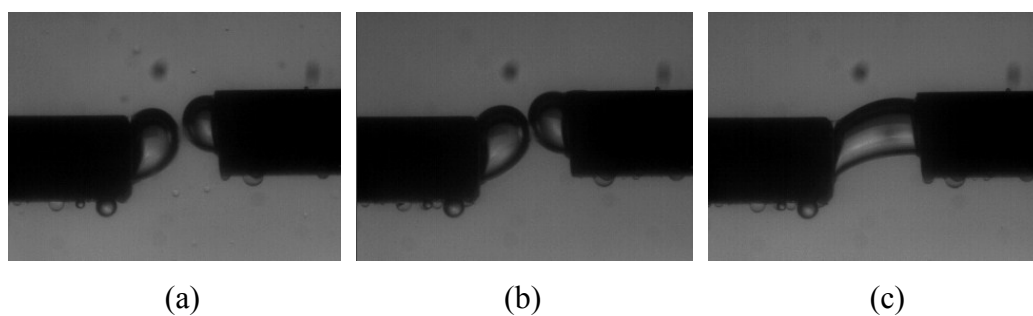


Fig. 5.13. Setup 2: 50 ppm MIBC and 1600 ppm solvent (time from a to c, ca. 65 - 70s)

5.3.2.2.3 MIBC and talc

When talc was circulated with the 50 ppm MIBC solution, the bubbles did not coalesce after an extended period of time (ca. 3 min), as shown in Figure 5.14.

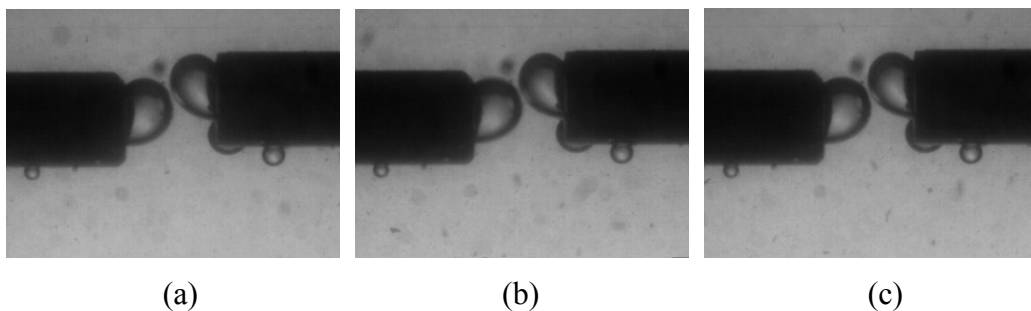


Fig. 5.14. Setup 2: 50 ppm MIBC and 0.02 % w/w talc.

5.3.2.2.4 MIBC, talc and solvent

When both talc and solvent were circulated with 50 ppm MIBC, bubbles did not coalesce after an extended period (ca. 3 min), as shown in Figure 5.15.

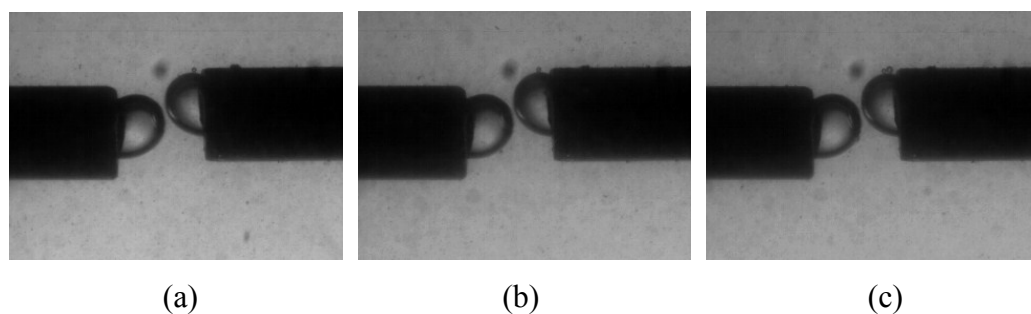


Fig. 5.15. Setup 2: 50 ppm MIBC, 0.02 % w/w talc, and 1600 ppm solvent.

5.3.2.3 In presence of PPG 425

5.3.2.3.1 PPG 425 alone

In 10 ppm PPG 425 solution, no coalescence was observed after an extended period of time (ca. 3 min), shown in Figure 5.16.

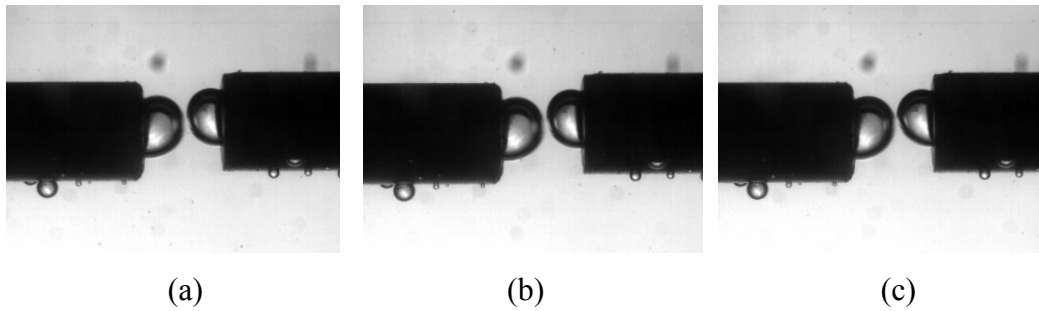


Fig. 5.16. Setup 2: 10 ppm PPG 425.

5.3.2.3.2 PPG 425 and solvent

When solvent droplets were circulated with the 10 ppm PPG 425 solution, coalescence was observed after about the same lapse of time (ca. 62 - 70 s) noted in the other coalescence events. As with MIBC and solvent, the bubbles seem to be drawn closer to each other until they coalesce (Figure 5.17).

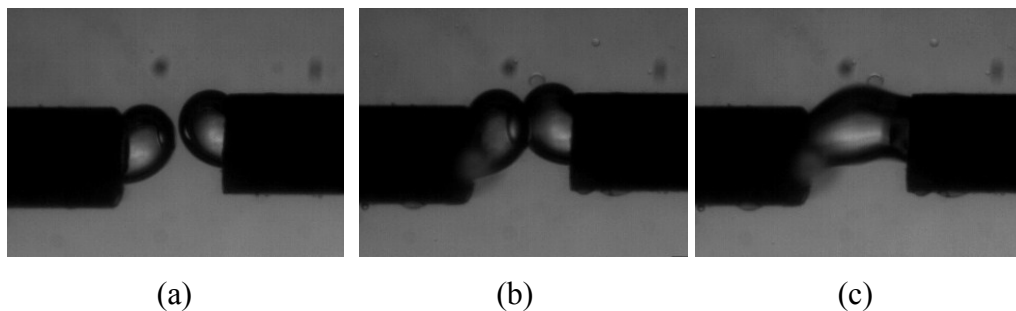


Fig 5.17. Setup 2: 10 ppm PPG 425 and 1600 ppm solvent

When solvent was circulated in 10 ppm PPG 425 solution, an occurrence where a solvent droplet was held between two bubbles was captured (D_d / D_b ca. 0.2). Video sequences indicate that the solvent droplet draws the bubbles closer to each other (Figure 5.18). After about 17 s, the two bubbles held together (bridged) by the solvent droplet coalesced.

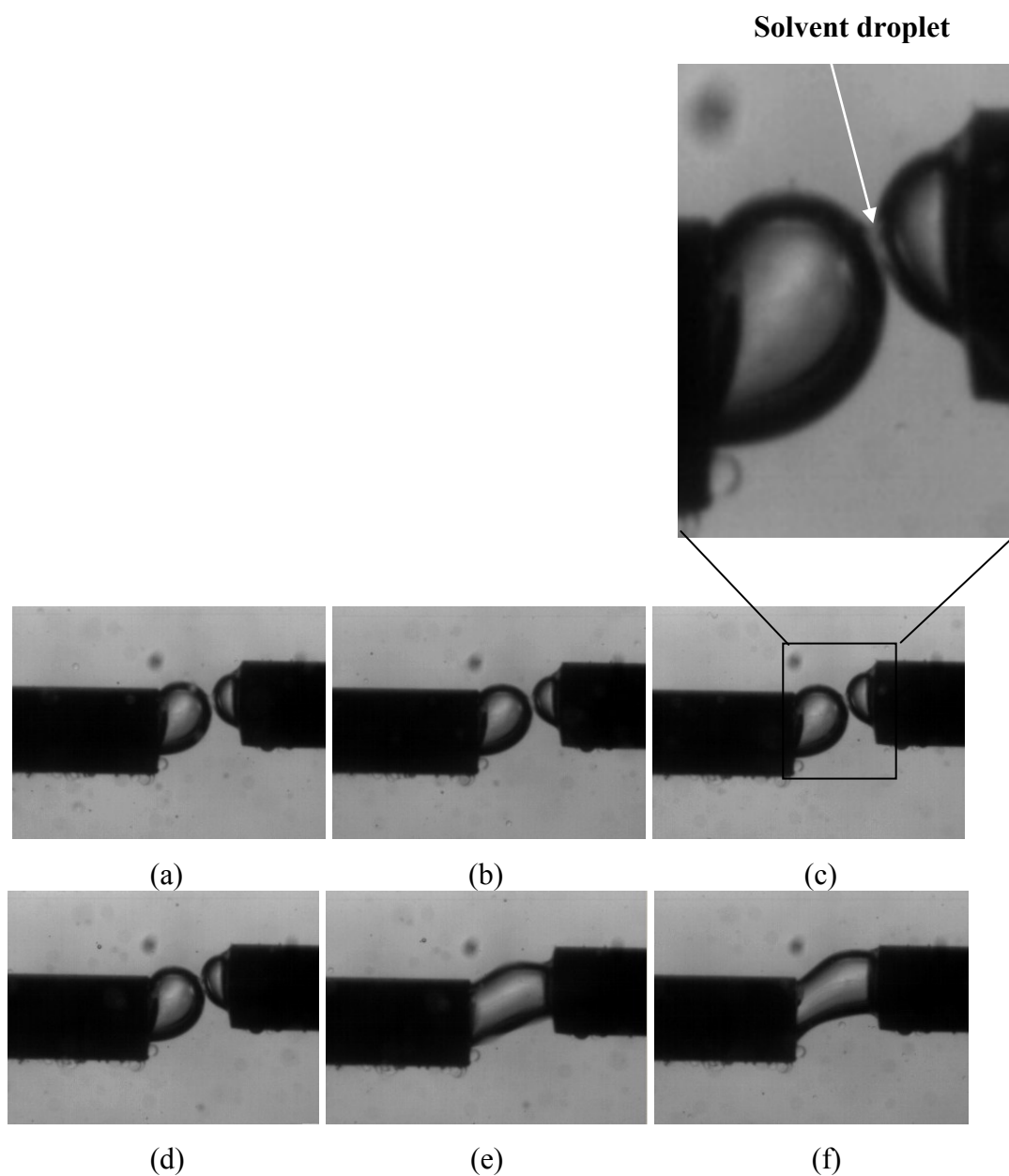


Fig. 5.18. Setup 2: Solvent droplet attaches (a) and bridges the two bubbles (b – d) causing coalescence (e – f) with 10 ppm PPG 425 (D_d / D_b ca 0.2)

5.3.2.3.3 PPG 425 and talc

With addition of talc circulating with the 10 ppm PPPG solution, coalescence was observed after an elapse of time (ca. 62 - 70 s), as shown in Figure 5.19.

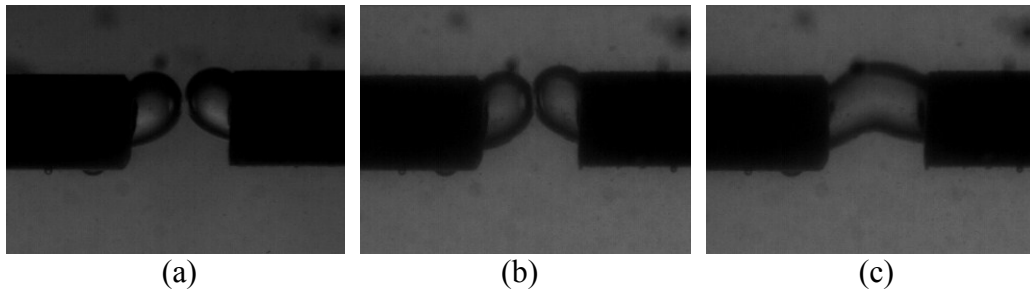


Fig. 5.19. Setup 2: 10 ppm PPG 425 and 0.02 % w/w talc.

5.3.2.3.4 PPG 425, talc, and solvent

When the talc - solvent mix was circulated with 10 ppm PPG 425, coalescence was observed after ca. 63 - 71 s, as shown in Figure 5.20.

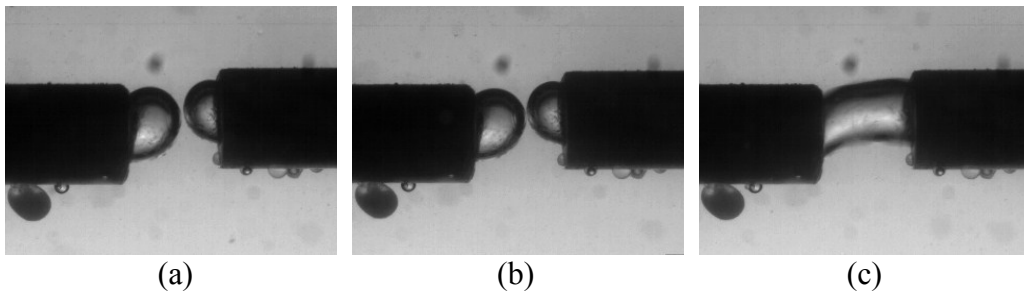


Fig. 5.20. Setup 2: 10 ppm PPG 425, 0.02 % w/w talc and 1600 ppm solvent .

5.3.2.4 In presence of NaCl

5.3.2.4.1 NaCl alone

In 0.4 M NaCl solution, no coalescence event was observed after an extended period of time (ca. 3 min), as shown in Figure 5.21.

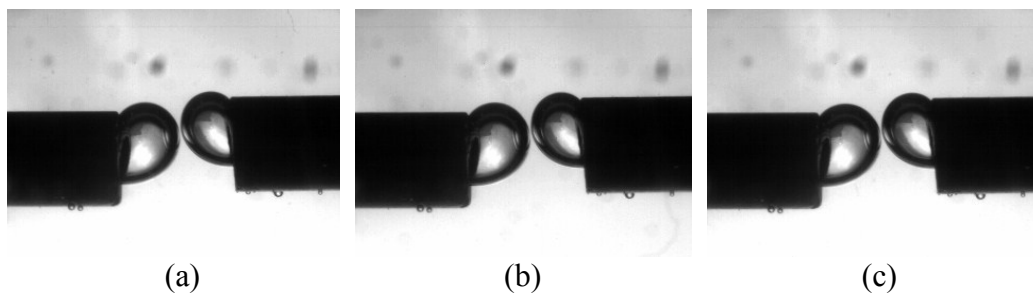


Fig. 5.21. Setup 2: 0.4 M NaCl.

5.3.2.4.2 *NaCl and solvent*

When solvent was circulated with the 0.4 M solution, coalescence was observed after a certain elapse of time (59 - 67 s), as shown in Figure 5.22.

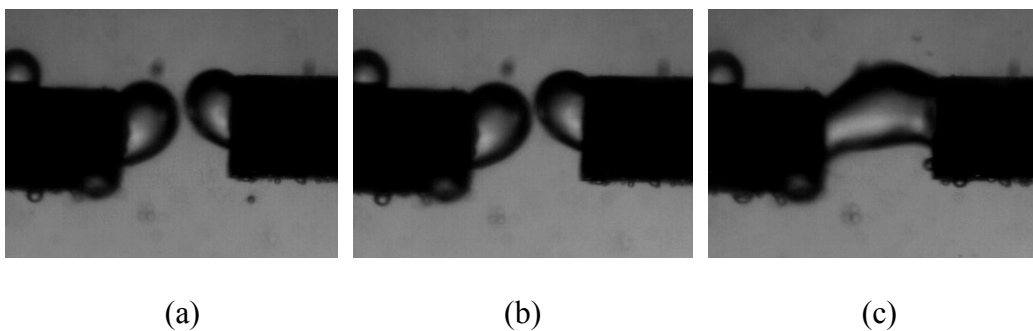


Fig. 5.22. Setup 2: 0.4 M NaCl and 1600 ppm solvent

5.3.2.4.3 *NaCl and talc*

In 0.4 M NaCl solution when talc was added, coalescence was not observed for up to ca. 3 min), as shown in Figure 5.23.

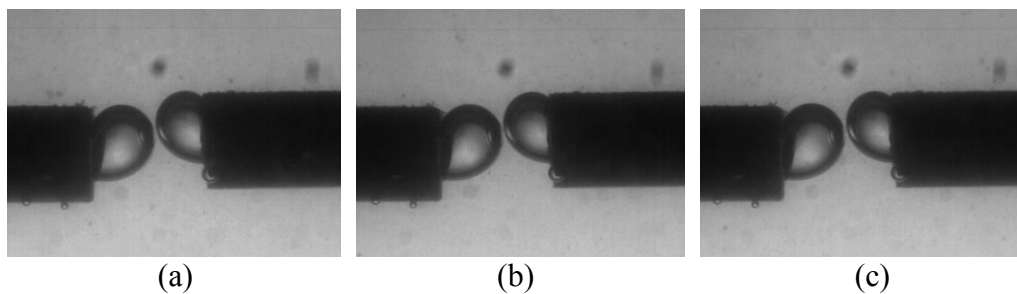


Fig. 5.23. Setup 2: 0.4 M NaCl and 0.02 % w/w talc.

5.3.2.4.4 NaCl, talc and solvent

In 0.4 M NaCl solution, in presence of solvent and talc, coalescence was not observed even after an extended period of time (ca. 3 min), as shown in Figure 5.24.

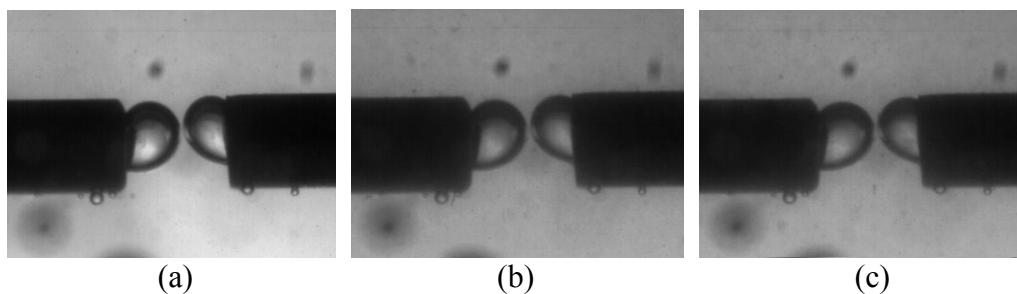


Fig. 5.24. Setup 2: 0.4 M NaCl, 0.02 % w/w talc and 1600 ppm solvent .

5.3.2.4.5 NaCl and graphite

In 0.4 M NaCl solution, when graphite was added, coalescence was not observed after an extended elapse of time (ca. 3 min), as shown in Figure 5.25.

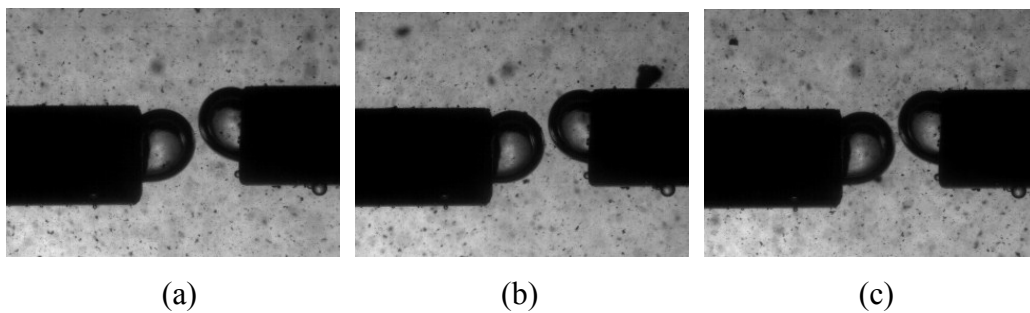


Fig. 5.25. Setup 2: 0.4 M NaCl and 0.02 % w/w graphite.

5.3.2.4.6 NaCl, graphite, and solvent

In 0.4 M NaCl solution, in presence of solvent and graphite, coalescence was observed after ca. 67 - 75 s, as shown in Figure 5.26.

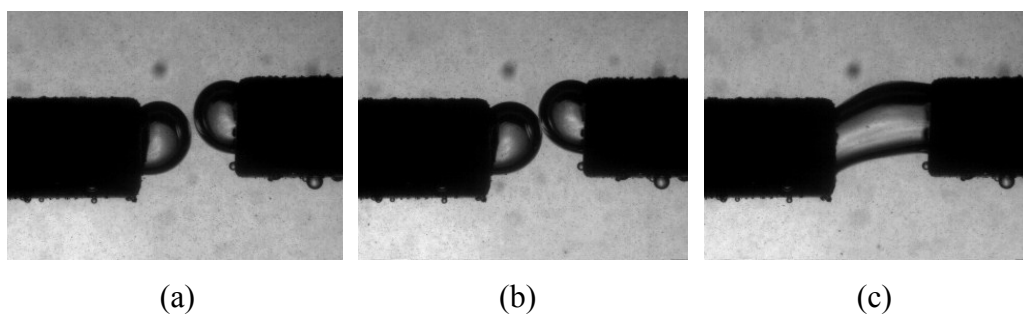


Fig. 5.26. Setup 2: 0.4 M NaCl, 0.02 % w/w graphite and 1600 ppm solvent.

5.3.2.5 Summary

Table 5.1 summarizes the outcome for each scenario.

Table 5.1 Coalescence, yes or no, for each condition tested.

Dispersion	Alone	With solvent	With talc	With talc and solvent	With graphite	With graphite and solvent
Water	No	No (but spreads)	Yes	-	Yes	-
50ppm MIBC	No	Yes	No	No	-	-
10 ppm PPG 425	No	Yes	Yes	Yes	-	-
0.4M NaCl	No	Yes	No	No	No	Yes

5.3.3 Surface and interfacial tensions

The measurements are shown in Table 5.2. Substituting in equations 3.4 to 3.6 (Chapter 3), the entry coefficient (E), bridging coefficient (B), and spreading coefficient (S) for spreading of a solvent droplet in water, 50 ppm MIBC, 10 ppm PPG 425, and 0.4 M NaCl solutions were calculated. In all cases, the E, B and S were positive, i.e., the equations predict that the solvent droplet (LIX:Kerosene 1:29) would enter the interface, form an oil bridge and spread, causing film rupture which leads to bubble coalescence.

Table 5.2. Measurements of interfacial tensions and computation of E, B and S coefficients for solvent (LIX:kerosene 1:29)-aqueous solution systems..

Aqueous phase	$\gamma_{W/A}$	$\gamma_{W/O}$	$\gamma_{O/A}$	Entry coefficient E	Bridging coefficient B	Spreading coefficient S
Water	73.5	22.0	26.9	68.6	5157	24.6
50 ppm MIBC	71.8	20.8	26.9	65.8	4870	24.1
10 ppm PPG 425	64.3	20.0	26.9	57.4	3815	17.5
0.4 M NaCl	74.5	22.3	26.9	69.9	5328	25.4

5.4 Discussion

In attempting to coat swarms of bubbles with solvent using the downcomer, bubble bed collapse was encountered, signified by rapid decrease in gas holdup and aspirated air rate and increase in bubble size (Chapter 3). The addition of solvent collapsed the bubble bed regardless of which coalescence inhibitor was used, MIBC (alcohol-based frother), PPG 425 (polyglycol-based frother) or NaCl, or how the solvent was introduced, into the bubble bed, into the feed solution, or into the air as aerosol. The mechanism of film rupture known in the case of foam caused by attachment, bridging and/or spreading of oil (solvent) droplets was speculated to be the origin of the bed collapse.

Both solid and liquid hydrophobic particles can bridge and cause coalescence of bubbles (Dippenaar, 1982; Pugh, 1996). Liquid particles however, have an extra feature, i.e., the spreading action at the interface (Figure 3.25, Chapter 3). Thus, it became a point of interest to examine the effect of hydrophobic solids on the bubble bed and compare to that of solvent. The last chapter (Chapter 4) was dedicated to that objective. The results showed that the two hydrophobic solids tested, talc and graphite, did not affect the bubble bed in the same way as the solvent, if anything tending to promote bed stability rather than disrupt.

This chapter aimed at direct observation of the mechanisms using a model setup of two bubbles held in close proximity (0.04 – 0.06 mm) and contacted by various combinations of solvent droplet, solid and solid/droplet. Results from the first approach (setup 1) where a solvent droplet was introduced showed that when the solvent droplet was larger than the bubbles ($D_d / D_b = 1.4$), no coalescence occurred but instead a rather extensive solvent layer (film) built up. The resulting film was stable over an extended period (more than 3 min). When the solvent droplet size was halved ($D_d / D_b = 0.7$), coalescence was observed regardless whether PPG 425, MIBC or NaCl was used. The film in the second case, it appears, was thin enough to rupture.

Setup 1 was replaced by setup 2 for all subsequent tests. This new arrangement better simulates the conditions in the downcomer where bubbles are exposed to circulating dispersions of solvent droplets. The setup also permitted solid particle dispersions to be examined, for which setup 1 was not suited. The circulation settings were selected such that in the absence of solvent and/or solids the bubbles did not coalesce (Table 5.1). This result, of course, was expected but did in addition serve the purpose of showing the separation distance was well maintained in face of the turbulence introduced by the circulating dispersions.

With the circulation of solvent droplets, coalescence occurred in all situations except in water alone where spreading and building of an intervening layer sufficient to resist rupture occurred. It is perhaps of some note that with all three coalescence inhibitors the solvent film is apparently thinner and prone to rupture.

The time to coalesce was always about the same. This is likely because time zero was the start of circulation and thus includes the time for particles (solvent or solid) to encounter a bubble and probably dwarfs the time over which the events of particle attachment, bridging, and spreading occur. In consequence the times have no quantitative value hence the summary (Table 5.1) is ‘yes’ ‘no’ in terms of coalescence.

The coalescence mechanism in the setup when solvent was introduced is speculated to be the same that induced collapse of the bubble bed, i.e., film rupture caused by the attachment, bridging and/or spreading of solvent droplets, as shown in Figure 3.25 (Chapter 3). Some evidence for this mechanism was captured in the case of 10 ppm PPG 425. The video shows that a solvent droplet ($D_d / D_b = 0.2$) attaches, bridges the two bubbles and induces coalescence (Figure 5.18) although spreading was not evident.

The results show that the hydrophobic solids, talc and graphite, exhibit a bridging/coalescence effect in water alone (Figure 5.10 and 5.11), but not in the presence of two of the coalescence inhibitors, MIBC and NaCl. The lack of coalescence in the presence of MIBC and NaCl corresponds with their being no bubble bed collapse in these cases either. It may be pertinent that the solid particle bridging/coalescence event described by Dippenaar (1982), shown in Figure 4.1 (Chapter 4), was with distilled water, no coalescence inhibitor apparently being tested. The presence of coalescence inhibitor appears to counter the destabilizing effect of hydrophobic solid particles. The exception was the talc/PPG 425 system, where adsorption of frother by the talc is known to occur (Kuan and Finch, 2010) and can be considered to have reduced coalescence inhibition, as argued in Chapter 4 regarding the loss of some bubble bed stability in the talc/PPG 425 system.

The results generally correspond to the observation of bubble bed collapse seen in the Chapters 3 and 4. Table 5.3 summarizes the observation of bubble bed collapse in the downcomer and coalescence in the bubble contact device. There is good correspondence the exception being talc/NaCl/solvent where coalescence was not observed but the bubble bed did collapse.

Table 5.3. Observations of bubble bed collapse in downcomer (A) and coalescence in the bubble contact setup (B).

Conditions	Alone		With solvent		With talc		With talc and solvent		With graphite		With graphite and solvent	
	A	B	A	B	A	B	A	B	A	B	A	B
50ppm MIBC	No	No	Yes	Yes	No	No	No	No	-	-	-	-
10ppm PPG 425	No	No	Yes	Yes	Yes	Yes	Yes	Yes	-	-	-	-
0.4M NaCl	No	No	Yes	Yes	No	No	Yes	No	No	No	Yes	Yes

The bubble contact results, and by inference the bubble bed collapse results, are predicted by the estimates of E, B and S. For the case of solvent introduced into 50 ppm MIBC, 10 ppm PPG 425, and 0.4 M NaCl, equations 3.4 to 3.6 (Chapter 3) indicate that the solvent droplet will enter the air-aqueous interface ($E > 0$), form an oil bridge ($B > 0$), and spread ($S > 0$) (Table 5.2).

The difference between hydrophobic liquids and solids, the former causing coalescence the latter not, appears to be related to spreading: both solid particles and solvent droplets can bridge, but solvent has the added feature of being able to spread whereas solids obviously cannot. Spreading was not readily evident in the videos, e.g. in Figure 5.18. The solid particles would bridge and cause coalescence in water only, the effect being retarded by the presence of MIBC and NaCl. In most cases, the subsequent addition of solvent causes coalescence and bubble bed collapse thus the de-stabilizing effect of the solvent (oil) is greater than any stabilizing effect of the solid particle/coalescence inhibitor combination. The exception is the MIBC/talc combination which resists the de-stabilizing effect of solvent, both in the bubble contact as well as bubble bed experiments.

This is attributed to a coalescence inhibiting effect due to packing of talc particles and MIBC molecules at the air-water interface (Figure 4.18, Chapter 4).

Coalescence of the two bubbles was not observed with the talc/NaCl/solvent combination whereas bubble bed collapse was observed. Interpretation is limited by a lack of understanding of the action of salt in inhibiting coalescence compared to surfactant. Such understanding might explain the lack of coalescence in the model two bubble contact case compared to the crowded bubble bed in the downcomer.

5.5 Conclusions

1. Where solvent droplet was larger than the bubbles ($D_d / D_b = 1.4$), no coalescence was observed. When the solvent droplet was halved ($D_d / D_b = 0.7$), coalescence was observed.
2. When two bubbles were held in proximity and solvent droplets were circulated, coalescence occurred in all scenarios except for water alone where only spreading occurred. The coalescence mechanism was speculated to be that which induced bubble bed collapse upon solvent introduction in the downcomer (Chapters 3 and 4), namely film rupture caused by the bridging and/or spreading of solvent droplets. Evidence of solvent bridging was captured in the case of 10 ppm PPG 425.
3. The hydrophobic solids talc and graphite exhibit a bridging/coalescence effect in water alone but not in the presence of coalescence inhibitors MIBC and NaCl.
4. It is speculated that the solvent is a more effective antifoaming agent than the hydrophobic solids due to its ability to spread.
5. The talc/MIBC system did resist coalescence by solvent which corresponds to its ability to resist bed collapse.

5.6 References

Denkov, N. D., Marinova, K.G., 2006. Antifoam effects of solid particles, oil drops and oil-solid compounds in aqueous foams. Colloidal particles at liquid interfaces. Cambridge University Press.

Dippenaar, A., 1982. The destabilization of froth by solids. I. The mechanism of film rupture, *International Journal of Mineral Processing*, 9, 1-14.

Kuan, S.H., Finch, J.A., 2010. Impact of talc on pulp and froth properties in F150 and 1-pentanol frother systems, *Minerals Engineering* 23, 1003-1009.

Pugh, R.J., 1996. Foaming, foam films, anti-foaming and defoaming. *Advances in Colloid and Interface Science* 64, 67-142.

Chapter 6 – Unifying discussion

6.1 Summary of findings

The initial target of the thesis was to determine if a downcomer, similar to that in the Jameson Cell, could be used as a ‘reactor’ to coat bubbles with solvent and provide scale-up of the air-assisted solvent extraction (AASX) process. Chapter 3 explored this application but encountered the phenomenon of collapsing bubble bed almost immediately upon introduction of solvent. Though copper extraction near 70% exceeded the target (50%) and turbidity was minimized with the use of MIBC and NaCl (hence, low solvent loss to solution), these successes were overshadowed by the bubble bed collapse which was counter-productive to solvent coating. The attractive feature of high gas holdup in the bubble bed, one reason the downcomer was chosen as the ‘coating reactor’, deteriorated rapidly with the advent of small amounts of solvent.

The deterioration (gas holdup reduction) increased with progressive addition of solvent such that in certain situations, e.g. where NaCl was used, gas holdup reached zero towards the end of the experiment, equivalent to an aqueous/organic (a/o) ratio of ca. 900. The gas holdup reduction was accompanied by decreased aspirated air rate as well as formation of air slugs. Neither changing the solvent introduction technique nor changing solvent composition (LIX:Kerosene ratio) alleviated the situation. The mechanism of bed collapse was attributed to the known de-foaming properties of oil droplets. Because conditions in the bubble bed in the downcomer approach those of foam (gas holdup > 45%), this de-foaming mechanism could well be responsible, the solvent droplet taking on the role of antifoaming agent. The antifoaming action is associated with a solvent droplet attaching to a bubble surface and by bridging and/or spreading causing coalescence. The unexpected bed collapse prompted reorientation of the thesis to examine the bubble bed collapse phenomenon.

The literature teaches that both hydrophobic liquid droplets and hydrophobic solid particles can act as de-foaming agents by promoting coalescence. Chapter 4 investigated the effects of hydrophobic materials on bed stability by comparing solvent with two hydrophobic solids, talc and graphite. The overall result was that the solids did not produce bed collapse, if anything enhancing stability, suggesting it is the ability of the solvent to spread that gives it the de-foaming (bed collapse) effect.

Only able to compare the solids in the NaCl system (graphite adsorbs frothers), small additions (up to 0.07 % w/w) of both talc and graphite showed an initial increase in gas holdup with corresponding decrease in bubble size (an indication of increased bed stability) but at higher additions their effect diverged: with graphite the gas holdup decreased and bubble size remained constant while with talc gas holdup and bubble size remained constant. The gas holdup decrease in the case of graphite was attributed to an increase in bubble rise velocity.

Subsequent addition of solvent with solids present resulted in bed collapse with one notable exception: the MIBC/talc/solvent combination where gas holdup and bubble size remained stable. This stability in the face of solvent was speculated as due to close packing of talc particles and MIBC molecules at the air-water interface that prevented the droplets from attaching and/or spreading.

Experimenting with the downcomer is limited in what it reveals of mechanisms. A model setup was required to provide control over the participating components. In Chapter 5 a bubble contact setup was built to view the coalescence event between two bubbles in close proximity (0.04 – 0.06 mm) when exposed to circulating dispersions of solvent, solid, and solvent/solid combinations. The conditions giving coalescence in the setup generally agreed with those yielding bed collapse, including the MIBC/talc/solvent case where neither coalescence nor bed collapse occurred. The act of solvent bridging was captured on video although spreading was not observed. The findings support the solvent attachment/bridging mechanism of bubble bed collapse.

In the absence of coalescence inhibitor, both talc and graphite cause coalescence, reasonably attributed to the attachment/bridging mechanism, but this was suppressed by MIBC and NaCl. This hints that either the bridging/coalescence property of solvent is greater than that of its two solid counterparts or the unique ability of the solvent to spread is involved in coalescence which the bubble contact setup could not reveal.

6.2 Solvent bridging and spreading effect

The solvent bridging/spreading effect is destructive in that it induces coalescence and consequent bed collapse. Thus the irony is that the very act of spreading central to coating swarms of bubbles for AASX actually causes collapse of the bubble bed in the downcomer that seemed so attractive at the outset. When only sequences of single bubbles were produced (Tarkan and Finch, 2005), this problem was not encountered as the bubbles never came close enough for the coalescence mechanism(s) to act. Similarly in the aerosol/Venturi system used by Tarkan et al. (2012) to produce coated bubbles injected into a column, the bubbles were never sufficiently crowded for contact and coalescence to be a factor. Indeed a column is characterized by the bubble swarm expanding as it moves away from the area of generation, i.e., the individual bubbles are moving away from each other thus reducing the possibility of coalescence. The downcomer, in contrast, does not allow the generated swarm to expand but rather constrains it with, as evident here, the potential for different outcomes. Future work on scaling up AASX should reconsider use of a column.

6.3 Solids bridging effect

In the context of coalescence and bubble bed collapse, the talc and graphite hydrophobic solid particles were not as effective as the solvent. They did not induce bubble coalescence in the presence of coalescence inhibitors neither did they cause bed collapse (except when PPG 425 was used with talc explained by adsorption of the frother by talc). They did however, exhibit bubble bridging effects in water alone leading to bubble

coalescence in the bubble contact experiments. Hydrophobic solids are known to aid formation of stable froth in flotation, as they did here noted in Chapter 4. The bridging/coalescence effect with talc and graphite in water alone implies that, to act as froth stabilizers, solid particles and coalescence inhibitors are best acting in concert. In flotation this is the common situation. However, in a follow up study Dippenaar (1982b) observed destabilization by hydrophobic quartz and galena) in presence of a frother (1,1,3-triethoxy butane). At the other extreme, Pugh (2007) was able to generate aqueous foams from surfactant-free dispersions of hydrophobic anatase (titanium oxide) nano-particles. The role of solid particles/frother/salt combinations is ripe for research both in terms of bubble production and foam (froth) stabilization.

6.4 The MIBC/talc combination

The only case where the bubble bed did not collapse upon introduction of solvent was MIBC/talc. Though functional in the sense that gas holdup and bubble size remained stable with addition of solvent, the impracticality of the combination does not lend itself to AASX. As such at this juncture extraction experiments were not performed with this scenario.

6.5 Industrial use of downcomer in organic removal

Experiments showed that at the typical range of 50 to 200 ppm in organic content in solvent extraction plants, the Jameson Cell would continue to function without excessive bubble bed collapse. Even with substantial bed collapse at 900 ppm solvent the present results show that organic (tramp droplet) removal was achieved although inefficiently. Unlike the unit used in this work, Jameson Cell plant installations do not have sensors to measure gas holdup thus the extent of collapse, if any, is unknown. Expanding use of the Jameson Cell to de-oiling in general for water treatment, e.g. on off-shore oil rigs for oil spill cleanup, may need to consider the possibility of bed collapse.

Recent efforts have seen the Jameson Cell considered for flotation of organic carbon from flotation streams (e.g. Smith et al., 2008) and in the secondary recovery of bitumen in oil sands processing (Neiman et al., 2012). The possibility of bed collapse is probably not a factor in these cases as the hydrophobic material is either solid (the first case) or highly viscous and therefore solid-like (the second case) and the current results have demonstrated that solids do not cause bed collapse.

6.6 References

Dippenaar, A., 1982b. The destabilization of froth by solids II. The rate determining step, *International Journal of Mineral Processing* 9, 15-27.

Neiman, O., Hilscher, B., Siy, R., Secondary recovery of bitumen using Jameson downcomers, 2012. 44th Annual Canadian Mineral Processors Conference, Ottawa, Canada. January 17 -19.

Pugh, R.J., 2007. Foaming in chemical surfactant free aqueous dispersions of anatase (titanium oxide) particles, *Langmuir* 23, 7972-7980.

Smith, T., Lin, D., Brigitte, L., Anderson, G., 2008. Removal of organic carbon with a Jameson cell at Red Dog Mine, 40th Annual Canadian Mineral Processors Conference, Ottawa, Canada. January 22 -24.

Tarkan, H. M., Finch, J.A., 2005. Air-assisted solvent extraction: towards a novel extraction process. *Minerals Engineering* 18, 83-88.

Chapter 7 – Conclusions, contributions, and future work

7.1 Conclusions

The following conclusions can be drawn from the study:

1. In the attempt to use a downcomer as a 'reactor' to coat bubbles with solvent and provide scale-up of the air-assisted solvent extraction (AASX) process, the phenomenon of collapsing bubble bed was encountered almost immediately upon introduction of solvent. The attractive feature of high gas holdup in the bubble bed, the reason the downcomer was chosen as the 'coating reactor', deteriorated rapidly with the advent of small amounts of solvent.
2. Bubble bed collapse was indicated by decrease in gas holdup and aspirated air rate and increase in bubble size. Changing the solvent introduction method or changing the solvent composition (LIX:Kerosene ratio) did not alleviate the problem.
3. The mechanism of bed collapse was attributed to the known de-foaming properties of oil droplets. Because conditions in the bubble bed approach those of foam (gas holdup > 45%), this mechanism could be responsible, the solvent droplet taking on the role of antifoaming oil. The antifoaming action is associated with a solvent droplet attaching to a bubble surface and by bridging and/or spreading causing coalescence.
4. Investigation of the effects of hydrophobic materials on bed stability by comparing solvent with two hydrophobic solids, talc and graphite, showed that the solids did not produce bed collapse, if anything enhancing stability, suggesting it

is the ability of the solvent to spread that gives it the de-foaming (bed collapse) effect.

5. Subsequent addition of solvent to the solids resulted in bed collapse with one exception the MIBC/talc combination where gas holdup and bubble size remained stable. The stability was speculated to be due to cooperative close packing of talc particles and MIBC molecules at the air-water interface that prevented the droplets from attaching and/or spreading. The impracticality of the combination, however, does not lend itself to AASX.
6. The bubble contact setup established to view the response of two bubbles held in proximity (0.04 – 0.06 mm) when exposed to circulating dispersions of solvent, solid and solvent/solid combinations showed that the conditions giving coalescence generally agreed with those yielding bed collapse, including the MIBC/talc/solvent case where neither coalescence nor bed collapse occurred. The act of solvent bridging was captured on video although spreading was not observed; nevertheless, the findings are in concert with bed collapse via the solvent attachment/bridging/spreading mechanism.
7. In water only, both talc and graphite cause coalescence through the attachment/bridging mechanism (also captured on video) but this was suppressed by MIBC and NaCl. This hints that either the bridging/coalescence property of solvent is greater than that of its two solid counterparts or the unique ability of the solvent to spread is involved in coalescence which the bubble contact setup could not reveal.
8. At the typical range of 50 to 200 ppm organic content in solvent extraction plants the Jameson Cell should continue to function without excessive bubble bed collapse. Expanding use of the Jameson Cell for de-oiling water treatment may need to consider the possibility of bed collapse.

7.2 Contributions to Knowledge

1. First attempt to create swarms of solvent-coated bubbles for the air-assisted solvent extraction process aimed at dilute metal effluent streams in a downcomer.
2. Discovery that introducing solvent into the downcomer induces bed collapse.
3. First to associate the antifoaming action of oil droplets to bubble bed collapse in a downcomer.
4. First to report a decrease in bubble size upon adding talc or graphite to NaCl solutions in a downcomer.
5. Development of set-up and procedure to observe response of two bubbles held in proximity to circulation of suspensions of solvent, solid and solvent/solid combinations.
6. Demonstration of solvent bridging mechanism as well as explanation of bubble bed collapse.

7.3 Suggestions for Future Work

1. The effect of viscous oil droplets such as bitumen on antifoaming action can be explored. The results would shed more light on the bridging and spreading action of oil in comparison with the bridging action of particles because bitumen droplets can behave like a solid particle or an oil droplet depending on temperature.
2. It may prove to be illuminating to assess the effect of high solids content (e.g. up to 20 % w/w) and particle size on the bubble bed in the downcomer.
3. It would be useful to revisit the technique developed by Tarkan et al. (2012) which combined the aerosol coating technique of Maiolo and Pelton (1998) with the Venturi bubble generator employed by Gomez et al. (2001). The ultrasonic generator used which limited the solvent rate can be replaced with one of a higher output, e.g. the recently developed atomizer by Xstrata called the 'Frothermiser' (Pokrajcic et al. 2005).

7.4 References

Dippenaar, A., 1982b. The destabilization of froth by solids II. The rate determining step, *International Journal of Mineral Processing* 9, 15-27.

Gomez, C.O., Acuna, C., Finch, J.A., Pelton, R., 2001. Aerosol enhanced flotation deinking of recycled paper. *Pulp & Paper Canada* 102, 28–30.

Kuan, S.H., Finch, J.A., 2010. Impact of talc on pulp and froth properties in F150 and 1-pentanol systems, *Minerals Engineering* 23, 1003-1009.

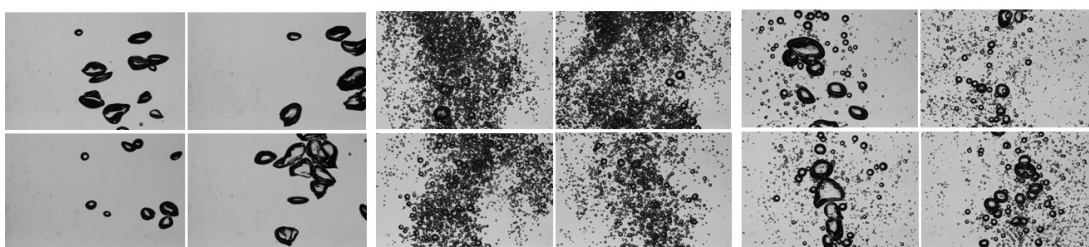
Maiolo, J., Pelton, R., 1998. Aerosol-enhanced flotation—a possible approach to improved flotation deinking. *Journal of Pulp and Paper Science* 24, 324–328.

Pokrajcic, Z., Cowburn, J.A., Harbort, G.J., Manlapig, E.V., 2005. Improving coal flotation using a new method of frother addition, *Centenary of Flotation 2005 Symposium*, Brisbane, Australia.

Pugh, R.J., 2007. Foaming in chemical surfactant free aqueous dispersions of anatase (titanium oxide) particles, *Langmuir* 23, 7972-7980.

Appendices

Appendix A - Supplementary Figures

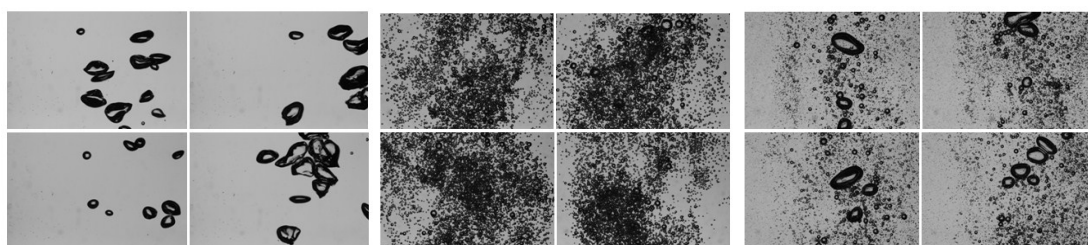


(a)

(b)

(c)

A1. (a) Bubbles in water. (b) Bubbles with addition of 90ppm MIBC. (c) Bubbles after 33.3 mL solvent injection in the presence of 90ppm MIBC.

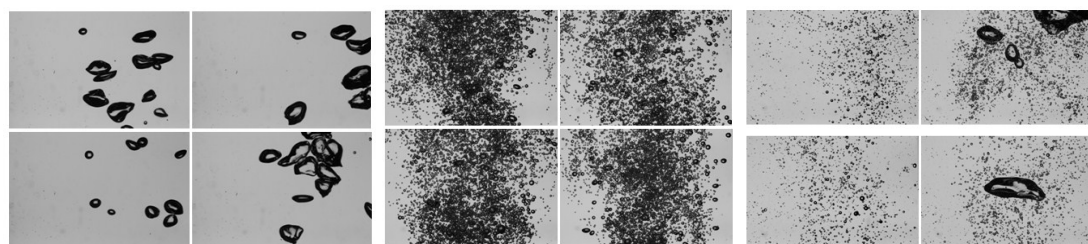


(a)

(b)

(c)

A2. (a) Bubbles in water. (b) Bubbles with addition of 30ppm PPG 425. (c) Bubbles after 33.3 mL solvent injection in the presence of 30ppm PPG 425.

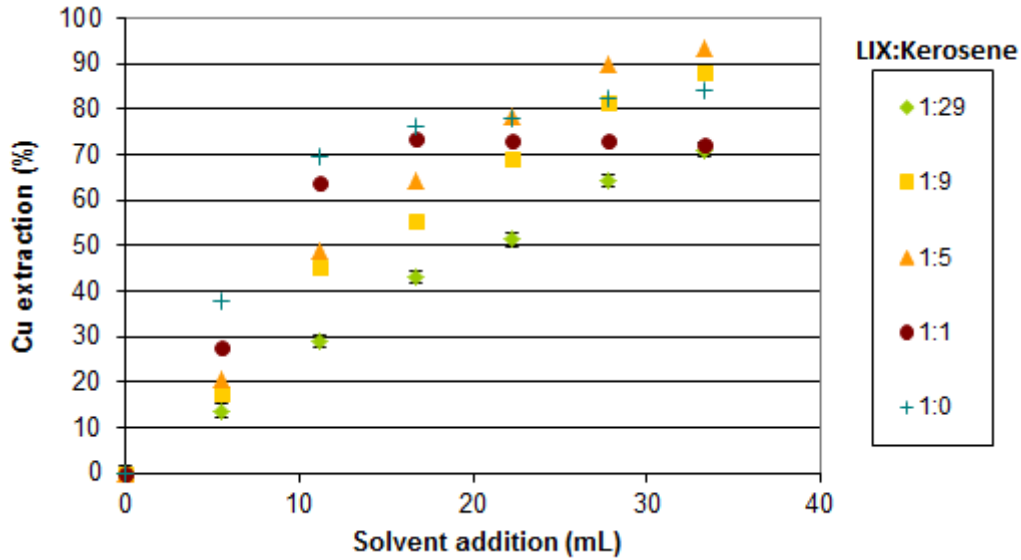


(a)

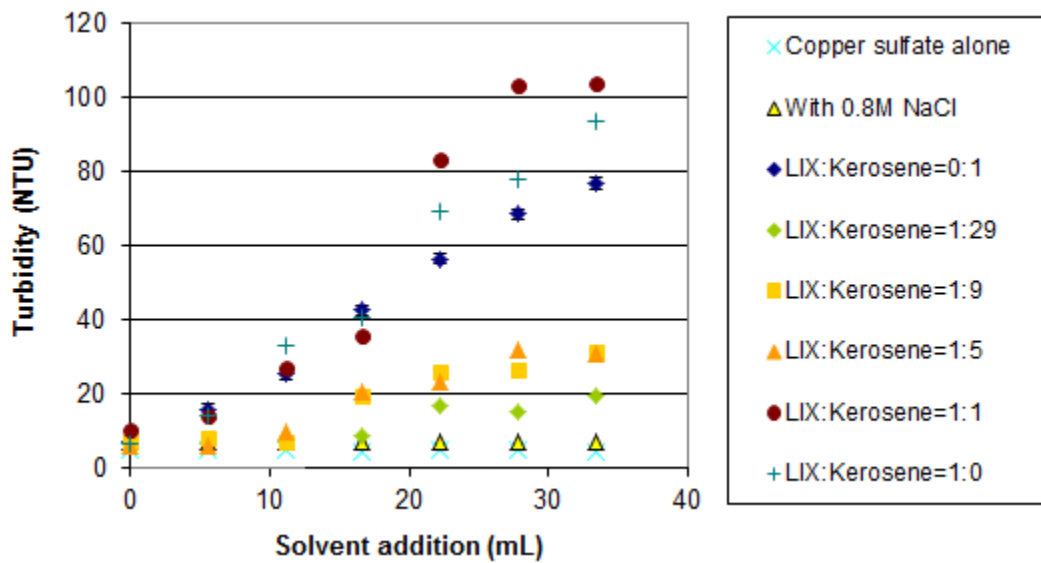
(b)

(c)

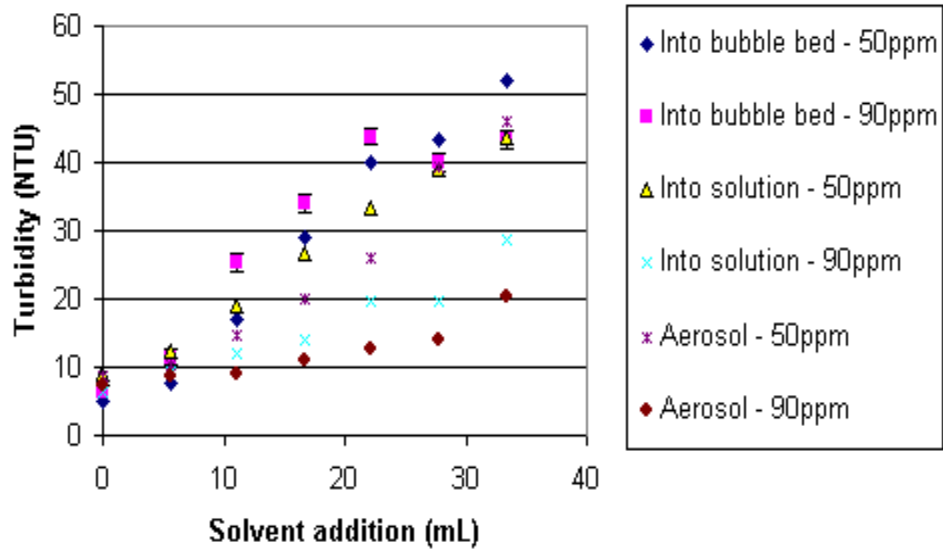
A3. (a) Bubbles in water. (b) Bubbles with addition of 0.8M NaCl. (c) Bubbles after 33.3 mL solvent injection in the presence of 0.8M NaCl.



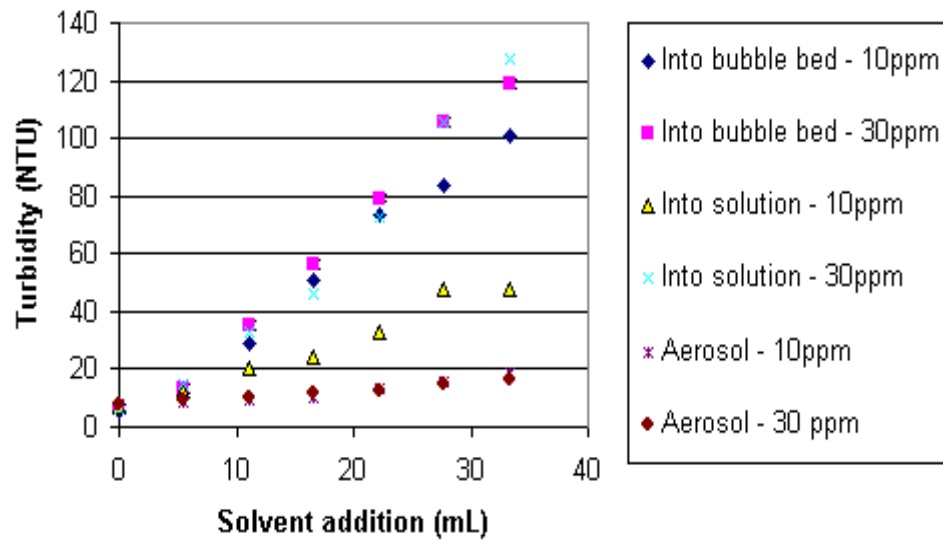
A4. Copper extraction with respect to solvent addition at different LIX to kerosene ratios



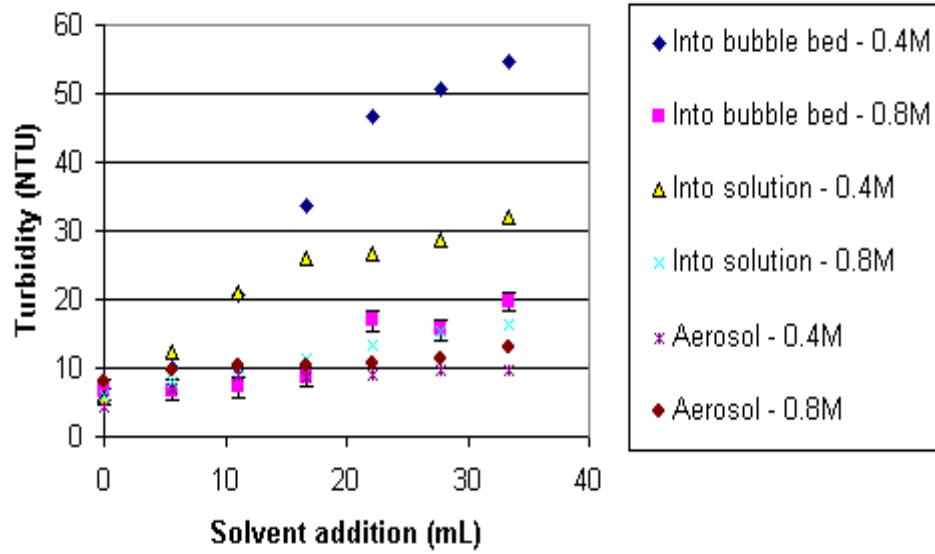
A5. Change of turbidity with respect to solvent addition at different LIX to kerosene ratios



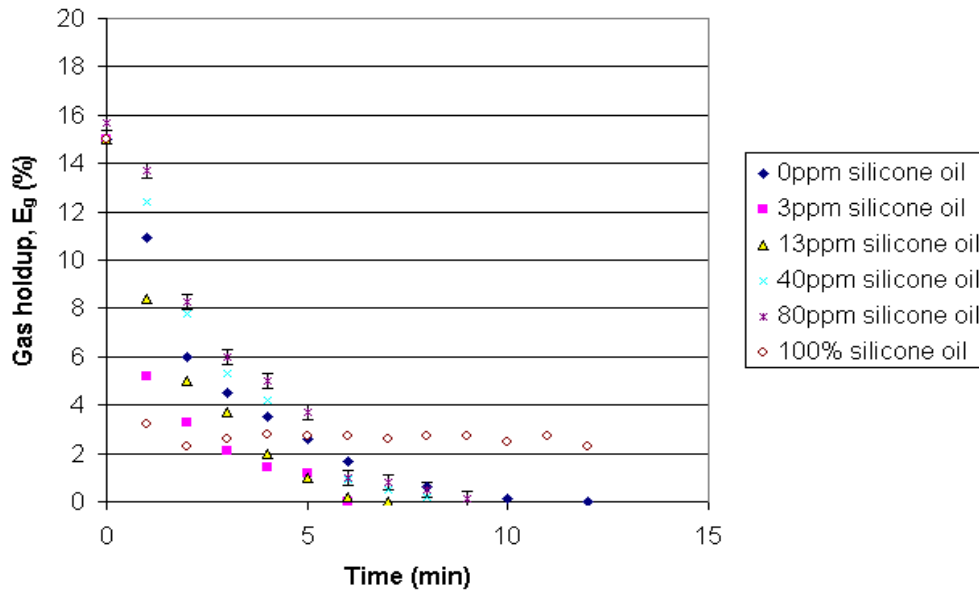
A6. Comparison of turbidity data for the three solvent introduction techniques (in bubble bed, in solution and in air) for MIBC systems



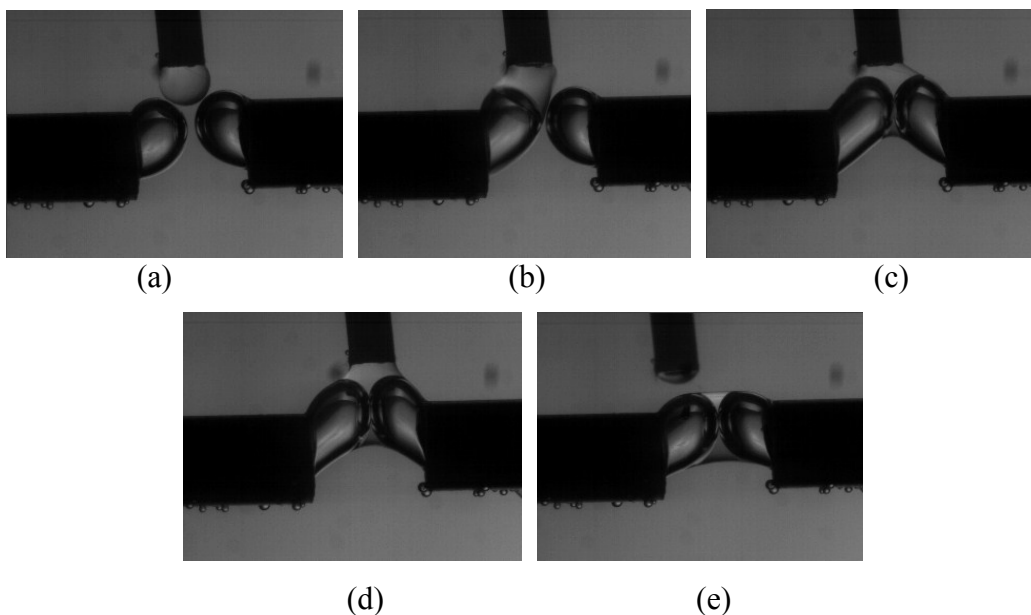
A7. Comparison of turbidity data for the three solvent introduction techniques for PPG 425 systems



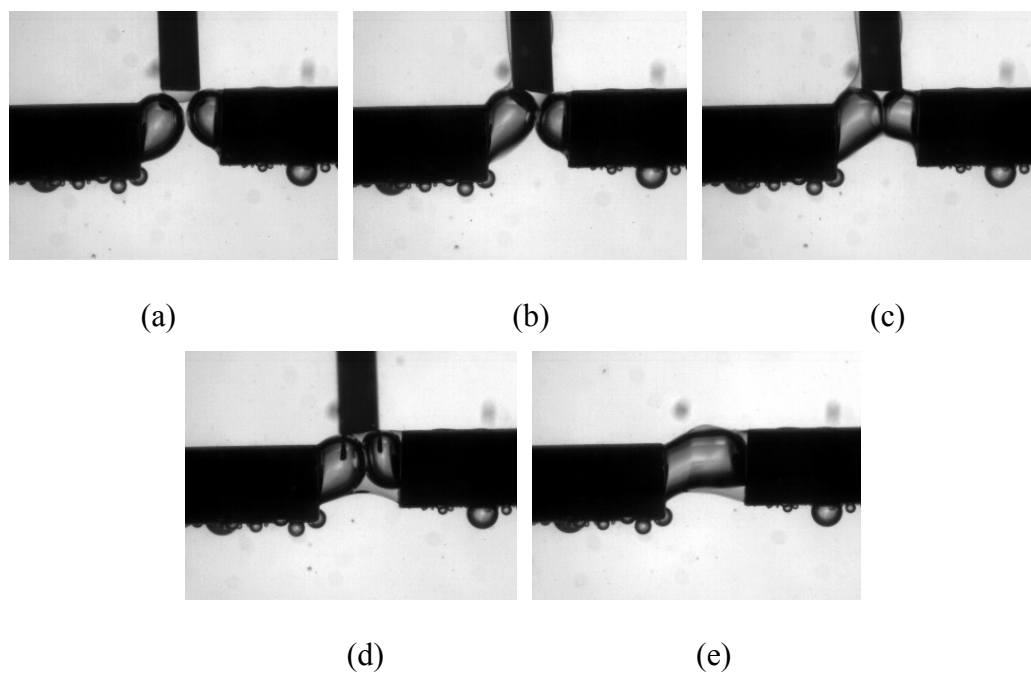
A8. Comparison of turbidity data for the three solvent introduction techniques for NaCl systems



A9. Effect of silicone oil concentration in solvent on gas holdup of separation tank. (0.8 M NaCl solution, solvent LIX:Kerosene 1:29, solvent flowrate = 0.04 mL/s, solvent volume = 33.3 mL).

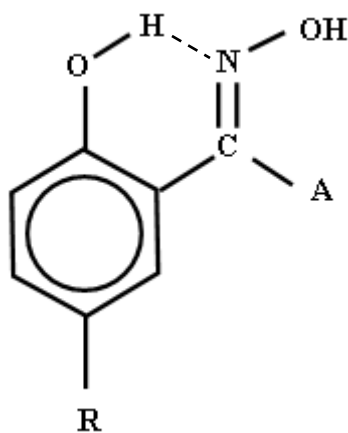


A10. Solvent droplet ($D_{drop} / D_{bubble} = 0.7$) in contact with two bubbles in presence of 50 ppm MIBC, LIX:Kerosene 1:29

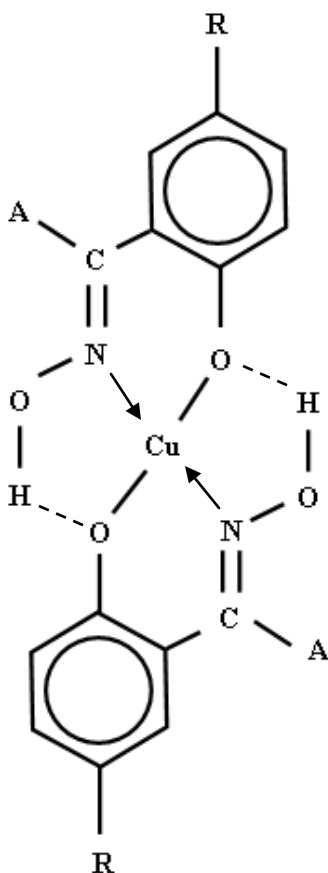


A11. Solvent droplet ($D_{drop} / D_{bubble} = 0.7$) in contact with two bubbles in presence of 0.4 M NaCl, LIX:Kerosene 1:29

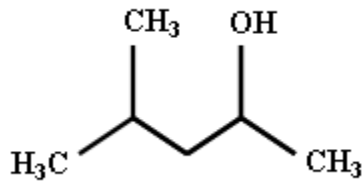
Appendix B – Molecular Structures



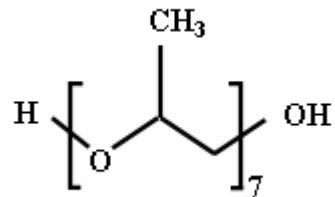
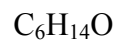
B1. Oxime molecule, R = C₉H₁₉ or C₁₂H₂₅, Salicylaldoxime: A = H, Ketoxime: A = CH₃ or C₆H₅. The commercial extractant used (LIX 973N) is a 7/3 volume blend of salicylaldoxime and ketoxime.



B2. Formation of copper complex with two oxime molecules.



B3. Molecular structure of 4-methyl-2-pentanol or methyl isobutyl carbinol (MIBC),



B4. Molecular structure of polypropylene glycol (PPG 425), $\text{H}(\text{C}_3\text{H}_6\text{O})_7\text{OH}$

Appendix C – Reproducibility

The sample standard deviation (s) was calculated using the following equation:

$$s = \sqrt{\frac{\sum (x - \bar{x})^2}{(n - 1)}} \quad (\text{C1})$$

where x , \bar{x} and n are the individual measurements, the average and the number of measurements.

Standard deviations of individual data sets were then pooled. The pooled standard deviation (s_p) was calculated as follows:

$$s_p^2 = \frac{\sum_{i=1}^k ((n_i - 1)s_i^2)}{\sum_{i=1}^k (n_i - 1)} \quad (\text{C2})$$

The 95% confidence interval was then computed as follows:

$$95\% \text{ confidence interval} = \pm 1.96 \frac{s_p}{\sqrt{n}} \quad (\text{C3})$$

The error bars indicated in the figures of this thesis correspond to the 95% confidence interval.